The Use of Well-Defined Molybdenum ROMP Initiators in the Synthesis of Fluorescent Poly(arylenevinylene) Homopolymers and Copolymers

Thesis by

Delwin Lerone Elder

In Partial Fulfillment
of the Requirements for the Degree of
Doctor of Philosophy

California Institute of Technology
Pasadena, California

2000

(Defended August 16, 1999)

To my family

"And death shall have no dominion.
Dead men naked they shall be one
With the man in the wind and the west moon;
When their bones are picked clean and the clean bones gone
They shall have stars at elbow and foot;
Though they go mad, they shall be sane,
Though they sink through the sea they shall rise again;
Though lovers be lost love shall not;
And death shall have no dominion . . . ".

— Dylan Thomas

Acknowledgment

First and foremost, I would like to thank Bob Grubbs for his support, patience, and advice in all aspects of my research during my thesis. The research environment that he has fostered has been an excellent place to do and learn organometallic, polymer, and organic chemical methods.

I would like to thank several people who have had a direct and major impact on my thesis research. Jérôme Claverie got me started on my initial project in the Grubbs group and taught me about olefin metathesis, taught me numerous Schlenk line and drybox techniques, and introduced me to the Bruker AM500, the finest instrument ever built. Eric Dias was a great help to me in my initial project, interpreting NMR spectra, giving advice, and was the general go-to guy whenever I was lost; and Eric always had answers. Shojiro Kaita worked with me for a few months on my initial project, and his assistance was greatly appreciated. Scott Miller's enthusiasm and optimism was always inspirational to me, and I thank him for that. Mike Wagaman got me started on the conjugated polymer project and taught me a lot about polymer synthesis and isolation, LEDs, and fluorescence spectoscopy. I would like to thank Erika Bellmann, Sean Shaheen, Kelly Killeen, Shannon Rice, Jason Brooks, and all of the members of the Center for Advanced Multifunctional Polymers and Non-Linear Optical Materials for teaching me about fluorescent materials and the many aspects of LEDs.

There are many people and institutions who have helped my academic development, too many to name here, but I would specifically like to acknowledge Governor's School, Jim Adcock, Maurice Brookhart, Francis Rix, Katie Carrado, Master

Yoda, and Howard Katz for being mentors to me and teaching much about science and doing research in different environments.

I would also like to thank the members of my thesis committee for taking the time to follow my progress, advise, and read and comment on my thesis, John Bercaw, Dennis Dougherty, and Harry Gray.

I would like to give a heartfelt and sincere "thank you" to all of the members of the Grubbs group (and spouses and friends), past and present, who have all helped me in many little ways concerning science, instrumentation, and personal well-being. Particularly, I would like to thank Osamu for being a great friend, a great chemist, and a great hiker. I cannot say enough about the generosity of Osamu; he once even offered to run a comumn for me. I'd like to thank Helen, Dave, Cassandra, Scott, Jan-Karel, Mary Shepard, Amy Pangborn Giardello, Mike "Psycho" Giardello, Todd, Jason, Janis, Heather, Erika, Michèle, Chris, Melanie, Thomas R., Yves, BZ, Arnab, Bill, and Sheldon for generally being cool people to hang out with; EricD. for playing his guitar, Eric C. for playing his flute, Helen for playing her violin; Tom Kirkland for being a good roommate; Tom Wilhelm for sharing a bench; Mike Ulman for sharing bay; Eric D., Marcus, Adam, Mike W., Mike U., Peter, J.P., Jason, Eric "the Flute" Connor, and Rob for making our end of the lab a fun and musically interesting place to work. TAK, Marcus, Sylvia, Helen, and Mike Johnson for all of the adventures in the Dungeon; everyone on the camping trips and in the softball games; Dan for the jambalaya; Dian Buchness and Linda Clark have also been a great help, answering questions, and keeping me (somewhat) organized. There are certain non-grubbs group members whom I would like to acknowledge also, like Adrian H. and Caroline for Sci-Fi nights, Adrian P. and Jim for the Sci-Fi movies;

Christine for being a good neighbor and cooking me dinner whether I wanted it or not; Adrian, Jim, Tom, Dario, Derek, Gabe, and others on the soccer team; Claudine and Deanna for all of the rollerblading and hiking adventures; Adrian H. for introducing me to the Derby and Molly, Roscoe, Eric, Sylvia and everyone else at the Derby for a swingin' time.

A special thanks goes to Connie Calderon, Cheryl, Ramona, Yuny, and everyone in NSBE and CLASES for support and making social life here a Caltech a little bit better.

Last, but certainly not least, I would like to thank my family and dedicate this Thesis to them for always being there for me, supporting me, and keeping me happy.

Abstract

We have discovered that ring-opening metathesis polymerization (ROMP catalysts of the type $Mo(CHMe_2Ph)(N\text{-}2,6\text{-}C_6H_3{}^iPr_2)(OCMe(CF_3)_2)_2$ (**1**) may be greatly activated by the addition of one or more equivalents of the cocatalyst $HOCMe(CF_3)_2$ (hexafluoro-*t*-butanol, HFB). In general, HFB increases the rate of initiation relative to propagation for the ROMP of low strain cyclic olefins. The ratio or propagation to initiation has been measured and found to decrease by up to three orders of magnitude upon the addition of HFB to polymerizations of cyclooctene, cyclooctadiene, and 3,4,6-trichloro-5-octyl-benzobarrelene (**2**) initiated by **1**. With **2** we were able to measure k_p and k_i as well as k_p/k_i and found that HFB increases both k_p and k_i, but k_i increases to a greater degree. High strain cyclic olefins such as norbornene display no such enhancement of initiation. The mechanism of this "alcohol effect" is not yet well understood.

New conjugated poly(1,4-naphthalenevinylene)s (PNVs) disubstituted by electron-donating alkoxy substituents (**3**) have been synthesized by ROMP of new dialkoxy-benzobarrelene monomers (**4**) followed by aromatization with DDQ. Polymerizations were initiated with catalyst $Mo(CHCMe_2Ph)(N\text{-}2,6\text{-}C_6H_3\text{-}{}^iPr_2)(OCMe_2(CF_3))_2$ (**5**) whose performance was superior to initiator **1**. This ROMP-Aromatization Route is a mild synthesis procedure and provides polymers of controlled molecular weight that are low in polydispersity and soluble in common organic solvents. The wavelengths of photoluminescence of **3** are from 534-546 nm with quantum efficiencies of (5-15%).

Block copolymers diester-PPV-*block*-dialkoxy-PNV (**6**) and dialkoxy-PNV-*block*-alkyl-PNV (**7**) and random copolymers diester-PPV-*random*-dialkoxy-PNV (**8**)

have been synthesized by the ROMP-Aromatization Route utilizing initiator **2**. The diester-PPV segments have a larger HOMO-LUMO gap than the dialkoxy-PNV segments allowing the polymer to be able to execute through-bond (non- Förster) energy transfer. Upon photoexcitation of the large band gap segments, the block copolymers **6** however do not display energy transfer, but the block copolymer **7** and the random copolymers **8** do display moderate to efficient energy transfer. Remarkably, in the case of **8c**, photoluminescence is increased by a factor of 2 to 18%, and for **7**, the efficiency is increased by a factor of 10 to 5%. This copolymer strategy should be a general technique to increase the quantum efficiency of polyarylenevinylenes.

Table of Contents

List of Equations, Figures, and Tables

Chapter 1

Equations

Figures

Tables

Chapter 2

Figures

Chapter 3

Figures

Tables

Chapter 4

Figures

Tables

Chapter 1

The "Alcohol Effect":

Mechanistic Studies on the Enhancement of Initiation Rates of Molybdenum and Tungsten ROMP Initiators by the Cocatalyst Hexafluoro-*t*-butanol

Abstract

We have discovered that ring-opening metathesis polymerization (ROMP catalysts of the type M(CHR)(NAr)(OCMe$(CF_3)_2)_2$ and M(CHR)(NAr)(OCMe$(CF_3)_2)_2$L (M = Mo, W; R = CMe_2Ph, L = Lewis base) may be greatly activated by the addition of one or more equivalents of the cocatalyst HOCMe$(CF_3)_2$ (hexafluoro-*t*-butanol, HFB). In general, HFB increases the rate of initiation relative to propagation for the ROMP of low strain cyclic olefins. The ratio k_p/k_i (where k_p is the rate constant for propagation and k_i is the rate constant for initiation) has been measured and found to decrease by up to three orders of magnitude upon the addition of one or more equivalents of HFB to polymerizations of cyclooctene, cyclooctadiene, and 3,4,6-trichloro-5-octyl-benzobarrelene (**3Cl-BB**) initiated by Mo(CHR)(NAr)(OCMe$(CF_3)_2)_2$ (R = CMe_2Ph, Ar = 2,6-$C_6H_3{}^iPr_2$) (**1a**). With **3Cl-BB** we were able to measure k_p and k_i as well as k_p/k_i and found that HFB increases both k_p and k_i, but k_i increases to a greater degree. Fifteen equivalents of HFB was found to be optimal for rates and narrow polydispersity index. High strain cyclic olefins such as norbornene display no such enhancement of initiation. The mechanism of this "alcohol effect" has been investigated, but a complete explanation has not yet been found.

Introduction

Ring-opening metathesis polymerization (ROMP)[1] has been used to make a wide variety of important polymers including conducting polyacetylenes,[2] highly fluorescent poly(phenylenevinyene)s,[3,4] liquid crystalline polymers,[5] photocurable polymers,[6] telechelic polymers,[7] electroactive polymers,[8] and biomimetic polymers.[9,10,11] Because ROMP is a living polymerization system in many cases, good control of molecular weight can be achieved, and block copolymers may be readily prepared by sequential addition of monomers.[12] The most popular types of homogeneous, well-defined, single component ROMP initiators are ruthenium, molybdenum, and tungsten alkylidenes (see Figure 1).[13] The ruthenium-based catalysts have the advantage of being more functional group tolerant than the molybdenum or tungsten ones, which allows for the polymerization of monomers bearing functional groups such as alcohols and carboxylic acids,[14] and the polymerization in aqueous media.[15]

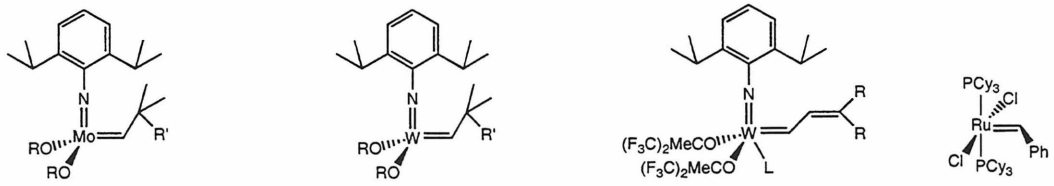

1a, R = $CMe(CF_3)_2$, R' = Ph
1b, R = $CMe_2(CF_3)$, R' = Ph
1c, R = CMe_3, R' = Ph
1d, R = $CMe(CF_3)_2$, R' = Me

2a, R = $CMe(CF_3)_2$, R' = Ph
2b, R = $CMe_2(CF_3)$, R' = Ph
2c, R = CMe_3, R' = Ph
2d, R = $CMe(CF_3)_2$, R' = Me

3a, L = , R = Ph
3b, L = , R = Me

4

Figure 1. Popular well-defined, single-component olefin metathesis alkylidene initiators.

The tungsten and molybdenum catalysts have the advantage of being highly active, and are necessary to ROMP some low-strain monomers such as cycooctatetrenes[16] and benzobarrelenes[17] and effect the metathesis polymerization of acetylenes.[1,18] Compounds **1a** and **2a** are among the most active metathesis catalysts known.[1,12b,19,20,21]

Their high activity is partly a result of them being coordinatively unsaturated, 16-electron, very electrophilic compounds. Without sterically bulky ligands to protect the metal center and prevent bimolecular- and other decomposition pathways, these reactive compounds would be unstable.

An undesired consequence of requiring bulky ligands is that, during ROMP, catalysts **1** and **2** tend to initiate much slower than they propagate. Thus, monodisperse polymers are not able to be prepared, and large quantities of monomer (in some cases several hundred equivalents) are required to achieve full initiation, which is often impractical. It has been explained that differences in reactivity between initiating and propagating alkylidenes is because the propagating alkylidene is less bulky than the initiating alkylidene, and thus more apt to bind monomer (Figure 2). For catalysts such as **4**, initiation has been shown to be much faster than propagation (by an order of magnitude), but it is unable to polymerize low-strain cyclic olefins to high molecular weights.

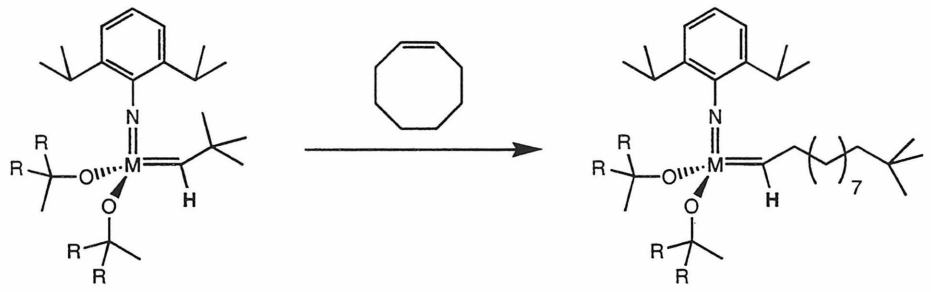

Figure 2. Initiating and propagating alkylidenes during ROMP.

The problem of how to increase the rate of initiation relative to propagation in tungsten and molybdenum metathesis catalysts has been investigated previously and a

partial solution disclosed. It has been found that the relative rate of initiation can be increased by the addition of Lewis bases such as phosphines, amines, and ethers, but this *only* works for highly strained monomers such as norbornenes and cyclobutenes. For example, **2d** in the presence of 10 equivalents of PMe_3 was used to ROMP 20 equivalents of cyclobutene in toluene solvent, resulting in polymer with a polydispersity index (PDI) of 1.07. Without the phosphine, or with a bulky phosphine which is not able to coordinate completely (ca. $PMePh_2$), the PDI is ~2 under analogous reaction conditions. This result is brought about presumably because the phosphine binds more tightly to the propagating carbene—which has a more crowded ligand sphere—slowing down propagation by hindering monomer coordination. The rate of initiation does not actually increased, but it does increase *relative* to propagation.

A second strategy was developed that is applicable to a wider range of monomer types. This strategy uses tungsten initiator **3**, and is successful at increasing the relative rate of initiation because the steric bulk of the initiating alkylidene (a vinylalkylidene) is less. A fifth ligand, typically a phosphine or ether, is necessary to stabalize and isolate these compounds, making them 18-electron, coordinatively saturated species.[22,23] Mechanistic details suggest that the lewis base is able to dissociate, leaving a coordinatively unsaturated species which reacts with monomer (Figure 3). Since the

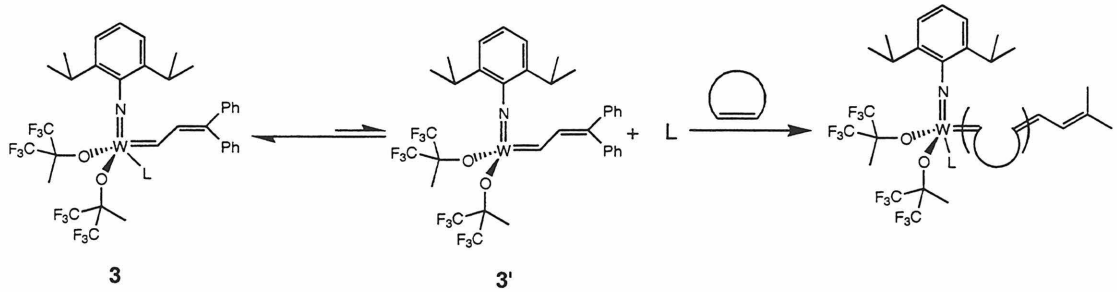

Figure 3. Initiation of a 5-coordinate tungsten vinylalkylidene.

ligand bulk of **3'** is less than that of **2a**, **3'** demonstrates a relative initiation rate that is an order of magnitude faster than that of **2a**. However, rates of polymerization were slow, and PDI values obtained are rarely below 1.3, so we were encouraged to seek other ways to increase initiation.[24]

An observation was made that all of the tungsten and molybdenum alkylidene compounds containing hexafluoro-*t*-butoxide ligands studied by this research group contained an impurity of $HOC(CH_3)(CF_3)_2$ (hexafluoro-*t*-butanol, HFB) (usually 1-5 mol%).[24] Attempts to remove the alcohol by dynamic vacuum, recrystallization, and "alcohol sponges" such as $MgSO_4$ and molecular sieves were never completely successful. Thus it became imperative to learn more about the influence of HFB on catalyst reactivity.

Shortly before joining the Grubbs group, Jérôme Claverie and others discovered somewhat accidentally that HFB can be used as a cocatalyst with compounds **1a**, **2a**, and **3** to increase the relative rate of initiation.[24] This became known as the "alcohol effect." When I joined the group, we began examining this affect more carefully, and reported here are our efforts to quantitate how much the rates of initiation and propagation were altered by HFB and determine limitations, examine differences with different monomers, and determine the mechanism of enhancement.

Results and Discussion

Results from k_p/k_I Measurements

An investigation of how HFB affects k_p and k_i in ROMP initiated by **1a** was undertaken (k_i is the rate constant for initiation, Equation 1, and k_p is the rate constant for propagation, Equation 2). Compound **1a** is probably the most popular of the

molybdenum and tungsten metathesis initiators and is commercially available. Since the polymerization of intermediate- to high strain olefins such as norbornene (NBE), *cis-cis*-1,5-cyclooctadiene (COD), and *cis*-cyclooctene (COE) is very rapid, evaluation of k_p and k_i is difficult by common techniques such as NMR spectroscopy. However, the ratio k_p/k_i may be readily evaluated using equation 1 according to the method of Gold[25] if one knows the initial monomer concentration, M_o, the final monomer concentration, M, the initial initiator concentration, I_o, and the final initiator concentration, I (Equation 3).[26,27] Initial concentrations can be controlled experimentally, and final concentrations can be determined by ^{1}H NMR spectroscopy, integrating the alkylidene resonances of initiator and propagating species (Figure 4).

$$I + M \xrightarrow{k_i} IM \tag{1}$$

$$IM + M \xrightarrow{k_p} IM_n \tag{2}$$

$$\frac{k_p}{k_i} = \frac{(M - M_0) - (I - I_0)}{(I - I_0) + \ln\left(\frac{I}{I_0}\right)} \tag{3}$$

k_p/k_i Measurements were made using Equation 3 for the polymerization of common ROMP monomers COD, COE, and NBE at room temperature in C_6D_6 solvent,

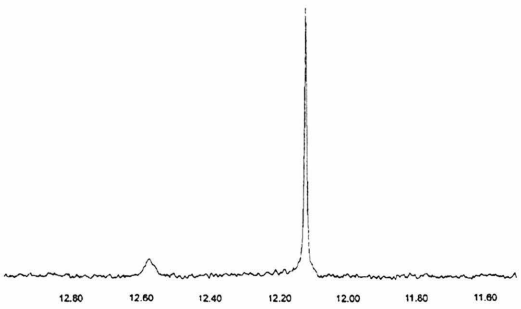

Figure 4a. ^{1}H NMR spectrum from 13.0 to 11.0 ppm after COD polymerization. The alkylidene signal of catalyst **1a** is at 12.13 ppm and the propagating carbene is at 12.56 ppm.

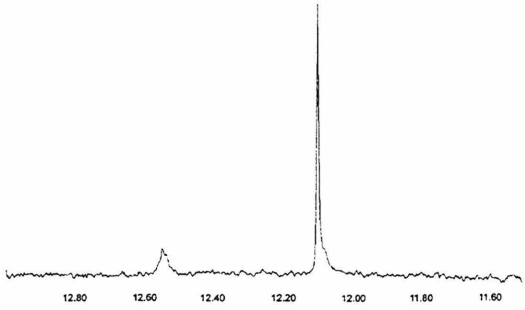

Figure 4b. ^{1}H NMR spectrum from 13.0 to 11.0 ppm after COE polymerization. The alkylidene signal of catalyst **1a** is at 12.13 ppm and the propagating carbene is at 12.55 ppm.

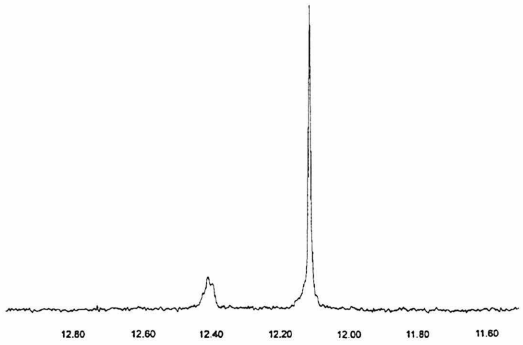

Figure 4c. ^{1}H NMR spectrum from 13.0 to 11.0 ppm after COD polymerization. The alkylidene signal of catalyst **1a** is at 12.13 ppm and the propagating carbene is at 12.41 ppm.

and were complete in less than five minutes unless otherwise noted. Results are shown in Table 1. For the ROMP of COD without the addition of HFB, Entry 1, propagation is 8300 times faster than initiation. Entry 1 shows 2 mol% HFB relative to initiator, which is the native amount of alcohol in this batch of catalyst; none has been added. Repetition of this experiment in the presence of 30 equivalents of HFB decreases k_p/k_i to 1800, or, stated another way, the relative rate of initiation increases by a factor of 4.6. As little as one equivalent of HFB increases the relative rate of initiation to nearly the same degree, but excess was typically used to ensure maximal enhancement. The lithium alkoxide of HFB ($LiOC(CH_3)(CF_3)_2$, HFB-Li) also increases the relative rate initiation and to an even greater degree, as shown in Entries 3 and 4. In the presence of 0.9 equivalents of HFB-Li, k_p/k_i is 1900, and in the presence of excess HFB-Li (20 equivalents), k_p/k_i decreases to 930, a relative initiation rate increase of 8.9-fold.

The effect of HFB on k_p/k_i for the polymerization of COE by **1a** is shown in Table 1, Entries 6 and 7. Without adding HFB, the degree of initiation is below the limit of detection by NMR spectroscopy, so we are only able to set an upper limit of initiation: 0.5%. This results in a k_p/k_i value of 5×10^6 or greater. The overall rate of

polymerization is also slower than the previous cases, 28 min, as a result of the low level of initiation. In the presence of 30 equivalents of HFB, the relative rate of initiation increases dramatically, by a factor of 10^3 (k_p/k_i = 2700), and propagation is complete within 5 min.

In contrast to COD and COE polymerizations, ROMP of NBE in the presence of several equivalents HFB does not show a marked decrease in k_p/k_i. Entries 9-12 of Table 1 shows that large amounts HFB seem to have a *random* effect on NBE initiation and propagation rates.

The differences in magnitude of the alcohol effect on NBE, COD, and COE initiation rates can be explained by considering the amount of monomer ring strain. The major driving force for ROMP is the release of energy upon the relief of monomer ring strain.[1] Thus, highly strained monomers such as cyclobutene will polymerize rapidly, while low strain monomers such as cyclohexene do not undergo productive metathesis.[1,28] Monomer ring strain decreases as follows: NBE > COD > COE (the -ΔH values for conversion of liquid monomer to solid polymer have been measured to be 62, 25-33, and 13 kJ/mol, respectively).[1,29] The magnitude of the alcohol effect on relative rates of initiation increases with decreasing monomer ring strain. *That is, the alcohol effect is larger for low strain cyclic olefins.* Presumably, the timescale of HFB interaction with the catalyst is faster than the rate of COD polymerization and much faster than the rate of COE polymerization, resulting in a larger effect. However, the rate of NBE ROMP must be so fast that the alcohol is unable to compete, resulting in a negligible effect on rates.

Table 1. k_p/k_i Measurements for the ROMP of COD, COE, and NBE initiated by **1a**.

entry	monomer	equ. HFB	monomer equ.	k_p/k_i	solvent	% initiation
1	COD	0.02	30	8300	C_6D_6	7.9
2	COD	> 30	30	1800	C_6D_6	17
3	COD	0.02[a]	70	1900	C_6D_6	25
4	COD	0.02[b]	70	930	C_6D_6	33
5	COD	0.02	90	$> 5 \times 10^6$	THF/C_6D_6[c]	< 0.5[d]
6[e]	COE	0.05	70	$> 5 \times 10^6$	C_6D_6	< 0.5[d]
7	COE	> 30	70	2700	C_6D_6	21
8[f]	COE	0.05	80	$> 5 \times 10^6$	THF/C_6D_6[c]	< 0.5[d]
9	NBE	0.02	50	6800	C_6D_6	12
10	NBE	0.02	50	2400	C_6D_6	19
11	NBE	> 30	50	3900	C_6D_6	15
12	NBE	> 30	100	2600	C_6D_6	27
13	NBE	0.3	50	140	THF/C_6D_6[c]	63

[a]Instead of HFB, 0.9 equivalents of $LiOC(CH_3)(CF_3)_2$ (HFB-Li) was used. [b]Instead of HFB, 20 equivalents of HFB-Li was used. [c] Solvent mixture of 25-50% THF-d_8 in C_6D_6. [d] The degree of initiation was below the detection level of ^{1}H NMR, so an upper level of 0.5% is assumed. [e] This reaction took 28 min to reach completion. [f] This reaction took 3.3 hours to reach 88% completion.

While the failure of HFB to enhance the relative rates of initiation for high strain monomers may seem disappointing at first, recall that a convenient method for such enhancements has previously been reported as mentioned above: addition of Lewis bases. Table 1, Entry 13 shows that THF dramatically decreases k_p/k_i for NBE polymerization to 140. Contrarily, Entries 5 and 8 show that for COD and COE polymerizations, THF *increases* k_p/k_i, which is opposite to the effect of HFB. HFB and THF nicely compliment each other for relative initiation enhancement for a variety of monomers.

k_p and k_i Measurements in 3,4,6-trichloro-5-octylbenzobarrelene ROMP

Though HFB has resulted in the enhanced relative initiation rate of low strain monomers, initiation is still incomplete and typically less than 40% when close to 100

equivalents of monomer are used (Table 1). Because of this low degree of initiation, polydispersity is broad for all cases; PDI ≈ 2. Examining the kinetics of a monomer that initiated completely would allow us to gain more information about this system, and evaluate k_p *and* k_i, rather than just k_p/k_i: Once initiation is complete, propagation, Equation 2, is the only reaction occurring, and k_p may be determined from the integrated rate equation, Equation 4. k_p/k_i may be calculated as before (Equation 3), and from these two values, k_i may be deduced.

$$\ln\left(\frac{M}{M_0}\right) = -k_p \cdot IM \cdot dt \qquad (4)$$

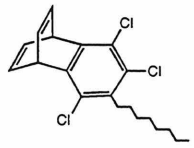

3Cl-BB

Figure 5. 3,4,6-trichloro-5-octyl benzobarrelene

If no HFB is added in the ROMP of 50 equivalents of 3,4,6-trichloro-5-octylbenzobarrelene (**3Cl-BB**) by **1a** in C_6D_6 at room temperature, the reaction takes two days to reach completion (Table 2, Entry 1). The slow polymerization is somewhat advantageous, in that we are able to monitor initiation and conversion by ^1H NMR. Unlike polymerizations of COD, COE, and NBE, initiation *does* reach completion well before the propagation is complete. Addition of only one equivalent of HFB to the reaction solution cuts both the reaction time and the initiation time in half to 1 day and 16 hours, respectively (Entry 2). Five equivalents of HFB further decreases both times several-fold (Entry 3). Higher levels of HFB—10, 15, 50 equivalents—continue to

decrease initiation and reaction times, but not as dramatically, to 1 hour for initiation and 5 hours for complete conversion.

With this monomer, we are able to evaluate the effect of HFB on k_p and k_i individually for the first time. Previously we did not know if the k_p/k_i decrease was a result of a k_i increase, a k_p decrease, or if they were both being altered. What we immediately learn from the data in Table 2 is that addition of HFB causes both k_p and k_i to increase. k_p increases by a factor of 2-3 each time as the concentration of HFB is increased from zero to one equivalent, then to five, then to 10 equivalents, then levels off (Entries 1-4). The maximum value of 35×10^{-3} $M^{-1}s^{-1}$ is obtained with 15 equivalents of HFB. The initial change in k_i is more dramatic: Upon the addition of one equivalent of HFB, k_i increases by a factor of 7.5, then by a factor of three, then two as HFB is increased further to five then 10 equivalents. Like k_p, k_i levels of at 10 equivalents of HFB, but has its maximum value in the presence of 15 equivalents, 3.7×10^{-3} $M^{-1}s^{-1}$.

As the amount of HFB is increased from zero to 50 equivalents, the ratio k_p/k_i decreases rapidly, then levels out (Table 2). k_p/k_i decreases by a factor of four, from 47 to 12, upon the addition of just one equivalent of HFB. Although the variation in k_p/k_i is small upon further addition of HFB, we know that k_p and k_i still increase several-fold, but they do so nearly proportionally.

PDI values also respond favorably to increased rates of initiation and propagation. Without the addition of HFB, the PDI is 5.83 (Table 2, Entry 1). This is much broader than expected considering that initiation reaches completion before propagation does. Because of the long reaction time, there is probably some catalyst termination, leading to

Table 2. k_p, k_i, and k_p/k_i measurements for the ROMP of **3Cl-BB** by initiator **1a** with varying degrees HFB present.

entry	equ. HFB	reaction time	initiation time	k_p/k_i	k_p (x 10^{-3} $M^{-1}s^{-1}$)	k_i (x 10^{-3} $M^{-1}s^{-1}$)	PDI	$\overline{M_n}$ (x 10^{-3})
1	0.02	2 days	16 hr	47	3.2	0.069	5.83	6.7
2	1	1 day	8.0 hr	12	6.4	0.52	1.49	11.1
3	5	9 hr	2.5 hr	11	16	1.4	1.98	10.2
4	10	6 hr	1.4 hr	9.7	31	3.2	1.58	11.0
5	15	6 hr	~1.4 hr	9.5	35	3.7	1.30	11.3
6	50	5 hr	1.0 hr	9.9	31	3.1	1.31	14.8

Attempts to Explain the Mechanism of the Alcohol Effect

Early on in this work, it was suggested that HFB might be acting to increase the rate of initiation in the same way as mentioned above for Lewis bases, which we know now to be untrue. Upon examining this, we found that HFB does not bind to catalysts such as **1a** even when as many as 50 equivalents excess of HFB are in solution. This conclusion is based on the failure of the ^{1}H NMR alkylidene signal of **1a** (12.13 ppm, singlet, C_6D_6 solvent) to shift upon addition of the alcohol. A wide variety of Lewis bases are known to alter the alkylidene chemical shift by ~1 ppm (upfield or downfield) upon binding, and this shift is quite diagnostic.[30] Coincidental identical chemical shifts of the HFB-bound and –unbound species can be ruled out because ^{19}F analysis reveals that the ligand symmetry of the **1a** does not change in the presence of HFB. Low temperature NMR analysis is unable to detect fluctional HFB binding down to –93 °C. Also, it is unlikely that HFB participates in hydrogen bonding to **1a** (one might expect the nitrogen or oxygens to be hydrogen bond acceptors). The hydroxyl NMR chemical shift of HFB (1.66 ppm, C_6D_6 solvent) is very sensitive to the polarity of its environment, but does not change in the presence of one equivalent of **1a**.

Molybdenum and tungsten alkylidenes of the type shown in Figure 1 exist as an equilibrium mixture of *syn* and *anti* isomers (Figure 6).[19] Equilibrium favors the *syn* isomer in almost all cases, and for **1a**, the *syn/anti* ratio is 1400.[31] However, work by Schrock and coworkers show that the *anti* isomer of **1a** is actually approximately two orders of magnitude more active than the *syn*. We have considered that HFB might be activating these initiators by acting as a catalyst to lower the energy barrier to *syn* $\leftrightarrow$ *anti* isomerization. Decreasing this barrier could result in enhanced activity by accelerating

the time it takes to replenish the depleted level of *anti* alkylidenes after they react with monomer.[32]

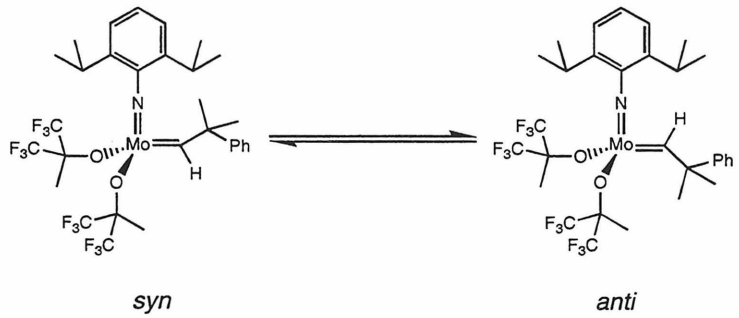

Figure 6. *syn* ↔ *anti* isomerization of molybdenum alkylidenes.

In light of these issues, we became interested in determining if HFB alters the barrier to *syn* ↔ *anti* isomerization of **1a**. This can be accomplished by measuring the observed rate constants of *anti* → *syn* isomerization (Equation 5, Figure 6) in the presence of HFB at various temperatures, and calculating $\Delta G^{\ddagger}$ from the Eyring equation (Equation 6).[33] Preliminary experiments showed that indeed, HFB did increase the rate of isomerization at low temperatures.

$$\frac{d[\text{anti}]}{dt} = -k[\text{anti}] \tag{5}$$

$$\ln\left(\frac{k}{T}\right) = -\frac{1}{T}\frac{\Delta H^{\ddagger}}{R} + \frac{\Delta S^{\ddagger}}{R} + 23.8 \tag{6}$$

Although the alkylidene resonance of the *anti* isomer of **1a** is hardly observable by ^{1}H NMR at room temperature, its concentration may be increased to ~15% by photolysis at –50 °C or lower for six hours as reported by Schrock and coworkers.[31] At this temperature, isomerization back to the *syn* isomer after photolysis is negligible over several hours.

Figure 7 shows the plot of ln[anti] versus time at –12, –19, and -37 °C, and Table 3 shows the observed rate constants for *anti* → *syn* isomerization measured at these temperatures in the presence of 1.6 equivalents HFB and toluene solvent. Figure 8 shows the Eyring plot of this data and compares it with kinetic data collected by Schrock and coworkers in the absence of HFB.[31] The activation parameters obtained are shown in Table 4, revealing that the activation energies of *anti* → *syn* isomerization are the same with and without HFB present; $\Delta G^{\ddagger}$ = 19 kcal/mol. Thus *syn* ↔ *anti* isomerization is likely not responsible for the initiation enhancements.

The enthalpy of activation ($\Delta H^{\ddagger}$) for *anti* → *syn* isomerization decreases significantly in the presence of HFB. The entropy of activation is a large negative value in the presence of HFB ($\Delta S^{\ddagger}$ = -24 cal mol^{-1} T^{-1}) indicating that the transition state becomes significantly more ordered during isomerization. It is interesting to note that in

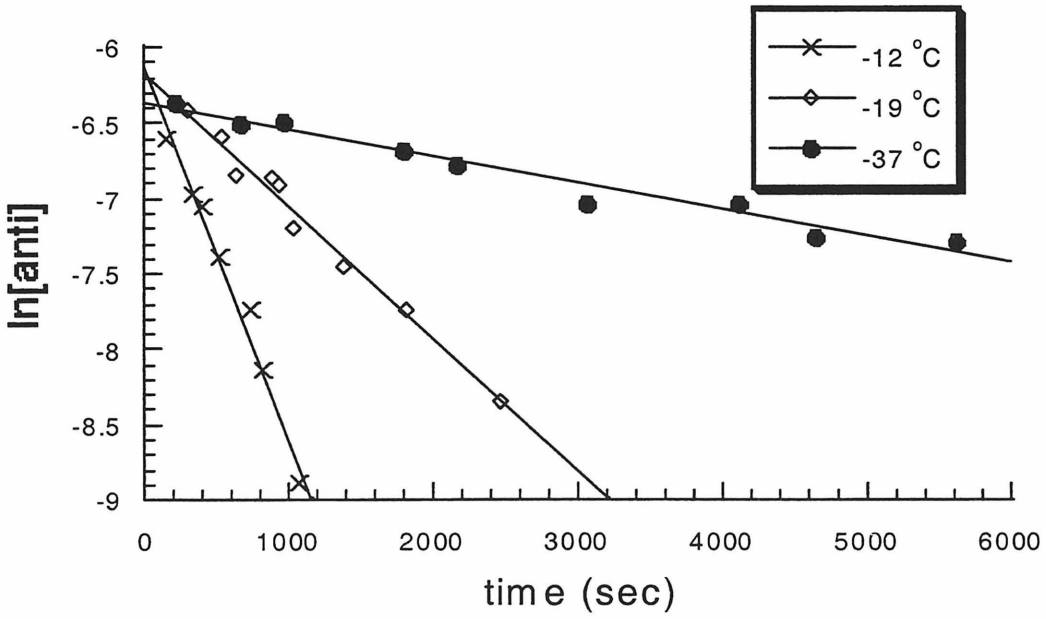

Figure 7. Plots of ln[*anti*] vs. time used to determine rate constants of *anti* → *syn* isomerization at various temperatures.

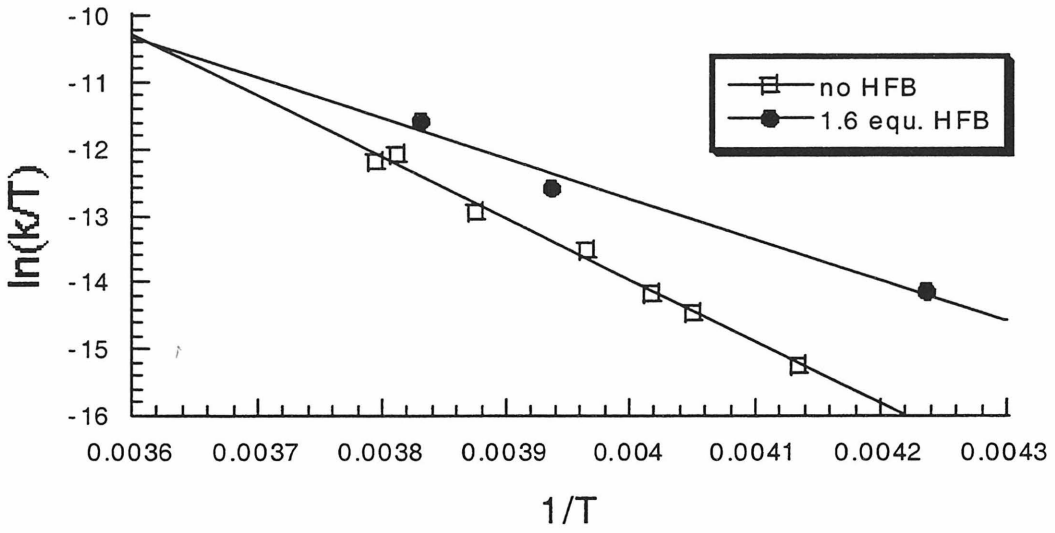

Figure 8. Eyring plot for *anti* → *syn* isomerization with and without the presence of HFB.

a coordinating solvent such as THF, Schrock and coworkers report a large positive $\Delta S^{\ddagger}$ (21 cal mol^{-1} T^{-1}), again indicating the opposite effect of HFB and lewis bases on catalysts such as **1a**.

Table 3. Rate constants for the *anti* → *syn* isomerization of the alkylidene ligand of **1a** in the presence of 1.6 equivalents of HFB, in toluene-d_8, at various temperatures.

temp (°C)	$k_{anti \rightarrow syn}$ ($M^{-1}s^{-1}$)
-12	2.45×10^{-3}
-19	8.63×10^{-4}
-37	1.70×10^{-4}

Table 4. Activation parameters for the rotation of the alkylidene ligand of **1a**.

	$\Delta H^{\ddagger}$ (kcal/mol)	$\Delta S^{\ddagger}$ (cal/mol·T)	$\Delta G^{\ddagger}$ (kcal/mol)
no HFB[31]	18.3	-2	18.8
THF solvent[31]	29.8	21	23.4
1.6 equ. HFB	12	-24	19

We have also been able to demonstrate that HFB affects the *syn* ↔ *anti* isomerization rates of Lewis base adducts of **1**. As Lewis base binding may be used as a model for olefin binding in these systems, the results may be relevant to metathesis

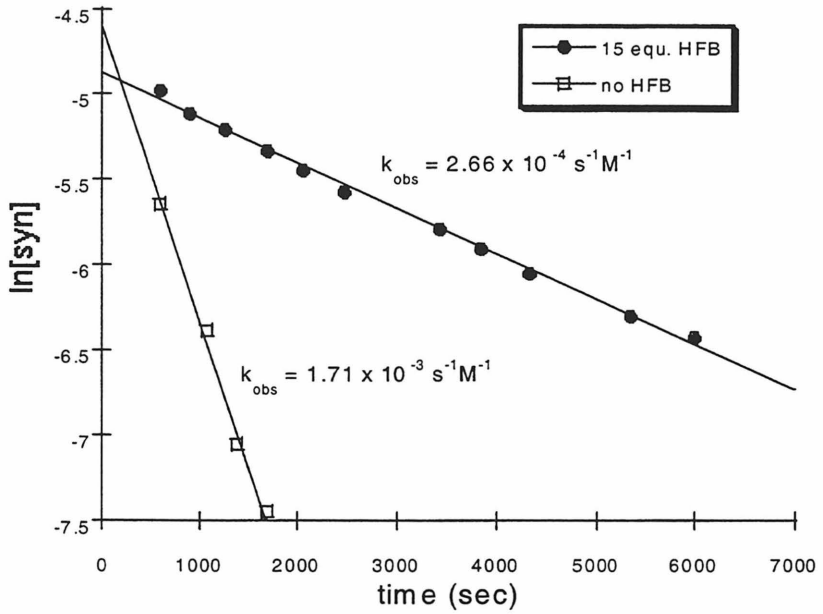

Figure 9. Plots of ln[*syn* carbene] vs. time for the *syn* → *anti* isomerization of **1a** in the presence of 10 equivalents of $P(OMe)_3$ either with or without HFB.

activity. Previous studies have shown that many small Lewis bases such as PMe_3, $P(OMe)_3$, pyridine, and nitriles bind to the *syn* alkylidene as the kinetic product and slowly isomerize to the *anti* analog.[30,39] We have been able to quantitate that 15 equivalents of HFB slows the rate of *syn* → *anti* isomerization of **1a**, when $P(OMe)_3$ is bound, by an order of magnitude from 1.71 x 10^{-3} $M^{-1}s^{-1}$ to 2.66 x 10^{-4} $M^{-1}s^{-1}$ at room temperature in C_6D_6 (Figure 9).

Reactivity of 1 with Acids

Through magnetization transfer experiments,[34,35,36] we have confirmed that HFB in solution slowly exchanges with metal-bound alkoxides of complexes **1**, **2**, and **3** (see Experimental section for details). We have considered that there might be a cationic intermediate of high activity during this exchange that is responsible for the increased initiation rates observed in the presence of HFB (Figure 10). To further investigate the

significance of a possible cationic intermediate, we attempted to synthesize stable cationic molybdenum alkylidenes by, protonating off an alkoxide, and comparing its initiation and propagation rates to those of neutral species. However, the reaction with 1-1.3 equivalents of *p*-toluenesulfonic acid with **1a** in C_6D_6 yielded 5-10 new alkylidene species evidenced by ^1H NMR in the 13.1 to 15.5 ppm range, even when THF or $P(OMe)_3$ stabilizing ligands were present. The multiple products could be a result of *syn/anti* isomers and differing coordination geometries of 5-coordinate complexes. Reaction with one equivalent triflic acid in C_6D_6 also produced many alkylidene complexes from 14.2 to 15.7 ppm, while 1.8 equivalents led to rapid decomposition in the presence of $P(OCH_3)_3$.

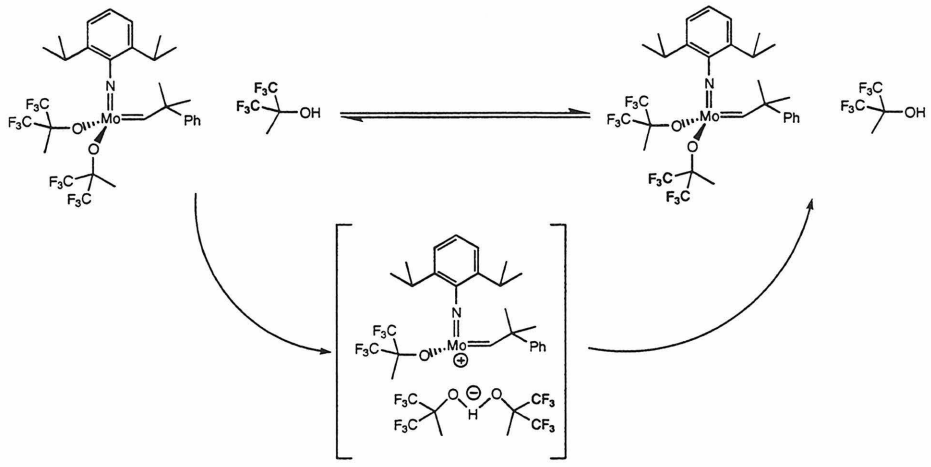

Figure 10. Alcohol/alkoxide exchange and possible cationic intermediate.

Addition of 1 equivalent of trifluoroacetic acid to **1a** immediately produces a 50:50 mixture of **1a** and the biscarboxylate complex **7a** cleanly, indicated by their ^1H NMR carbene resonances at 12.13 and 14.99 ppm, respectively (Table 5, Figures 11-13). The products and product distributions are stable for hours at room temperature. The monoalkoxide-monocarboxylate species **5a** is not observed, either because it is not formed, or more likely, because it disproportionates to **1a** and **7a**.[37] Addition of a second

equivalent of trifluoroacetic acid to the solution gives complete conversion to **7a** cleanly and quantitatively (Figures 12-13). Addition of much more than two equivalents trifluoroacetic acid to **1a** leads to rapid decomposition. Attempts to isolate **7a** were unsuccessful; perhaps the carboxylates are not bulky enough to protect the complex from bimolecular decomposition.[38] When **7a** is synthesized *in situ*, it is able to ROMP 100 equivalents of COD to greater than 95% completion in two hours at room temperature.

Table 5. ^{1}H NMR alkylidene chemical shifts of alkylidene complexes **5-7** resulting from addition of one equivalent of carboxylic acid to catalysts **1a-b**.

catalyst	R [a]	bisalkoxide [b]	alkoxide/ carboxylate [c]	biscarboxylate [d]
1a	CF_3	12.12 (50%)[e]	**5a**, (0%)	**7a**, 14.99 (50%)
1a	Ph	12.12 (13%)	**5b**, 13.20 (74%)	**7b**, 14.34 (13%)[f]
1a	CH_3	12.12 (23%)[g]	**5c**, 13.12 (54%)	**7c**, 14.11 (23%)
1b	CF_3	11.68 (48%)	**6a**, 13.08 (4%)	**7a**, 14.99 (48%)
1b	Ph	11.68 (30%)	**6b**, 12.91 (40%)	**7b**, 14.34, 14.86 (30%)[h]
1b	CH_3	11.68 (25%)	**6c**, 12.79 (50%)	**7c**, 14.11 (25%)
1b	*p*-NO_2Ph	11.68 (19%)[i]	**6c**, 12.97 (62%)	**7d**, 14.37, 14.74 (19%)[j]

[a] Substituent of RCOOH. [b] Chemical shift and abundance of starting alkylidene **1a** or **1b**. [c] Chemical shift and abundance of **5** or **6**. [d] Chemical shift and abundance of **7**. [e] In parentheses is shown the percent of each alkylidene present. [f] When a second equivalent of benzoic acid is added, two alkylidene signals are observed for **7b** at 14.86 ppm and 14.34 ppm, corresponding to ***anti*-7b** and ***syn*-7b**, respectively, in a 1:3 ratio. [g] The relative amounts of alkylidenes are only estimates as slightly more than one equivalent of acetic acid was added. [h] The signals at 14.86 ppm and 14.34 ppm correspond to ***anti*-7b** and ***syn*-7b** and are observed in a 1:3 ratio. [i] The relative amounts of alkylidenes are only estimates as slightly less than one equivalent of nitrobenzoic acid was added. [j] The signals at 14.74 ppm and 14.37 ppm correspond to ***anti*-7d** and ***syn*-7d**, respectively, and are observed in a 1.33:1 ratio.

Interestingly, the reaction of other carboxylic acids with catalysts **1** gave different products in widely product distributions. Reaction of benzoic acid with **1a** yielded three

rather than two alkylidene products: starting material (**1a**), the biscarboxylate compound **7b**, and the "intermediate" alkoxide/carboxylate complex **5b** (Table 5, Figure 14). Although the alkoxide/carboxylate complex **5a** was not observed by ^{1}H NMR when trifluoromethylacetic acid was used, the alkoxide/carboxylate complex **5b** is much more abundant (74%) than **1a** or **7b** (both 13%) when benzoic acid is used. The products are formed rapidly (less than 10 minutes) and the product distribution is stable for hours at room temperature. The ^{1} NMR alkylidene resonance of **7b** (14.34 ppm) is the farthest downfield of the three, and the alkylidene chemical shift of **5b** (13.20 ppm) is intermediate. Addition of a second equivalent of benzoic acid converts the mixture completely to **7b**. Two ^{1}H NMR alkylidene resonances are observed for **7b** when it is in pure form, but not when in a mixture with **1a** and **5b**. They occur at 14.86 ppm and 14.34 ppm and probably correspond to the *anti* and *syn* alkylidenes, respectively, in a 1:3 ratio. The resonance at 14.86 ppm was assigned as ***anti*-7b** partially because the *anti* alkylidene is nearly always farther downfield than the *syn* isomer.[31,39]

The addition of acetic acid to **1a** results in the formation of molybdenum alkoxide/carboxylate complex **5c** and the biscarboxylate complex **7c** with alkylidene chemical shifts (13.12 ppm and 14.11 ppm, respectively) comparable to the previous

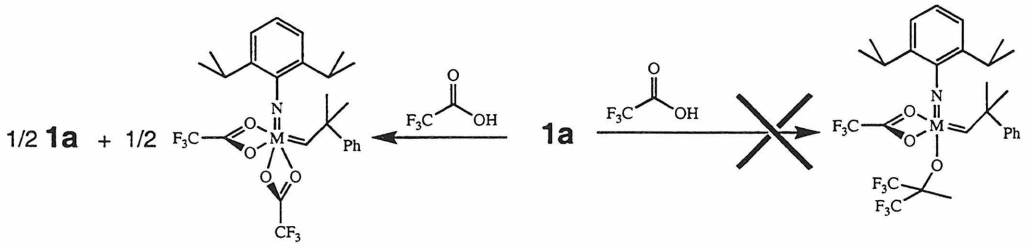

Figure 11. Reaction of **1a** with trifluoroacetic acid. The biscarboxylate complex **7a** is formed, but the alkoxide/carboxylate complex **5a** is not produced.

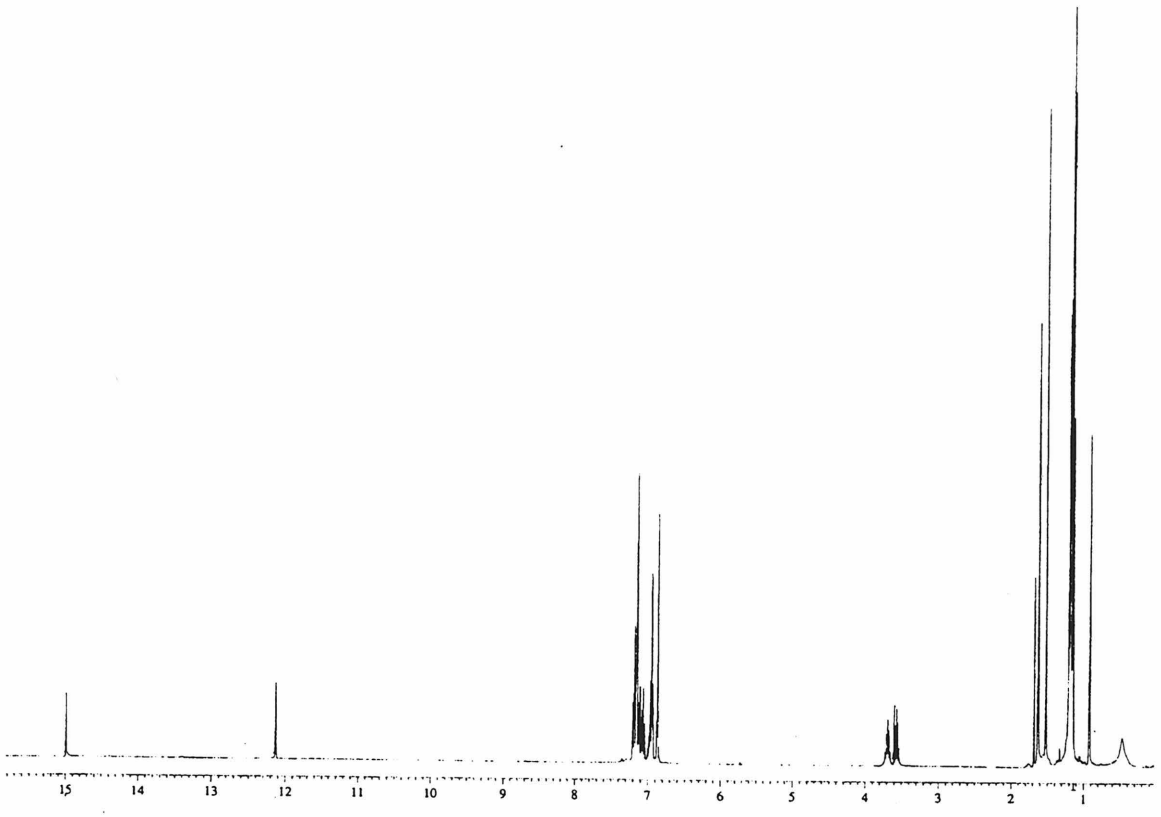

Figure 12. ^{1}H NMR spectrum of 50:50 mixture of **1a** (alkylidene signal, 12.13 ppm) and **7a** (alkylidene signal, 14.99 ppm) resulting from addition of one equivalent of trifluoroacetic acid to **1a**.

compounds (Table 5). Addition of a second equivalent of acetic acid resulted in full conversion to **7c**, and only one isomer was observed (presumably the *syn* isomer).

Similar but enlightening results were observed when carboxylic acids were reacted with catalyst **1b**. When **1b** was reacted with 1 equivalent of trifluoroacetic acid, the biscarboxylate complex **7a** was formed in 48% along with the alkoxide/carboxylate complex **6a** which was not observed with **1a** (Table 5, Figure 14). The amount of **6a** (alkylidene ^{1}H NMR resonance at 13.08 ppm) was low, 4%, but the fact that it was observed and **5a** was not suggests that $(CF_3)Me_2CO$- is better at stabilizing the alkoxide/carboxylate complex than is $(CF_3)_2MeCO$-.

Reaction of **1b** with benzoic acid produces **1b**, the alkoxide/carboxylate complex

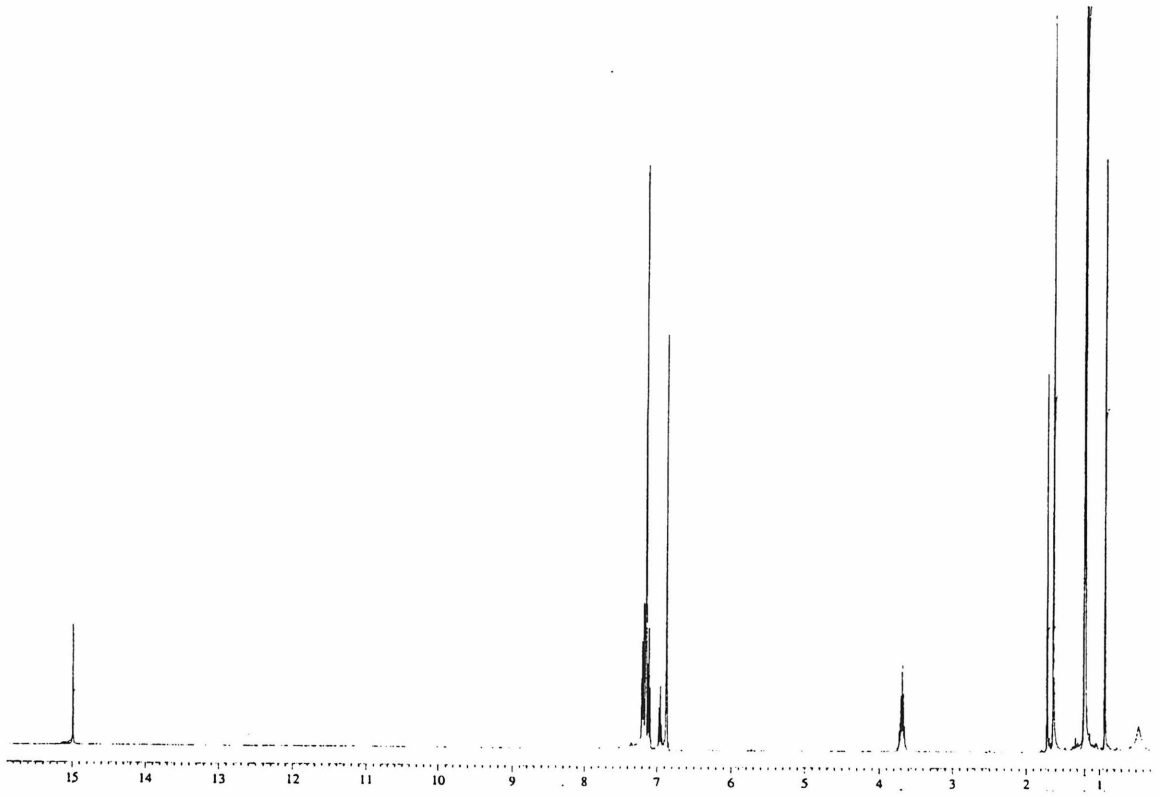

Figure 13. ^{1}H NMR spectrum of **7a** resulting from the addition of two equivalents of trifluoroacetic acid to **1a**.

6b, and the biscarboxylate complex **7b** in a 30%:40%:30% distribution, respectively (Table 5). The alkylidene ^{1}H NMR chemical shift of **6b** (12.91 ppm) is intermediate to **1b** and **7b**. As in the case of reaction of benzoic acid with **1a**, the alkoxide/carboxylate complex is most abundant. Unlike the case of reaction with **1a**, both *syn* and *anti* isomers of **7b** are observed in the presence of **1b** and **6b**. The collective content of ***anti-*** and ***syn-*** **7b** is 30% and the relative ratio is 1:3 as observed above. The ratio is maintained when the mixture is converted fully to **7b** by the addition of a second equivalent of benzoic acid.

Addition of one equivalent of acetic acid to **1b** interestingly produces a statistical mixture of **1b**, **6c**, and **7c**, 25%:50%:25% (Table 5). Reaction of one equivalent of *p*-nitrobenzoic acid with **1b** produces, besides the alkoxide/carboxylate complex **6d**, *syn*

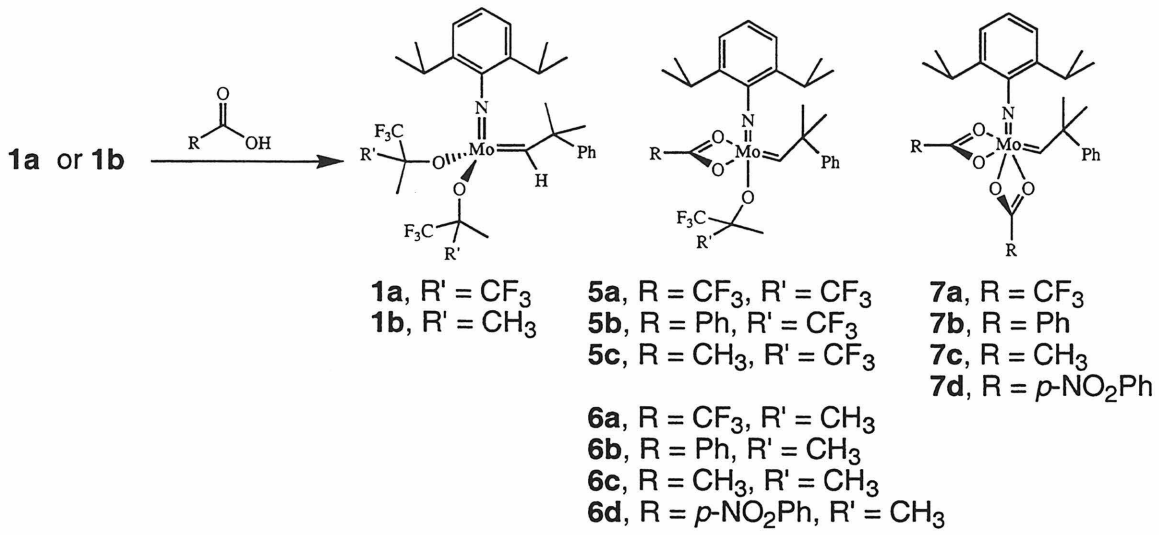

Figure 14. Reaction of carboxylic acids with catalysts **1a** or **1b** and formation of alkoxide/carboxylate complexes **5** or **6** and biscarboxylate complexes **7**.

and *anti* isomers of the biscarboxylate complex **7d**. Interestingly, the downfield alkylidene NMR resonance of **7d** (14.74 ppm), presumably the *anti* isomer, is in greater abundance (57%) than the upfield resonance and presumably *syn* isomer (14.37 ppm, 43%). It is unusual that the *anti* isomer would be in greater abundance, but not rare, especially when a fifth ligand is bound to the metal center.

This group of experiments shows that multiple products are accessible from protonation of alkylidenes **1** and **2**, and that exclusive protonation of the alkoxides and ligand exchange is most likely.

Compound **7a** was treated with Lewis bases such as THF and 1,2-dimethoxyethane (DME) in order to generate cationic complexes such as **8a** and **8b** (Figure 15). However, this was unsuccessful, as the carboxylates were bound too tightly to be displaced by ethers, even with mild heating. We attempted to generate a cationic molybdenum alkylidene **9** with a much weaker coordinating counterion by treating **1a** with the lewis acid $B(C_6F_5)_3$ in the presence of five equivalents of DME as a stabilizing

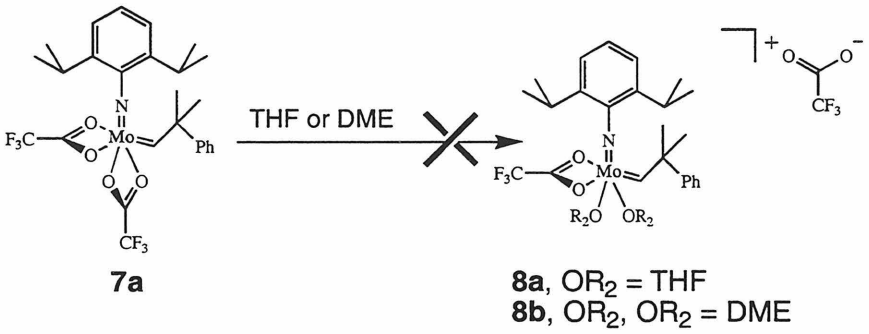

Figure 15. Attempted synthesis of cationic molybdenum alkylidenes.

base, in CD_2Cl_2 as shown in Figure 16. However, $B(C_6F_5)_3$ was too bulky to abstract an alkoxide, and no reaction was observed. From these experiments, we have learned that there is greater likelihood of generating a cationic molybdenum alkylidene by reaction of **1** with a Bronsted acid, and that one that is more weakly coordinating than carboxylates should be used.

Preliminary results show that there is little or no alcohol-induced rate enhancement in ring-closing metathesis (RCM).[40] However, since the molybdenum and tungsten catalyst resting state in RCM is a metallacyclobutane rather than an alkylidene, the mechanism of HFB involvement may be altered.

It is unlikely that an impurity in the HFB is responsible for the alcohol effect. Support for this is based on the observation that HFB and the alkoxide HFB-Li affect rate enhancements of the same scale. And it is highly unlikely that an impurity present in liquid HFB, which is purified by vacuum transfer from a drying agent, is also present in solid HFB-Li, which is purified by washing with pentane then drying under high vacuum. Furthermore we have used different batches of HFB to the same degree of success.

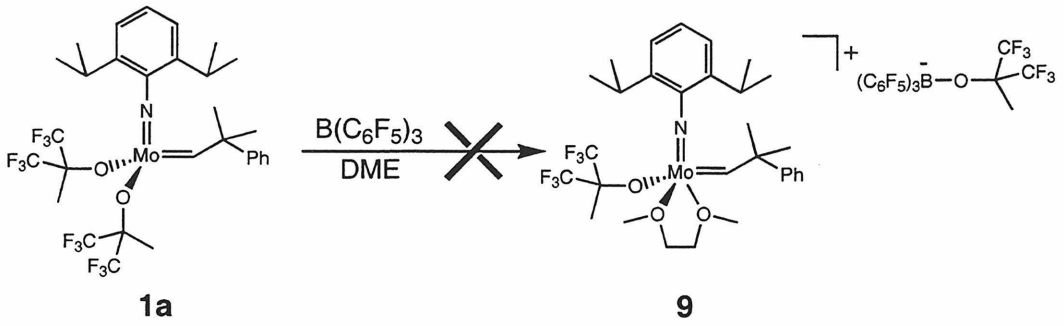

Figure 16. Attempted synthesis of cationic molybdenum alkylidenes using $B(C_6F_5)_3$.

Acknowledgments

I would like to thank Jérôme Claverie for initiating this project, giving me direction during my early months in the Grubbs group, and teaching me many experimental techniques in organometallic and polymer chemistry. The intellectual assistance and advice of Dr. Eric L. Dias was incredibly valuable in many little ways, and I would like to thank him for always taking the time to help. I would also like to thank Dr. Mike Wagaman for discussions and experimental suggestions regarding the alcohol effect and Dr. Shojiro Kaita for conducting the k_p, k_i, and k_p/k_i measurements for the ROMP of **3Cl-BB**. This research was generously supported by grants from NSF and NIH, I think.

Experimental

General Considerations. All manipulations of air- and/or water-sensitive compounds were performed using standard high-vacuum or Schlenk techniques in an argon atmosphere purified by passage through BASF R3-11 catalyst (Chemalog) and 4-Å molecular sieves (Linde), or carried out under nitrogen in a Vacuum Atmospheres dry box equipped with MO-40-1 purification catalyst. NMR spectra[41] were recorded with either a QE-300 Plus (300.10 MHz ^{1}H; 75.49 MHz ^{13}C) spectrometer, a JEOL GX-400

(399.65 MHz ^{1}H; 376.01 MHz ^{19}F; 100.50 MHz ^{13}C), or a Brucker AM 500 (500.14 MHz ^{1}H; 470.56 MHz ^{19}F; 125.76 MHz ^{13}C). All coupling constants are reported in Hz. All ^{1}H and ^{13}C chemical shifts are reported in ppm downfield from tetramethylsilane (TMS) and referenced to residual protons in the solvent or TMS. ^{19}F spectra were referenced externally to a $CFCl_3$ sample. Photolysis was achieved with a 450 W medium-pressure mercury Hanovia lamp using a filter for $\lambda_{max,ex}$=362 nm. Gel permeation chromatograms were obtained on an HPLC system using an Altex Model 110A pump, a Rheodyne Model 7125 injector with a 100 mL injection loop, two American Polymer Standards 10 mm mixed bed columns, and a Knauer differential refractometer detector using CH_2Cl_2 as eluent at a 1.0 mL/min flow rate.

Materials. Benzene, benzene-d_6, tetrahydrofuran (THF), ether, toluene, and hexane were degassed by bubbling a stream of argon through the solvents and dried by passage through solvent purification columns.[42] Pentane was dried in the same fashion or was stirred over concentrated H_2SO_4 to remove olefins, dried over $MgSO_4$ and CaH_2, transferred onto sodium-benzophenone ketyl solubilized with tetraglyme, and then vacuum transfered. Toluene-d_8, THF-d_8, and 1,2-dimethoxyethane (DME) were dried over sodium-benzophenone ketyl, vacuum transferred, then degassed by three continuous freeze-pump-thaw cycles. Methylene chloride-d_2, *cis,cis*-1,5-cyclooctadiene, and *cis*-cyclooctene was dried over CaH_2, vacuum transferred or distilled, then degassed by three continuous freeze-pump-thaw cycles. Hexafluoro-*t*-butanol was dried over activated $MgSO_4$, vacuum transferred, and degassed by three freeze-pump-thaw cycles. Norbornene was dried over sodium, vacuum transferred, and stored in the dry box at -30°C. A fresh supply of $P(OMe)_3$ was degassed, filtered through activated alumina, and

stored under nitrogen. *p*-Toluenesulfonic acid was recrystallized from water and dried *in vacuo* at 100 °C, triflic acid was used as received (in an ampule opened in a nitrogen dry box), benzoic acid and *p*-nitrobenzoic acid were dried *in vacuo*, acetic acid was dried over $KMnO_4$, and trifluoroacetic acid and $B(C_6F_5)$ were used as received. All other chemicals were obtained from Lancaster Synthesis, Inc.; Aldrich Chemical Co.; or Strem Chemicals, Inc. Alkylidenes **1a**,[21a] **1b**,[43] and **3**,[22] and **3Cl-BB**[44] were prepared as previously reported.

k_p/k_i Measurements. k_p/k_i for a polymerization with incomplete initiation may be calculated using Equation 3 where I_o is the initial initiator concentration, I is the final initiator concentration, M_o is the initial monomer concentration, and M is the final monomer concentration.[25,26] A representative example will be given. In the dry box a 0.0249 M solution made from 0.0069 g (0.0105 mmol) **1a** in 0.42 mL C_6D_6 was prepared in an NMR tube and 0.020 mL (0.158 mmol, 15 equivalents) $HOC(CH_3)(CF_3)_2$ was added. The NMR tube was capped with a rubber septum, as was a vial containing a 2.89 M solution of COD in C_6D_6. The catalyst solution was checked by NMR, then 0.11 mL (30 equ.) of the COD solution was added via a gastight syringe to the NMR tube followed by vigorous shaking to ensure mixing. Analysis by ^1H NMR was made within 5 min to ensure the polymerization was complete, and to measure I/I_0, then k_p/k_i was calculated. ^1H NMR alkylidene chemical shifts of the propagating species for polymerization of COD, 12.56 ppm (multiplet); COE, 12.55 ppm (multiplet); NBE, 12.42 ppm (broad). In the presence of THF the chemical shifts of the propagating species for NBE was 12.84 ppm (doublet). The standard deviation in k_p/k_i measurements was 20-40%, partly due to the difficulty of mixing rapidly reacting reagents in an NMR tube.

Independent Measurement of k_p and k_i. Before initiation is complete, k_p/k_i can be calculated as mentioned above at multiple times and the values averaged. After initiation is complete, k_p may be calculated from Equation 4 as outlined in the text.[33]

General Procedure for Benzobarrelene Polymerizations. A 0.11 mL aliquot from a 0.00452 M stock solution of **1a** (0.0038 g, 0.00497 mmol) was added to a solution of 0.0927 g (0.250 mmol, 50 equ.) benzobarrelene in 0.6 mL C_6D_6. If HFB was used, it was added just prior to addition of monomer. Reactions were monitored by ^{1}H NMR. The chemical shift of the propagating species for polymerization was at 11.90 ppm (br). Reactions were terminated by the addition of degassed benzaldeyde, followed by precipitation of the polymer into degassed methanol and washing twice. The polymers were stored under nitrogen, as they are somewhat oxygen sensitive.

Photolysis Experiments and k_{obs} Measurements for *anti*→*syn* Alkylidene Isomerization. A representative example will be given. In a nitrogen-filled dry box 0.15 mL of a 0.0649 M stock solution of **1a** (0.00973 mmol) was diluted to 0.70 mL with toluene-d_8, and 0.0019 mL (0.0154 mmol) HFB was added. This was placed in a teflon-sealed NMR tube. After obtaining a ^{1}H NMR spectrum, the tube was cooled to –60 °C with a heptane/liquid nitrogen cold bath in a clear glass dewar. A high pressure mercury lamp, filtered for maximum emission at 362 nm, was used to photolize the solution for 4 hr. The solution was immediately frozen in liquid nitrogen and inserted into the precooled -70° C NMR probe[45] and equilibrated for at least 10 minutes before acquisition of spectra. The ratio of *anti:syn* alkylidene (13.28 ppm and 12.13 ppm, respectively) was found to be 1:6. *Anti*→*syn* isomerization was very slow at this temp, so the spectrometer probe was heated to -37° C, equilibrated for 10 min, then analyzed spectroscopically

every 10 min until the *anti* signal decayed fully. The observed rate constant for *anti*→*syn* isomerization, k_{obs}, was calculated from the equation $\ln(A_t) = -k_{obs}t + \ln(A_o)$ where A_t is the concentration of *anti* isomer at time t and A_o is its concentration at time zero. Activation parameters were calculated from the Erying equation (Equation 6) using observed rate constants obtained at different temperatures.

Mo(CHCMe$_2$Ph)(N-2,6-C$_6$H$_3$^{i}Pr$_2$)(OOCCF$_3$)$_2$ (5). In the dry box **1a** (0.0132 g, 0.020 mmol) was dissolved in 0.60 mL C_6D_6 followed by addition of one equivalent CF_3COOH (0.0015 mL, 0.02 mmol). The solution became slightly darker over minutes. ^{1}H NMR was taken after 30 minutes and showed a 50:50 mixture of **1a** and **5** and one equivalent of HFB. ^{1}H NMR of **1a**: δ 12.13 (s, 1, Mo=C*H*), 7.3-6.85 (m, 8, Ar*H*), 3.58 (heptet, 2, Ar(CH(CH_3)$_2$)$_2$), 1.54 (s, 6, OC(CH_3)(CF$_3$)$_2$), 1.18 (d, 12, Ar(CH(CH_3)$_2$)$_2$), 1.17 (s, 6, Mo=C(H)C(Ph)(CH_3)$_2$); ^{1}H NMR of **5**: δ 14.99 (s, 1, Mo=C*H*), 7.3-6.85 (m, 8, Ar*H*), 3.69 (heptet, 2, Ar(C*H*(CH$_3$)$_2$)$_2$), 1.63 (s, 6, Mo=C(H)C(Ph)(CH_3)$_2$), 1.20 (d, 12, Ar(CH(CH_3)$_2$)$_2$); ^{1}H NMR of HFB: δ 1.72 (s, 1, *H*OC(CH$_3$)(CF$_3$)$_2$), 0.93 (s, 3, HOC(CH_3)(CF$_3$)$_2$). ^{19}F NMR: δ -74.645 (s, *F*$_3$CCO$_2$[Mo]), -78.01 (s, (C*F*$_3$)$_2$MeCO[Mo]), -79.26 (s, HOCMe(C*F*$_3$)$_2$). Addition of an additional 1.1 equivalents CF_3COOH (0.0017 mL, 0.022 mmol) gave full conversion to **5** and the release of a second equivalent HFB. Attempted isolation led to decomposition.

Reaction of 1a with Acids. The same general procedure outlined in the previous paragraph was followed for reacting **1a** with other carboxylic acids, *p*-toluenesulfonic acid, and triflic acid. THF and $P(OMe)_3$ stabilizing ligands may have been added either before or after the acid. Most of these reactions led to a mixture of carbene complexes evidenced by ^{1}H NMR.

General Procedure for Alcohol Exchange Rate Measurements. Magnetization transfer (inversion spin transfer) experiments were used to study the following equilibrium,

$$A \underset{k_{-1}}{\overset{k_1}{\rightleftharpoons}} B$$

where A is metal-bound hexafluoro-*t*-butoxide and B is free HFB. **1a** (0.007 g) was dissolved in C_6D_6 along with 0.9 equivalents HFB. A room temperature 470.56 MHz ^{19}F NMR spectrum with spectral width from -35,718.30 Hz (-75.90 ppm) to -37,695.62 Hz (-80.01 ppm) showed two singlet resonances at -78.009 ppm (**1a**) and -79.262 ppm (HFB). The pulse sequence for the spin inversion and aquisition was: $\pi/2_x(\nu_A)$-τ_1- $\pi/2_{\pm x}$-τ_2-$\pi/2_{\pm x\pm y}$-acquisition, where $\pi/2$ is a 90° pulse (11 μs) for the resonance at ν_A, ν_A is the frequency of the downfield resonance, $\tau_1 = 1/(2|\nu_A - \nu_B|) = 0.848$ μs, ±x and ±y refer to the rotating frame axis along which the rf irradiation is applied, and τ_2 is a variable delay.[46] After each acquisition a delay time of greater than 5 * T_1 (40 s) was observed to allow all nuclei to relax to their equilibrium positions before repeating the pulse sequence with a new τ_2. Twenty spectra were taken, each with a slightly greater τ_2 than the one before ranging from 0.0001 sec to 40 sec. Other references[35,36] show how to fit this data to the Bloch equations modified to include the effects of chemical exchange and extract rate constants k_1 and k_{-1}. The ^{19}F T_1 values of **1a** and HFB must be known and were measured independently to be 1.08 sec and 5.77 sec, respectively.

References and Notes

1. Ivin, K. J.; Mol, J. C. *Olefin Metathesis and Metathesis Polymerization*; Academic Press: San Diego, 1997.

2. (a) Moore, J. S.; Gorman, C. B.; Grubbs, R. H. *J. Am. Chem. Soc.* **1991**, *113*, 1704. (b) Gorman, C. B.; Gingburg, E. J.; Grubbs, R. H. *J. Am. Chem. Soc.* **1993**, *115*, 1397.

3. Conticello, V. P.; Gin, D. L.; Grubbs, R. H. *J. Am. Chem. Soc.* **1992**, *114*, 9708.

4. Wagaman, M. W.; Grubbs, R. H. *Macromolecules*, **1997**, *30*, 3978.

5. (a) Maughon, B. R.; Weck, M.; Mohr, B.; Grubbs, R. H. *Macromolecules*, **1997**, *30*, 257. (b) Weck, M.; Mohr, B.; Maughon, B. R.; Grubbs, R. H. *Macromolecules*, **1997**, *30*, 6430.

6. Maughon, B. R.; Grubbs, R. H. *Macromolecules*, **1996**, *29*, 5765.

7. (a) Hillmyer, M. A.; Grubbs, R. H. *Macromolecules*, **1995**, *28*, 8662. (b) Hillmyer, M. A.; Nguyen, S. T.; Grubbs, R. H. *Macromolecules*, **1997**, *30*, 718.

8. Bellmann, E.; Shaheen, S. E.; Thayumanavan, S.; Barlow, S.; Grubbs, R. H.; Marder, S. R.; Kippelen, B.; Peyghambarian, N. *Chem. Mater.* **1998**, *10*, 1668.

9. Fraser, C.; Grubbs, R. H. *Macromolecules*, **1995**, *28*, 7248.

10. Marsella, M. J.; Maynard, H. D.; Grubbs, R. H. *Angew. Chem. Int. Ed. Engl.* **1997**, *36*, 1101.

11. (a) Schueller, C. M.; Manning, D. D.; Kiessling, L. L. *Tetrahedron Lett.* **1996**, *37*, 8853. (b) Mann, D. A.; Kanai, M.; Maly, D. J.; Kiessling, L. L. *J. Am. Chem. Soc.* **1998**, *120*, 10575.

12. (a) Grubbs, R. H.; Tumas, W. *Science* **1989**, *243*, 907. (b) Schrock, R. R. *Acc. Chem. Res.* **1990**, *23*, 158.

13. (a) Schwab, P.; Grubbs, R. H.; Ziller, J. W. *J. Am. Chem. Soc.* **1996**, *118*, 100. (b) Schwab, P.; France, M. B.; Ziller, J. W.; Grubbs, R. H. *Angew. Chem., Int. Ed. Engl.* **1995**, *34*, 2039.

14. Maughon, B. R.; Grubbs, R. H. *Macromolecules*, **1997**, *30*, 3459.

15. (a) Mohr, B.; Lynn, D. M.; Grubbs, R. H. *Organometallics*, **1996**, *15*, 4317. (b) Lynn, D. M.; Mohr, B.; Grubbs, R. H. *J. Am. Chem. Soc.* **1998**, *120*, 1627.

16. (a) Korshak, Y. V.; Korshak, V.; Kansichka, G.; Hocker, H. *Makromol. Chem., Rapid Commun.* **1985**, *6*, 685. (b) Ginsburg, E. J.; Gorman, C. B.; Marder, S. R.; Grubbs, R. H. *J. Am. Chem. Soc.* **1989**, *111*, 7621.

17. (a) Tasch, S.; Graupner, W.; Leising, G.; Pu, L.; Wagaman, M. W.; Grubbs, R. H. *Adv. Mater.* **1995**, *7*, 903. (b) Pu, L.; Wagaman, M. W.; Grubbs, R. H. *Macromolecules* **1996**, *29*, 1138.

18. Schrock, R. R.; Luo, S.; Lee, J. C., Jr.; Zanetti, N. C.; Davis, W. M. *J. Am. Chem. Soc.* **1996**, *118*, 3883.

19. Feldman, J.; Schrock, R. R. *Prog. Inorg. Chem.* **1991**, *39*, 1.

20. Schrock, R. R.; DePue, R. T.; Feldman, J.; Yap, K. B.; Yang, D. C.; Davis, W. M.; Park, L.; DiMare, M.; Schofield, M.; Anhaus, J.; Walborsky, E.; Evitt, E.; Kruger, C.; Betz, P. *Organometallics*, **1990**, *9*, 2262.

21. (a) Schrock, R. R.; Murdzek, J. S.; Bazan, G. C.; Robbins, J.; DiMare, M.; O'Regan, M. *J. Am. Chem. Soc.* **1990**, *112*, 3875. (b) Oskam, J. H.; Fox, H. H.; Yap, K. B.; McConville, D. H.; O'Dell, R.; Lichtenstein, B. J.; Schrock, R. R. *J. Organomet. Chem.* **1993**, *459*, 185.

22. Johnson, L. K.; Grubbs, R. H.; Ziller, J. W. *J. Am. Chem. Soc.* **1993**, *115*, 8130.

23. Johnson, L. K.; Frey, M.; Ulibarri, T. A.; Virgil, S. C.; Grubbs, R. H.; Ziller, J. W. *J. Am. Chem. Soc.* **1993**, *115*, 8167.

24. Claverie, J. P., Ph.D. Thesis, California Institute of Technology, 1995.

25. Gold, L. *J. Chem. Phys.* **1958**, *28*, 91.

26. Benedicto, A. D.; Claverie, J. P.; Grubbs, R. H. *Macromolecules*, **1995**, *28*, 500.

27. In Equations 1 and 2, I is the concentration of initiator and IM_n is the concentration of propagating alkylidene.

28. For strain energy calculations of various cyclic olefins, please see (a) Allinger, N. L.; Sprague, J. T. *J. Am. Chem. Soc.* **1972**, *94*, 5734. (b) Schleyer, P. v. R.; Williams, J. E.; Blanchard, K. R. *J. Am. Chem. Soc.* **1970**, *92*, 2377.

29. (a) Lebedev, B.; Smirnova, N.; Kiparisova, Y.; Makovetsky, K. *Makromol. Chem.* **1992**, *193*, 1399. (b) Lebedev, B.; Smirnova, N. *Macromol. Chem. Phys.* **1994**, *195*, 35.

30. Schrock, R. R.; Crowe, W. E.; Bazan, G.; DiMare, M.; O'Regan, M. B.; Schofield, M. H. *Organometallics* **1991**, *10*, 1832.

31. (a) Oskam, J. H.; Schrock, R. R. *J. Am. Chem. Soc.* **1993**, *115*, 11831. (b) Oskam, J. H.; Schrock, R. R. *J. Am. Chem. Soc.* **1992**, *114*, 7588.

32. It is important to note that *syn* and *anti* alkylidenes react with monomers to form new *syn* alkylidenes (Ref. 31). So every time an *anti* alkylidene undergoes metathesis, the concentration of the *anti* isomers decreases. The rate at which this equilibrium is reestablished could be crucial to k_p/k_i.

33. Wilkins, R. G. *Kinetics and Mechanism of Reactions of Transition Metal Complexes*; VCH: Weinheim, 1991.

34. Sandström, J. *Dynamic NMR Spectroscopy*; Academic Press: New York, 1982.

35. Robinson, G.; Kuchel, P. W.; Chapman, B. E. *J. Mag. Res.*, **1985**, *63*, 314.

36. Robinson, G.; Chapman, B. E.; Kuchel, P. W. *Eur. J. Biochem.* **1984**, *143*, 643

37. Feast, W. J.; Gibson, V. C.; Marshall, E. L. *J. Chem. Soc., Chem. Commun.* **1992**, 1157.

38. Shattenmann, F. J.; Schrock, R. R.; Davis, W. M. *J. Am. Chem. Soc.* **1996**, *118*, 3295.

39. Elder, D. L.; Grubbs, R. H., unpublished results.

40. Tested by ring-closing diethyl diallylmalonate with **1a**.

41. The following reference was used for help with NMR spectra interpretation: Silverstein, R. M.; Bassler, G. C.; Morrill, T. C. *Spectrometric Identification of Organic Compounds*, 5th ed., John Wiley & Sons: New York, 1991; pp 165-265.

42. Pangborn, A. B.; Giardello, M. A.; Grubbs, R. H.; Rosen, R. K.; Timmers, F. J. *Organometallics* **1996**, *15*, 1518.

43. (a) Schrock, R. R.; DePue, R. T.; Feldman, J.; Schaverien, C. J.; Dewan, J. C.; Liu, A. H. *J. Am. Chem. Soc.*, **1988**, *110*, 1423-1435. (b) Schrock, R. R.; DePue, R. T.; Feldman, J.; Yap, K. B.; Yang, D. C.; Davis, W. M.; Park, L.; DiMare, M.; Schofield, M.; Anhaus, J.; Walborsky, E.; Evitt, E.; Krüger, C.; Betz, P. *Organometallics*, **1990**, *9*, 2262-2275.

44. (a) Wagaman, M. W.; Bellmann, E.; Grubbs, R. H. *Phil. Trans. R. Soc. Lond. A* **1997**, *355*, 727. (b) Wagaman, M. W.; Grubbs, R. H. *Synth. Met.* **1997**, *84*, 327.

45. Spectrometer probe temperature was calibrated with methanol.

46. τ_2 is the delay time between inversion of the two resonances and aquisition. That is, the the amount of time magnitization transfer can occur before aquisition.

Chapter 2

Introduction to Conjugated Polymers in LEDs

Introduction to Conjugated Polymers in LEDs

Since the discovery of electroluminescence in organic polymers in 1990, research into the synthesis of semiconductor, conjugated polymers and their incorporation into light-emitting diodes (LEDs) has grown tremendously.[1] Many conjugated polymers conveniently have a HOMO-LUMO energy gap that provides luminescence in the visible wavelengths. Initially, poly(*p*-phenylenevinylene)[32] (PPV) was the conjugated polymer most popularly investigated, and more recently poly(*p*-phenyleneethynylene)s,[2,3] poly(thiophene)s, poly(*p*-phenylene)s, and poly(fluorene)s have received much attention (Figure 1).[4,5,6,7,8]

A schematic diagram of a simple LED is shown in Figure 2. An LED is a layered device—each layer approximately 100 nm thick—in which a luminescent semiconductor is sandwiched between two electrodes. When a large enough voltage is applied across

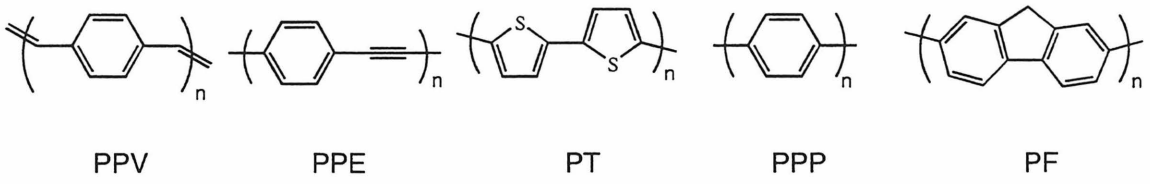

Figure 1. Popular families of conjugated polymers for luminescence applications: poly(*p*-phenylenevinylene) (PPV), poly(*p*-phenyleneethynylene), poly(thiophene) (PT), poly(*p*-phenylene) (PPP), poly(fluorene) (PF).

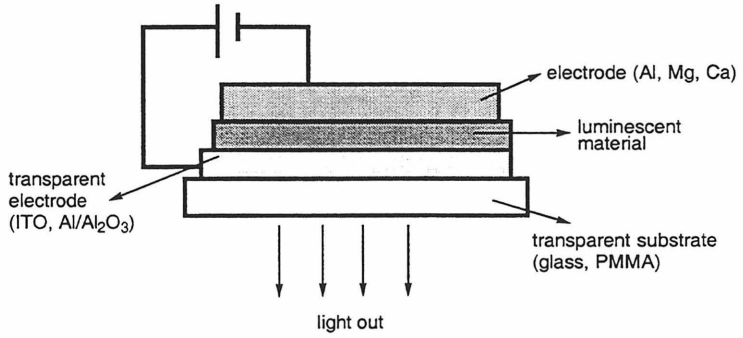

Figure 2. Schematic diagram of a simple LED.

the electrodes, luminescence occurs.[6,9] One of the electrodes should be transparent so that the light can be observed; this it typically the anode, which is usually indium tin oxide (ITO). The cathode is typically a compound with a low ionization potential (work function) such as calcium, aluminum, or magnesium. During LED fabrication, the luminescent material is deposited onto ITO-coated glass (commercially available) by spin casting from solution or vacuum deposition for small molecules. The metal cathode is then vacuum deposited on top. To protect the reactive metal from oxidation, it is often coated a thick (1000 nm) layer of a more inert metal such as silver or coated in air-impermeable epoxy.

Electroluminescence can be compared to photoluminescence, for in both, light is given off by radiative relaxation of a triplet excited state (often called exitons when

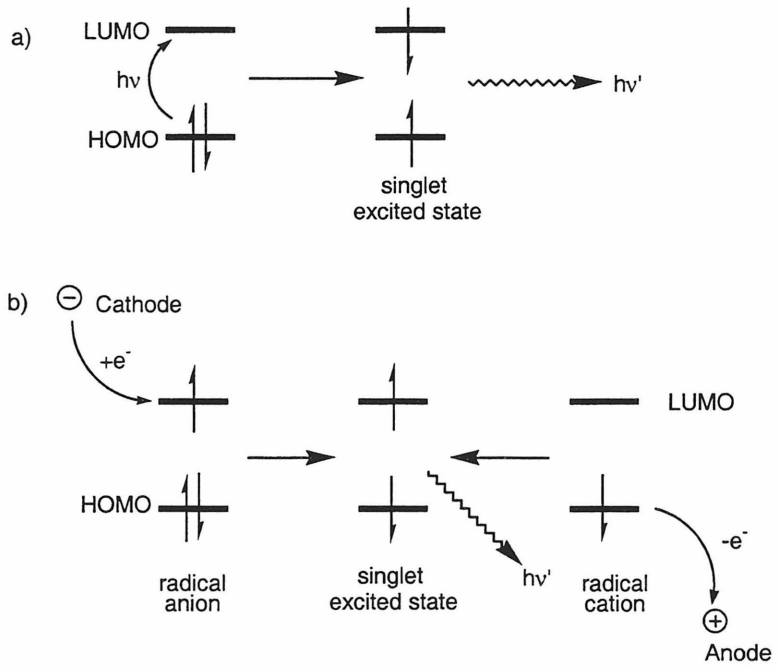

Figure 3. a) Photoluminescence: irradiation (hν) excites an electron from the HOMO to LUMO energy level to form an excited state. Luminescence occurs from the same molecule, but at a longer wavelength hν' due the Stoke's shift. b) Electroluminescence: Electrons are injected into the LUMO by the cathode, and holes into the HOMO by the anode. The charges migrate from one molecule to another until they meet in the same molecule. The result is the formation of the same excited state achieved by photoluminescence, followed by emission.

referring to conjugated polymers and solid state materials) to a singlet ground state (Figure 3).[6] The major difference is how the excited state is formed. In photoluminescence, excitation results in direct formation of the excited state (Figure 3a). In electroluminescence, charge injection at the electrode surfaces results in formation of radical cations or anions (often called positive or negative polarons in conjugated polymers) (Figure 3b). It is important to realize that the polarons are formed in different molecules. The electrons injected from the cathode migrate by electron hopping to the positively charged anode, and the holes[10] formed at the anode migrate to the cathode. Ideally the rates of migration of electrons and positive charges (holes) should be nearly the same; the ability to transport charge and the rates of transport are extremely important. Eventually the positive and negative polarons collide—combine in the same molecule—forming an excited state identical to that formed in photoluminescence. If the rates of electron and hole migration are widely different, it is likely that recombination will take place at one of the electrode surfaces, rather than within the emissive material, resulting in fluorescence quenching .[8,11]

The scientific community has been very excited about the use of conjugated polymers as the emissive component in LEDs because they offer a number of potential advantages over liquid crystal (LC) displays, cathode ray tube (CRT) displays, and LEDs based on inorganic emitters.[4,9] People have envisioned displays for televisions or laptop computers in which each pixel is an LED with a polymeric emitter. These "plastic LEDs" are expected to be thin, lightweight, and flexible so that one could unroll it like a projector screen or carry it around like a poster and hang it on the wall to show video with the brightness and quality of current televisions.[12] This is still quite a futuristic

dream, but it is believed that organic emitters rather than the inorganic semiconductor materials used in current commercial LEDs will be necessary to fulfill the physical properties requirements. Besides being lightweight and flexible conjugated polymers have the advantage of being able to be fabricated over a large area considerably cheaper than one could fabricate a crystalline inorganic phosphor. As long as the polymer is soluble, it may be readily spin cast into a film of high uniformity over large areas during LED fabrication,[1b] whereas the equipment and power cost of fabricating a single-crystalline inorganic film by evaporative vapor deposition over a large area is very expensive. A third potential advantage to using polymer LEDs is that the power consumption is less than that of LC displays. Also, LED displays are expected to have better large-angle viewing than LC displays of, for example, laptop computers. A fifth selling point often brought up is that the color of emission, adhesion, thermal behavior, and other properties, may be more rationally altered in conjugated polymers—by electron-donating or -withdrawing substituents and varying the molecular weight for example—than in inorganic phosphors. In order to create a full-color display, sharp red, green, and blue LED pixel elements are necessary for color mixing to achieve a full-color display. Alternatively, white LEDs—emitting over the entire visible spectrum—have been fabricated and are valuable because any wavelength can be selected by color filtering. Finally it should be mentioned that polymeric emitters are favored over small molecules[13] because small molecules tend to crystallize over time forming spacial gaps which act as luminescence quenching sites.

Two of the main challenges facing LED fabrication with polymers are increasing the emission quantum yield[14] and increasing the operation lifetime/stability.[5]

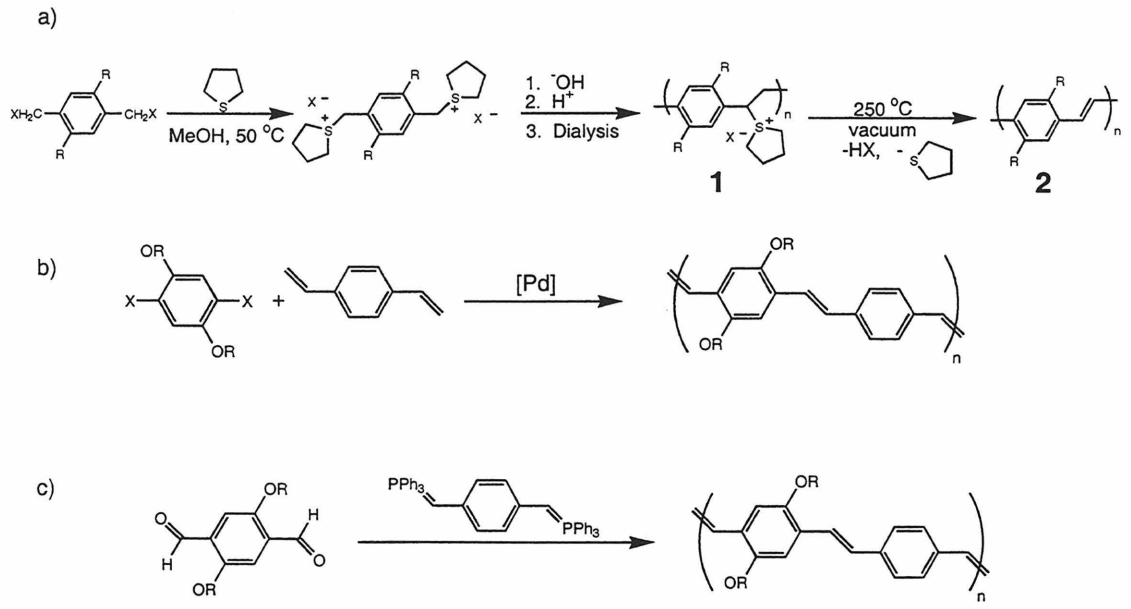

Figure 4. Shown here are the most common PPV synthesis routes. a) Halogen precursor route; b) palladium-catalyzed Heck coupling; c) Wittig-type coupling.

Nevertheless polymer LEDs are starting to appear on the market and are expected to have a bright future. Chapter 4 will present some of our efforts regarding the development of a general method to increase luminescence quantum yields of polyarylenevinylenes.

Though the development of new conjugated polymers presented in the next two chapters is directed mainly toward LEDs, there are some other applications that these materials and other PPV derivatives may be ideal for. These include materials for light-emitting electrochemical cells (LECs),[15] photovoltaics,[16,17,18] highly conductive polymers upon doping,[19] lasers,[20,21,22] nonlinear optical materials,[23] and light-harvesting/artificial photosynthesis systems.[24,25,26]

There are three different PPV synthesis routes that are commonly employed. The first one to be utilized for LED polymers is the halogen-elimination route or halogen percursor route (Figure 4a).[1b,6] In the first step of this three step procedure, a bis(α-halomethyl)-benzene is reacted with a thioether to form a water-soluble sulfonium salt. Treatment with base induces polymerization and elimination of one equivalent of

thioether to form the water-soluble polymer **1**. This polymer may be cast into a film (on ITO coated glass for LED fabrication) and heated to 250 – 300 °C for 10 hours under vacuum, eliminating thioether and HX, resulting in fully conjugated polymer **2** in good yields and good film uniformity. If R is a long alkyl chain, **2** is typically soluble in organic solvents and films may be spin cast *after* synthesis.

The second method has become equally as popular as the halogen precursor route. It is a palladium catalyzed Heck reaction and is an excellent way to prepare alternating copolymers (Figure 4b).[6,27,28,29] The third method, Witting-type coupling, may also be used to prepare alternating copolymers, but has been utilized less-frequently (Figure 4c).[30,31,32]

From a polymer synthesis point of view, one disadvantage these three methods share is that the polymer molecular weight obtained is difficult to control. This is important because, although the emissive properties of polymers do not change beyond a threshold of about 10 repeat units, many physical properties such as elasticity and modulus *are* molecular weight dependent. These properties may certainly be important for polymer processing, important if the LEDs are deposited on flexible substrates, or operate in environments with large temperature variations.

Our group has developed a synthesis method for PPV, poly(naphthalenevinylene) (PNV), and their derivatives in which excellent molecular weight control can be achieved.[33,34,35] Molecular weight control is achieved by ring-opening metathesis polymerization (ROMP,[36] Figure 5), which is a living polymerization procedure[37] for many monomers including those which lead to PPVs and PNVs.[34] Since there is no chain transfer and no chain termination in a living polymerization, each initiator produces one

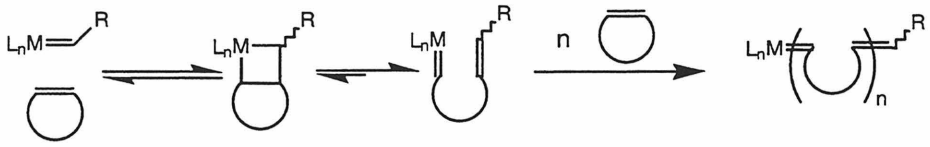

Figure 5. General ROMP reaction. A metal alkylidene reacts in a [2+2] fashion with the double bond of a cyclic olefin forming an intermediate metallacyclobutane which undergoes a retro [2+2] cycloaddition resulting in chain extension and a new alkylidene. The new alkylidene continues to consume monomer and elongate the polymer.

polymer chain, and increasing the monomer/catalyst ratio linearly increases the polymer molecular weight.

Our method of PPV synthesis, the ROMP-aromatization route, is a two step procedure involving ROMP of a barrelene[38] monomer[39] **3** initiated by a transition metal alkylidene **4**, followed by aromatization with an oxidant such as DDQ (Figure 6). The reaction conditions are quite mild and proceed at room temperature.[40] The barrelene may be functionalized with functional groups R to influence the solubility of the polymer and whose electronic contribution may alter the HOMO and LUMO energy levels, rationally controlling the color of emission.[41,42,43]

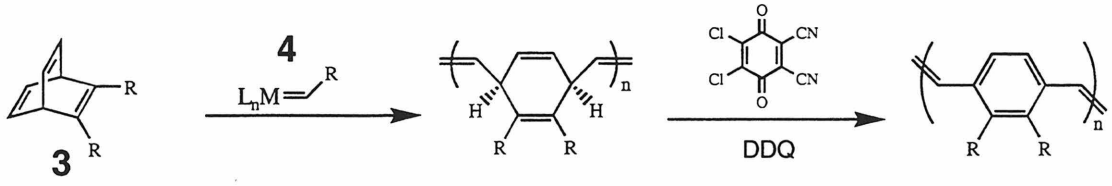

Figure 6. ROMP-Aromatization route to PPV synthesis. After the polymerization step, the initiator is quenched to cleave the metal from the polymer and terminate the catalyst.

It is notable that the ROMP-aromatization route to PPVs places substituents in the 2 and 3 positions on the phenyl ring (Figure 6) while the PPV synthetic methods mentioned above (Figure 4) typically situate the substituents in the 2 and 5 positions. Thus ROMP-Aromatization PPVs are novel and may have slightly different degrees of twisting, which leads to different conjugation lengths, different solubilities, differences in

solid state packing, and possibly different efficiencies and emission lifetimes. This reason along with the ability to make polymers with greater control (such as block copolymers) are the major reasons we have undertaken the investigation of emissive polymers and believe that we can discover some interesting and useful data to drive this field forward.

Figure 7 shows the complete list of PPVs and PNVs that had been synthesized by the time the work reported in the next two chapters of this thesis was begun.[33,34,39,41,42,43]

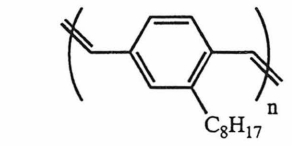

$\lambda_{max,em}$=495 nm
film = 535 nm

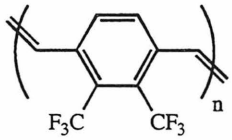

$\lambda_{max,em}$=449 nm (20%)
film = 458 nm

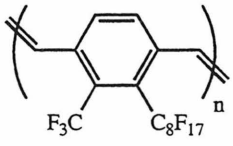

$\lambda_{max,em}$=443 nm[a] (65%)
film = 465 nm

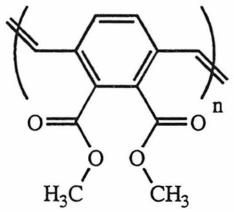

$\lambda_{max,em}$=479 nm (33%)

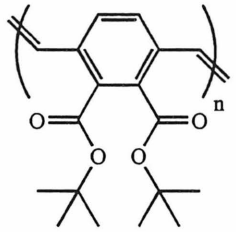

$\lambda_{max,em}$=479 nm (~100%)
film = 553 nm

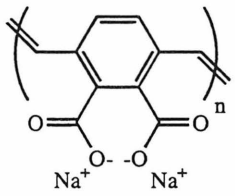

$\lambda_{max,em}$=491 nm[b] (16%)

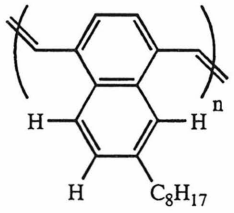

$\lambda_{max,em}$=561 nm (0.5%)
film = 593 nm

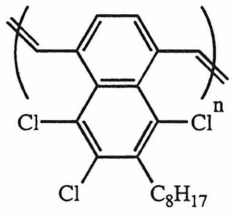

$\lambda_{max,em}$=569 nm (14%)
film = 570 nm

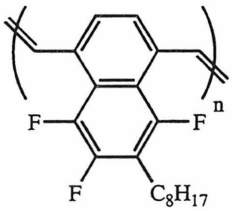

$\lambda_{max,em}$=568 nm (0.05%)

Figure 7. PPVs and PNVs produced by the ROMP-Aromatization route along with photoluminescence λ_{max} values in solution and of films. Quantum yields are reported in parentheses (referenced relative to $Ru(bpy)_3Cl_2$). Measurements are made in $CHCl_3$ solutions unless otherwise noted. [a] Solvent is C_6F_6. [b]Solvent is 0.1 N NaOH (aq.).

References and Notes

1. a) Partridge, R. H. *Polymer* **1983**, *24*, 755. b) Burroughes, J. H.; Bradley, D. D. C.; Brown, A. R.; Marks, R. N.; Mackay, K.; Friend, R. H.; Burn, P. L.; Holmes, A. B. *Nature* **1990**, *347*, 539.

2. Yang, J. S.; Swager, T. M. *J. Am. Chem. Soc.* **1998**, *120*, 11864.

3. Weder, C.; Wrighton, M. S. *Macromolecules* **1996**, *29*, 5157.

4. Sheats, J. R.; Antoniadis, H.; Hueschen, M.; Leonard, W.; Miller, J.; Moon, R.; Roitman, D.; Stocking, A. *Science* **1996**, *273*, 884.

5. Dodabalapur, A. *Solid State Commun.* **1997**, *102*, 259.

6. Kraft, A.; Grimsdale, A. C.; Holmes, A. B. *Angew. Chem., Int. Ed.* **1998**, *37*, 402.

7. Kido, J. *Trends Poly. Sci.* **1994**, *2*, 350.

8. Bradley, D. D. C. *Chem. Brit.* **1991**, *27 (8)*, 719.

9. Lovinger, A. J. *J. Mater. Res.* **1996**, *11*, 3174.

10. The term "hole" refers to the absence of an electron. That is, when an electron is removed from a molecule, a positive charge called a hole is left behind.

11. This is somewhat of an oversimplification because in electroluminescence either singlet *or* triplet excited states may be formed, but only singlet states emit efficiently.

12. Gustafsson, G.; Cao, Y.; Treacy, G. M.; Klavetter, F.; Colaneri, N.; Heeger, A. J. *Nature* **1992**, *357*, 477.

13. This introduction will not focus on small molecules used as emissive materials for LEDs, but shall highlight polymer fluorophores.

14. Electroluminescence quantum yield is defined here as the ratio of the number of photons emitted to the number of electron injected.

15. a) Pei, Q.; Yu, G.; Zhang, C.; Yang, Y.; Heeger, A. J. *Science* **1995**, *269*, 108. b) Pei, Q.; Yang, Y.; Yu, G.; Zhang, C.; Heeger, A. J. *J. Am. Chem. Soc.* **1996**, *118*, 3922.

16. Yu, G.; Zhang, C.; Heeger, A. J. *Appl. Phys. Lett.* **1994**, *64*, 1540.

17. Yu, G.; Heeger, A. J. ***1995***, 78, 4510.

18. Halls, J. J. M.; Walsh, C. A.; Greenham, N. C.; Marseglia, E. A.; Friend, R. H.; Moratti, S. C.; Holmes, A. B. *Nature* **1995**, *376*, 498.

19. (a) Lee, C. E.; Oh, D. K.; Jin, J. I.; Nam, B. K. *Synth. Met.* **1995**, *69*, 425. (b) Ahlskog, M.; Reghu, M.; Noguchi, T.; Ohnishi, T. *Synth. Met.* **1997**, *89*, 11.

20. Hide, F.; Schwartz, B. J.; Diaz-Garcia, M. A.; Heeger, A. J. *Chem. Phys. Lett.* **1996**, *256,* 424.

21. Berggren, M.; Dodabalapur, A.; Slusher, R. E.; Bao, Z. *Synth. Met.* **1997**, *91,* 65.

22. Berggren, M.; Dodabalapur, A.; Slusher, R. E.; Bao, Z. *Nature* **1997**, *389*, 466.

23. a) Yoon, C. B.; Shim, H. K. *J. Mater. Chem.* **1998**, *8*, 913. b) Klarner, G.; Former, C.; Martin, K.; Rader, J.; Mullen, K. *Macromolecules* **1998**, *31*, 3571.

24. Prathapan, S.; Johnson, T. E.; Lindsey, J. S. *J. Am. Chem. Soc.* **1993**, *115*, 7519.

25. Jullien, L.; Canceill, J.; Valeur, B.; Bardez, E.; Lefevre, J.-P.; Lehn, J.-M.; Marchi-Artzner, V.; Pansu, R. *J. Am. Chem. Soc.* **1996**, *118*, 5432.

26. a) Devadoss, C.; Bharathi, P.; Moore, J. S. *J. Am. Chem. Soc.* **1996**, *118*, 9635. b) Shortreed, M. R.; Swallen, S. F.; Shi, Z.-Y.; Tan, W.; Xu, Z.; Devadoss, C.; Moore, J. S.; Kopelman, R. *J. Phys. Chem. B* **1997**, *101*, 6318.

27. Heck, R. F. *Org. React.* **1982**, *27*, 345.

28. Peng, Z.; Zhang, J. *Chem. Mater.* **1999**, *11*, 1138.

29. Bao, Z.; Peng, Z.; Galvin, M. E.; Chandross, E. A. *Chem. Mater.* **1998**, *10*, 1201.

30. Yang, Z.; Sokolik, I.; Karasz, F. E. *Macromolecules* **1993**, *26*, 1188.

31. Yang, Z.; Hu, B.; Karasz, F. E. *J. Macromol. Sci. Pure Appl. Chem.* **1998**, *A35,* 233

32. Hörhold, H. H.; Opfermann, J. *Makromol. Chem.* **1970**, *131*, 105.

33. Tasch, S.; Graupner, W.; Leising, G.; Pu, L.; Wagaman, M. W.; Grubbs, R. H. *Adv. Mater.* **1995**, *7*, 903.

34. Wagaman, M. W. Ph.D. Thesis, California Institute of Technology, 1997.

35. Wagaman, M. W.; Grubbs, R. H. *Macromolecules* **1997**, *30*, 3978.

36. Ivin, K. J.; Mol, J. C. *Olefin Metathesis and Metathesis Polymerization*; Academic Press: San Diego, 1997.

37. (a) Grubbs, R. H.; Tumas, W. *Science* **1989**, *243*, 907. (b) Schrock, R. R. *Acc. Chem. Res.* **1990**, *23*, 158.

38. The official name for barrelene is bicyclo[2.2.2]octa-2,5,7-triene.

39. Wagaman, M. W.; Bellmann, E.; Cucullu, M.; Grubbs, R. H. *J. Org. Chem.* **1997**, *62,* 9076.

40. Heating is required for the DDQ aromatization of polymers with very strong electron-withdrawing groups such as fluorinated alkyls.

41. Pu, L.; Wagaman, M. W.; Grubbs, R. H. *Macromolecules* **1996**, *29*, 1138.

42. Wagaman, M. W.; Bellmann, E.; Grubbs, R. H. *Phil. Trans. R. Soc. Lond. A* **1997**, *355*, 727.

43. Wagaman, M. W.; Grubbs, R. H. *Synth. Met.* **1997**, *84*, 327.

Chapter 3

Synthesis of Dialkoxy-benzobarrelenes and Dialkoxy-PNVs by the ROMP-Aromatization Route

Abstract

New conjugated poly(1,4-naphthalenevinylene)s (PNVs) disubstituted by electron-donating alkoxy substituents (**4a-c** and **16**) have been synthesized by Ring-Opening Metathesis Polymerization (ROMP) of new dialkoxy-benzobarrelene monomers (**3a-c**) followed by aromatization with DDQ. Polymerizations were initiated with catalyst $Mo(CHCMe_2Ph)(N\text{-}2,6\text{-}C_6H_3\text{-}^iPr_2)(OCMe_2(CF_3))_2$ (**8b**) whose performance was superior to initiator $Mo(CHCMe_2Ph)(N\text{-}2,6\text{-}C_6H_3\text{-}^iPr_2)(OCMe(CF_3)_2)_2$ (**8a**) in terms of polymer polydispersity and polymerization rate. This ROMP-Aromatization Route is a mild synthesis procedure and provides polymers of controlled molecular weight that are low in polydispersity and soluble in common organic solvents such as methylene chloride, benzene, chloroform, and tetrahydrofuran. Furthermore, they are strongly photoluminescent in solution (quantum efficiencies 7-15%), making them good candidates for the emissive component of organic light-emitting diodes (LEDs). The wavelengths of photoluminescence of **4b-c** and **16** are from 534-546 nm (green to yellow-green) which is blueshifted relative to PNV with minimal electronic perturbations, contrary to the expected redshift for an electron-rich PNV. This blueshift is believed to be the result of stericly bulky alkoxy side chains causing twists in the polymer backbone, thus reducing the average conjugation length. To confirm this, a 6,7-dialkoxy-PNV (**17**), with alkoxy groups unable to interfere with the planarity of the polymer backbone, was synthesized, and displayed a solution photoluminescence λ_{max} of 598 nm. This is close to the wavelength one would expect based only on an electronic contribution of the alkoxy functional groups.

Introduction

Poly(*p*-phenylenevinylene) (PPV) derivatives and related π-conjugated polymers are considered to be organic semiconductors and many are highly fluorescent, emitting light in the visible spectrum.[1] They have been studied extensively over the past 10 years in both academia and industry for applications as emissive materials in light-emitting diodes (LEDs),[2,3,4] light-emitting electrochemical cells (LECs),[5] field effect transistors, electrically conducting polymers when doped,[6] light-harvesting/energy transfer systems,[7,8,9,10,11] fluorescent sensors,[12,13] nonlinear optical materials,[14] and lasers.[10,15,16]

Despite the tremendous amount of research in recent years involving PPV, there have been very few reports employing the related polyarylenevinylene poly(1,4-naphthalenevinylene) (PNV). PNVs may be synthesized in analogous fashions to PPVs,[17,18] so it is puzzling why it hasn't been exploited to a greater degree. What data has been obtained thus far has been promising, and PNV electroluminescence has been demonstrated.[19,20,21] Simple LEDs formed of ITO/200 nm PNV/Mg:In[22] have been shown to have a turn-on voltage[24] of 5 V, and an emission maximum at 605 nm.[19]

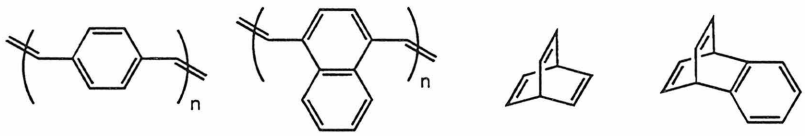

PPV PPV barrelene benzobarrelene

Among the differences in PNV and PPV is that PNV has a smaller HOMO-LUMO gap—due to the greater number of π system electrons—by ~0.4 eV, resulting in red shifted emission relative to PPV. A potential advantage of using PNVs in LEDs[23] is that it may more closely match electrode potentials of high work function metals than does PPV (see Figure 1). This is important because a high work function metal such as

aluminum is desirable because it is much less sensitive to degradation in oxygen than a low work function metal electrode like calcium. As a corollary, it should be noted that closely matching the emitter HOMO-LUMO energy levels to the electrode work functions results in more facile charge injection, thus lowering LED turn-on voltages.[24]

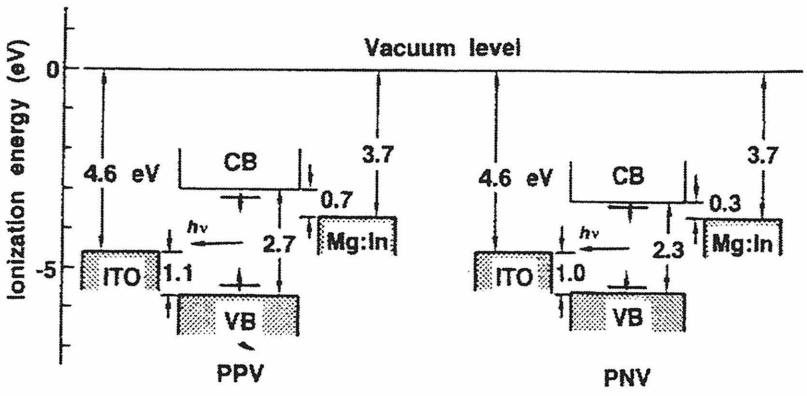

Figure 1. Energy diagram showing valence-band (VB or HOMO) and conduction band (CB or LUMO) energy levels of PPV and PNV.

Previous syntheses of PNV have been carried out following the Halogen Precursor Route (see Figure 2).[17,18] By this method, water-soluble polymer **1** is obtained and may be cast into films followed by thermolysis to yield an intractable yet uniform conjugated polymer, PNV. Researchers in our group have only recently presented the first, and so far only, reports of syntheses of soluble PNVs.[25,26,27,28] This is achieved by the ROMP-Aromatization Route as shown in Figure 3. ROMP is a living polymerization procedure; therefore one polymer chain is produced by each initiator. An identical procedure is used for PPV synthesis (see Chapter 2), except here a benzobarrelene monomer (**3**) is used. Functionalizing the monomer with alkyl groups allows the polymer to achieve solubility in common organic solvents. The polymer may also be substituted with electron-donating or –withdrawing moieties which are known to quite effectively

tune the HOMO-LUMO gap of conjugated polymers and is a logical way to effect the color of emission. Figure 4 shows a list of PNVs previously prepared by the ROMP-Aromatization Route. Electron-withdrawing halogen substituents slightly blue shift the emission, and most of the PPVs prepared by ROMP-Aromatization (see Chapter 2) also have electron-withdrawing groups to blue shift the emission. None have had strong electron-donating substituents. Thus the goals of this work were to synthesize electron-rich PNVs and compare the shifts in emission wavelengths, quantum yields, and other effects. Then we could begin to make unique copolymers with both electron-rich and –poor segments by the ROMP-Aromatization Route and explore their unique properties (see Chapter 4).

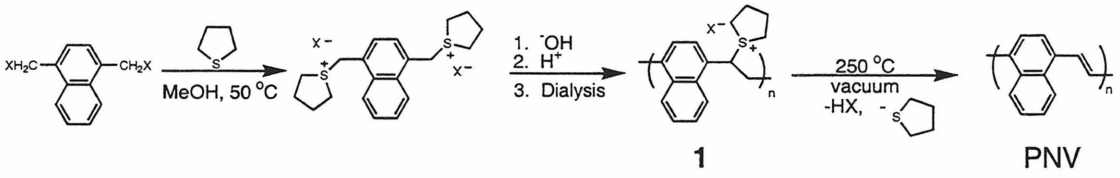

Figure 2. Halogen Precursor Route for PNV synthesis.

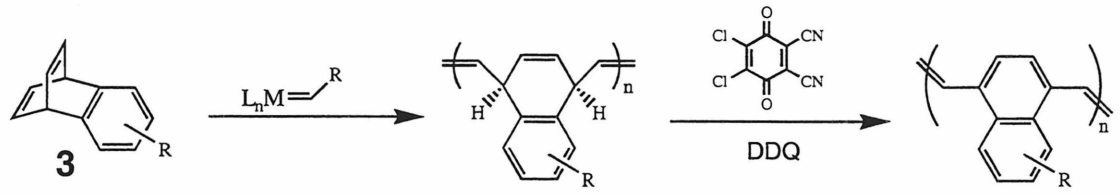

Figure 3. ROMP-Aromatization Route for synthesis of substituted PNVs.

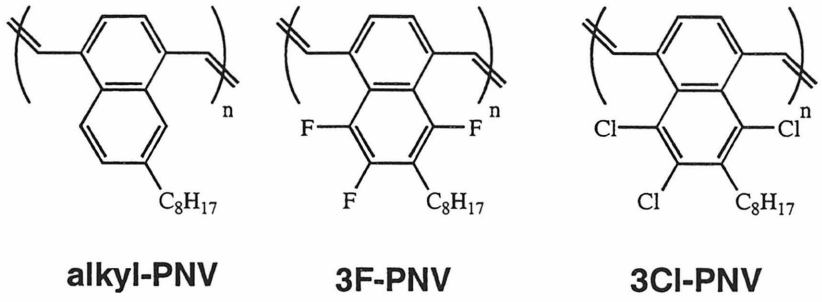

Figure 4. PNVs synthesized previously by ROMP-Aromatization route.

We chose dialkoxy-PNVs **4** as our target polymers. This was done in part because of the success others have had with dialkoxy-PPVs.[29,30] From these works we know that the alkoxy substituents are compatible with strong photo- and electroluminescence and can have a significant effect on emission wavelength.

Results and Discussion

Monomer Synthesis

Before we were able to prepare polymer, we had to develop a synthesis route for dialkoxybenzobarrelene monomers **3** as they were not known compounds. We followed a general strategy advanced for other benzobarrelene and barrelene syntheses.[26,27,31,32] In this strategy, *cis*-3,5-cyclohexadiene-1,2-diol undergoes a Diels-Alder reaction with a benzyne or activated alkyne followed by conversion of the diol to a double bond (Figure 5).[33]

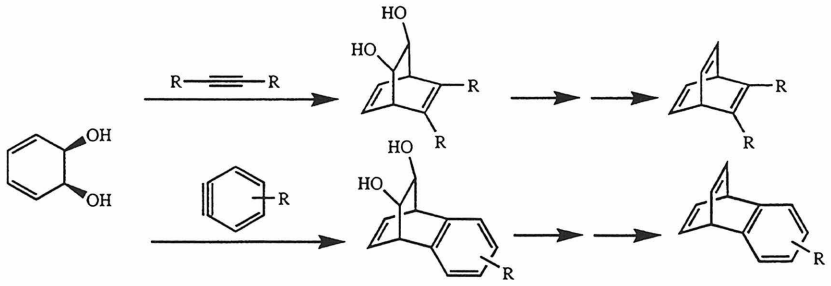

Figure 5. General strategy for barrelene and benzobarrele syntheses.

The synthesis of 3,6-dialkoxybenzobarrelenes we developed is shown in Figure 6. It is a four-step procedure starting from commercially available starting materials. Initially, *cis*-cyclohexadienediol is protected as an acetal (2-Phenyl-3a,7a-dihydro-benzo[1,3]dioxole, **2**) by reaction with benzaldehyde dimethylacetal and catalytic acid. Compound **2** is very sensitive to acid-catalyzed hydrolysis, and if the hydroscopic starting material has been in the presence of air for a long time, the reaction may fail.

Addition of molecular sieves seemed to diminish this problem. When the reaction does work, it proceeds in high yield and the product is used without further purification.[34] The second step, a Diels-Alder reaction between **2** and 1,4-benzoquinone, produces **5** in high yield and may be used without further purification.

Excess alkyl halide and two equivalents of base in DMSO solvent effected the next transformation, oxygen alkylation. Alkylation with iodoethane in the presence of KOH gave rise to **6a** in 30% yield, but under unoptimized conditions. A variety of bases were screened in this reaction, and all resulted in disappointingly low yields (Table 1). Comparing entries 2 and 3 shows that periodic addition of base is important: A 17% yield of **6b** is obtained when KOH is added at the beginning of the reaction all at once, and a 29% yield is obtained when it is added slowly over the first six hours of reaction when 1-iodo-2-ethylhexane is the alkylating agent. When NEt_3 or Na_2CO_3 was used as the base with slow addition, no desired product was obtained (Entries 4 and 5). *t*-BuOK produced a 19% yield, and the highest yield with this alkylating agent, 36%, was

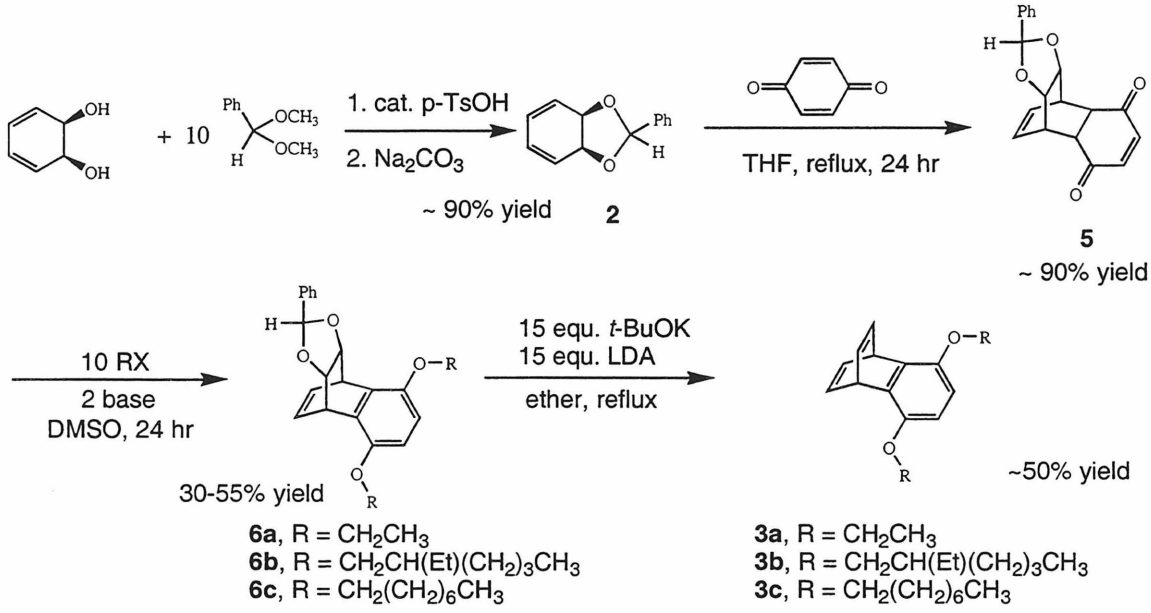

Figure 6. Synthesis of 3,6-dialkoxy-benzobarrelene.

obtained using LiOH. Under these same conditions, alkylation with 1-bromooctane resulted in a much greater yield, 55%. It is not clear why this reagent alkylates much better than the other two alkyl halides, but it may be an unexpected effect of the bromide.

Table 1. Synthesis of **5** under various alkyl halide and base conditions.

entry[a]	RX	base	yield
1	iodoethane	KOH	30%[c]
2	1-iodo-2-ethylhexane	KOH	17%[c]
3	1-iodo-2-ethylhexane	KOH	29%[b]
4	1-iodo-2-ethylhexane	NEt_3	0%[b]
5	1-iodo-2-ethylhexane	Na_2CO_3	0%[b]
6	1-iodo-2-ethylhexane	*t*-BuOK	19%[b]
7	1-iodo-2-ethylhexane	LiOH	36%[b]
8	1-bromooctane	LiOH	53-74%[b]

[a] Reactions carried out in DMSO solvent at room temperature for ~24 hours. [b] Base added periodically over the first six hours of reaction. [c] Base added all at once at the start of the reaction.

The final step in the monomer synthesis is a standard preparation[35] (ref) and converts the protected vicinal diol into a double bond producing **3a-c** in ~50% yield. The monomer is typically contaminated with 1-5% of the retro-Diels-Alder product **7**, which cannot be completely removed by silica gel chromatography (Figure 7).

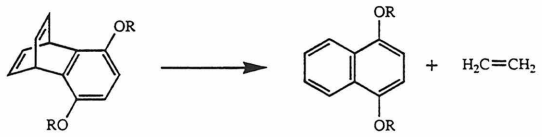

3a-c **7a-c**

Figure 7. Retro-Diels-Alder fragmentation of benzobarrelene **3**.

Polymerization

Molybdenum alkylidene **8a** or **8b**[36,37] is routinely used to initiate the ROMP of benzobarrelenes and barrelenes.[25,26,32] The ruthenium alkylidene **9** is not active enough to polymerize in high yield some of the barrelene and benzobarrelene monomers required for this study perhaps due to potentially coordinating Lewis basic functional groups, so it was not used in this study.[38]

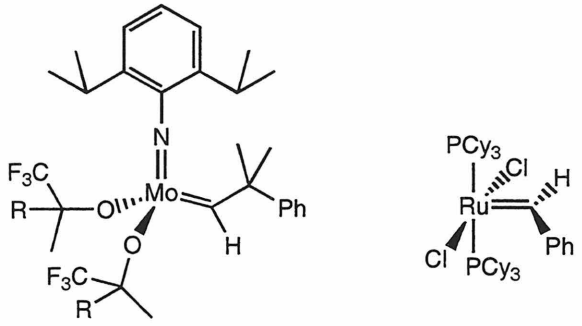

8a, R = CF_3
8b, R = CH_3

9

Figure 8. Popular single component, well-defined alkylidene ROMP initiators.

Polymerizations were carried out at room temperature in C_6D_6 solvent and monitored by ^1H NMR spectroscopy for initiation and propagation rates. Complete initiation of **3a** by **8a** was achieved in 10 minutes as evidenced by the new, broad[39] alkylidene resonance at 12.31 ppm for **10a** (the alkylidene proton of **8a** resonates at 12.13 ppm) (Figures 9 and 10 and Tables 2 and 3). That full initiation is achieved with **8a** was quite gratifying, as many ROMP monomers, such as norbornene, 1,5-cyclooctadiene, and cyclooctene, do not initiate completely in comparable monomer-to-catalyst ratios with initiator **8a**.[40] Propagation reached completion after 25 minutes, and the polymer was terminated by the addition of ~10 equivalents of benzaldehyde which undergoes a Wittig-type olefination cleaving the metal from the polymer and leaving a phenyl end group on

polymer **12a** (Figure 9).[41,42,43] The polymer is isolated by precipitation into methanol and purified by washing with methanol and reprecipitating twice or more until colorless. Gel permeation chromatography (GPC) revealed a monomodal molecular weight distribution of **12a** with a polydispersity index (PDI) of 1.24.

Hexafluoro-*t*-butanol (HFB) has been shown to be a cocatalyst with **8a** accelerating the rate of propagation and the rate of initiation relative to propagation in the ROMP of some intermediate to low strain monomers (see Chapter 1). Addition of 15 equivalents of HFB (relative to **8a**) to the reaction of **8a** and **3a** results in unexpected slower initiation time, slower propagation time, and bimodal molecular weight distribution (Table 2). This is indicative of the presence of two distinct propagating alkylidenes in solution, one polymerizing more rapidly (and initiating relatively slower), and thus to higher molecular weights. Interestingly however, ^{1}H NMR spectroscopy reveals only one propagating alkylidene, at 12.31 ppm. Perhaps the more active propagating alkylidene is in such a low concentration that it cannot be easily detected.[44,45] The effect of HFB is known to be monomer dependent and works well for monomers such as 1,5-cyclooctadiene, cyclooctene, and the trichloro-barrelene precursor to **3Cl-**

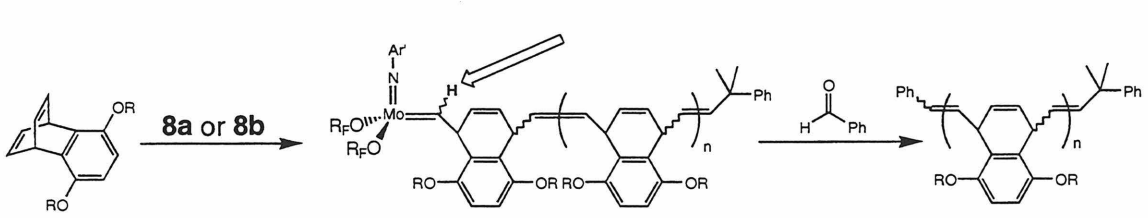

3a-c

10a, $R_F = CMe(CF_3)_2$, R = CH_2CH_3
10b, $R_F = CMe(CF_3)_2$, R = $CH_2CH(Et)(CH_2)_3CH_3$
10c, $R_F = CMe(CF_3)_2$, R = $(CH_2)_7CH_3$

11a, $R_F = CMe_2(CF_3)$, R = CH_2CH_3
11b, $R_F = CMe_2(CF_3)$, R = $CH_2CH(Et)(CH_2)_3CH_3$
11c, $R_F = CMe_2(CF_3)$, R = $(CH_2)_7CH_3$

12a-c

Figure 9. ROMP of **3a-c**. The arrow points to the alkylidene proton monitored by NMR spectroscopy.

PNV. The reason the "alcohol effect" does not operate in the ROMP of **3a** may be related to the potential coordination of the monomer's ether functional groups to the catalyst.

Initiating the ROMP of **3a** with **8b**—catalyst containing trifluoro-*t*-butoxide ligands rather than hexafluoro-*t*-butoxides—proceeds comparably to that of initiation with **8a**. Initiation is achieved within 10 minutes, and the propagating carbene **11a** can be observed as a broad signal at 11.82 ppm (the alkylidene proton of **8b** resonates at 11.68 ppm) (Tables 2 and 3 and Figure 10). Likewise, propagation is complete in 25 minutes, and a slightly broader PDI of 1.37 results.

Unlike monomer **3a**, **3b** polymerizes neither rapidly nor in a well-controlled fashion when initiated by **8a** (Table 2). No initiation of 40 equivalents of monomer is observed after 10 minutes, and the reaction takes 24 hours to reach completion. GPC reveals a bimodal molecular weight distribution with near baseline resolution. Peak molecular weights are M_n = 1,502,000 (PDI = 1.71) and M_n = 3800 (PDI = 1.07).[46] A molecular weight of 17,000 was targeted (Figure 11a). Even though there is only one propagating alkylidene observed by NMR spectroscopy (12.19 ppm, broad), GPC data suggests two. This difference in polymerization behavior of **3a** and **3b** with **8a** is very unusual considering how similar the monomers are.

Addition of 15 equivalents of HFB to the ROMP of **3b** by **8a** does not eliminate the bimodal molecular weight distribution. However, it does help to decrease the content of the more active alkylidene evidenced by the smaller relative size of the high molecular weight peak in the GPC trace (Figure 11b and Table 2).

Use of initiator **8b** with **3b** solves this problem. ROMP produces a polymer with a monomodal molecular weight distribution and a PDI of 1.15 (Figure 11c and Table 2). Furthermore, the reaction is more rapid when **8b** is used: Initiation reaches completion in 35 minutes and propagation reaches completion in 4 hours. Two broad resonances for the initiating carbene can be observed at 11.72 ppm and 11.62 ppm (Figure 10).

The high ROMP activity of **8b** is surprising because catalyst **8a** with more powerful electron-withdrawing alkoxides, and thus a more electrophilic metal, is thought to be more active. Indeed, the higher activity of **8a** towards cyclic and acyclic olefins has been demonstrated on a number of occasions.[47] The greater reactivity of **8b** here might be the result ligand sterics playing a more important role than electronics. The stericly smaller alkoxide ligands of **8b** may allow the metal center to be more accessible to olefin binding and subsequent metathesis.

Similar to what is observed for the polymerization of **3b**, initiation of 30 equivalents of **3c** by **8a** (with 15 equivalents of HFB)[48] produces polymer with a bimodal molecular weight distribution (Table 2). But when **8b** is the initiator, a monomodal polymer of PDI 1.28 is obtained, and both initiation and propagation are more than an order of magnitude faster. Interestingly, three propagating alkylidenes are observed by ^{1}H NMR when **8b** is the initiator (Figure 10 and Table 3). They must propagate at similar rates since a narrow PDI could still be obtained. NMR spectroscopy observes only one propagating alkylidene when **8a** is the initiator, once again suggesting that not all of the alkylidenes are discernible.[44]

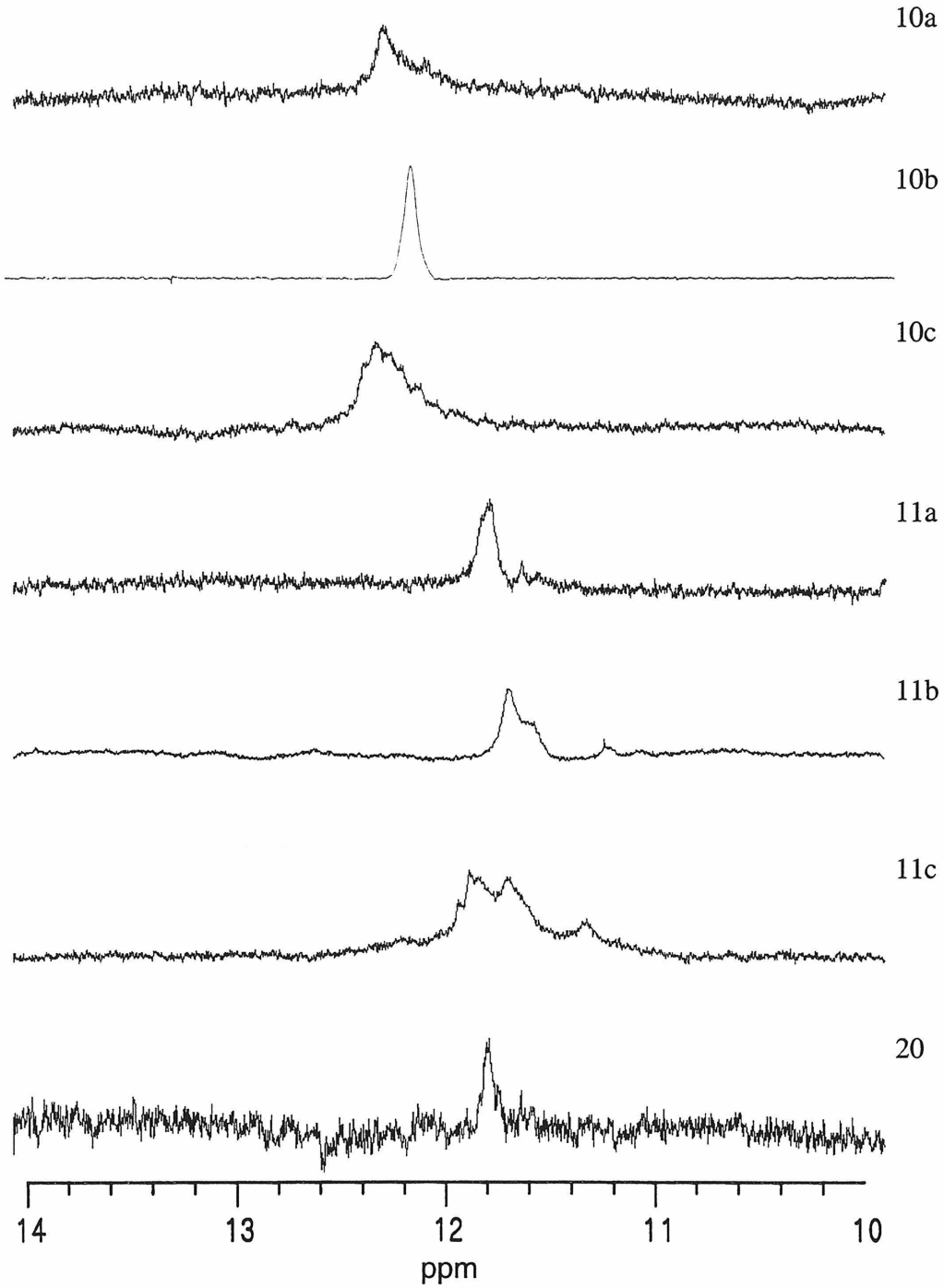

Figure 10. ^{1}H NMR spectra of the alkylidene region of propagating carbenes.

Table 2. Polymerization data of dialkoxy-PNVs.

initiator	monomer	M/I[a]	initiation time	propagation time	PDI[j]	M_n (obs.)[j]	MW (theory)
8a	**3a**	50	10 min	25 min	1.24	10,400	12,117
8a[b]	**3a**	51	10 min[c]	40 min	[d]	[d]	12,359
8b	**3a**	45	10 min	25 min	1.37	13,200	10,905
8a	**3b**	41	-[h]	24 h	[e]	[e]	16,839
8a[b]	**3b**	43	2 h	24 h[f]	[g]	[g]	17,660
8b	**3b**	41	35 mim	4 h	1.15	10,200	16,839
8a[b]	**3c**	30	~5 h	48 h	[i]	[i]	12,321
8b	**3c**	30	10 min	2.3 h	1.28	7200	12,321
8b	**18**	25	10 min	35 min	1.60	6100	10,043

[a] Monomer to initiator ratio. [b] 15 equivalents (relative to initiator) of hexafluoro-*t*-butanol added to catalyst solution. [c] Initiation 80% complete. [d] A bimodal molecular weight distribution was obtained. M_n = 562,000 (PDI = 2.25); M_n = 10,154 (PDI = 1.18). [e] A bimodal molecular weight distribution was obtained. M_n = 1,502,000 (PDI = 1.71); M_n = 3800 (PDI = 1.07). [f] Propagation 75% complete. [g] A bimodal molecular weight distribution was obtained. M_n = 600,000 (PDI = 2.12); M_n = 4300 (PDI = 1.87). [h] No initiation is observed after 10 minutes. [i] A bimodal molecular weight distribution was obtained. M_n = 24,000 (PDI = 1.64); M_n = 3000 (PDI = 1.32). [j] PDI and molecular weight data are relative to polystyrene standards.

Table 3. ^{1}H NMR alylidene chemical shift data for propagating alkylidenes.

propagating alkylidene[39]	alkylidene ^{1}H NMR chemical shift (ppm)[a]
10a	12.31
10b	12.19
10c	12.30
11a	11.82
11b	11.72, 11.62[b]
11c	11.88, 11.73, 11.37[b]
20	11.82

[a] ^{1}H NMR spectra recorded at room temperature in C_6D_6 solvent. [b] Multiple alkylidene resonances.

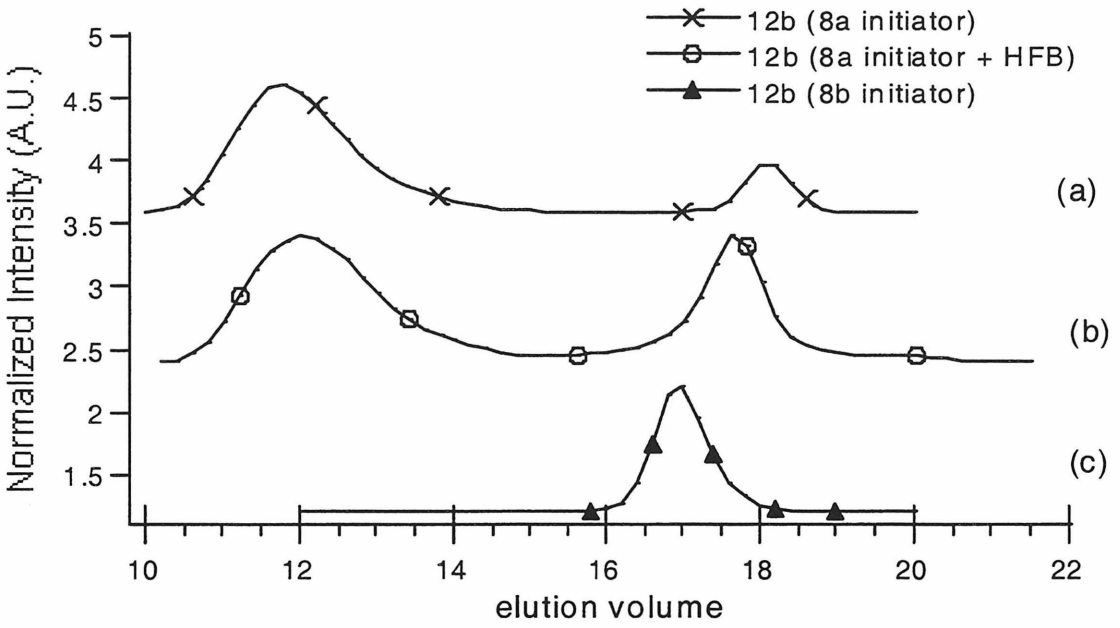

Figure 11. GPC traces of **12b** initiated with (a) **8a**, (b) **8a** and HFB, or (c) **8b**.

Polymer Aromatization

The aromatization procedure mirrors that used on other poly(benzobarrelene)s and poly(barrelene)s to form polyarylenevinylenes.[25,26,27,28,32] The oxidant 2,3-dichloro-5,6-dicyano-1,4-benzoquinone (DDQ) abstracts two hydrogen radicals from each polymer repeat unit resulting in PNVs **4a-c** (Figure 12). Aromatization of electron rich polymers such as **4** proceeds rapidly—less than 10 minutes—at room temperature in contrast to poly(barrelene)s **14** and **15** with strong electron-withdrawing groups which require several hours to reach completion or heating to 120 °C.[49] A slight excess of DDQ, 1.2 equivalents, is used to ensure complete reaction, and progress is monitored by ^{1}H NMR: olefin resonances disappear, shifting to the aromatic region. Another indication of aromatization is the color transformation; polymers change from white to yellow or yellow-orange. This cannot be used to quantitate the degree of conjugation, though, as they are highly colored even at low degrees of conjugation.

Reactions are typically carried out in methylene chloride since it is one of the best solvents to keep the polymers soluble. Solubility decreases dramatically upon conjugation as bond rotational degrees of freedom are restricted, and there is potential for polymer precipitation before achieving full conjugation. Aromatization can also be carried out in chloroform, aromatic solvents, and ethers if solubility permits. Polymer **4a** is nearly insoluble in the solvents mentioned above, but **4b** and **4c** with long branched or linear alkyl chains are quite soluble in CH_2Cl_2, $CHCl_3$, C_6H_6, and THF. The polymer is isolated by precipitation into methanol and purified by reprecipitation into methanol two times.

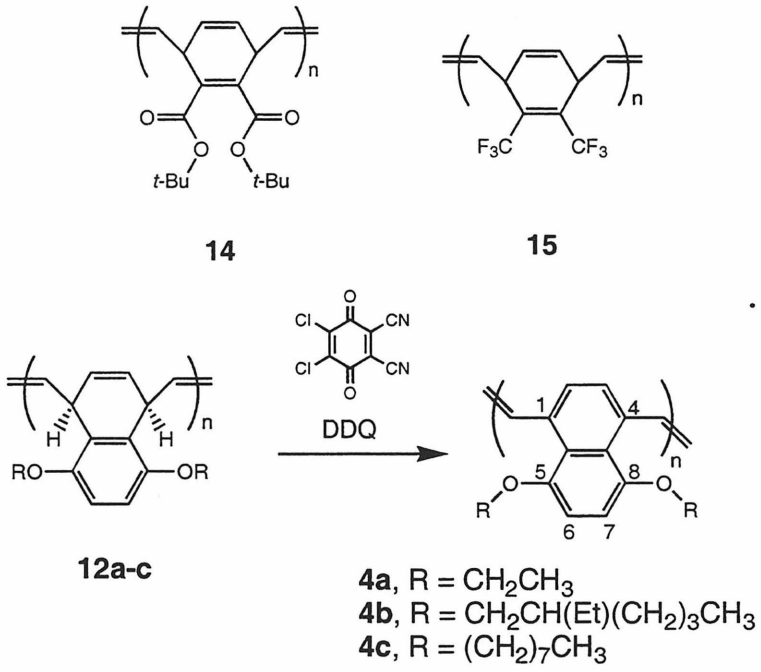

Figure 12. Polymer aromatization.

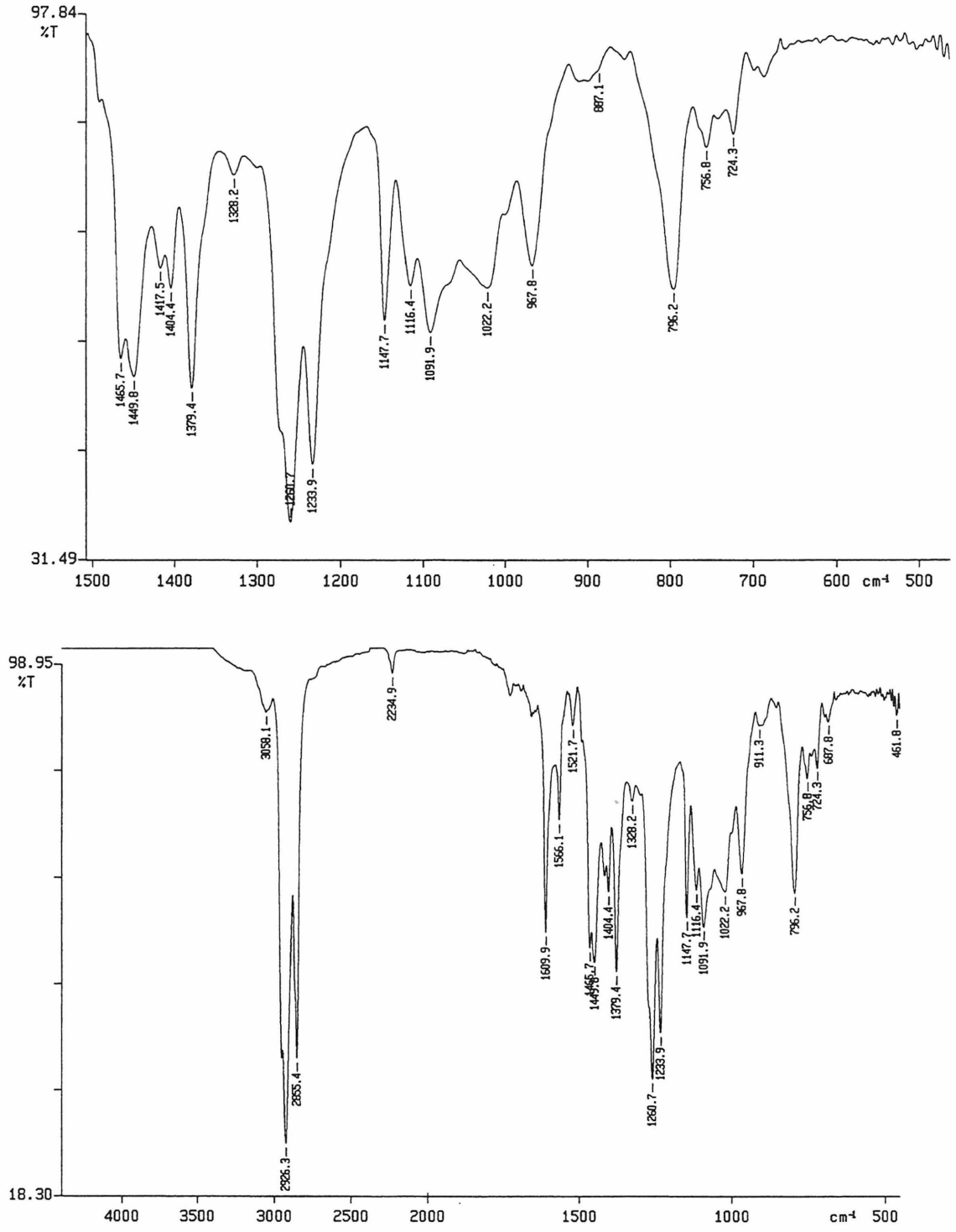

Figure 13. IR spectrua of **4c**.

Polymers **4a-c** have almost exclusively *trans* vinylene units as determined by IR spectroscopy. An IR spectrum of the fingerprint region of **4c** (Figure 13a) shows a peak

at 967.8 cm^{-1} which is characteristic of the *trans* C-H out-of-plane bending mode.[1,50] The absence of a peak at 882 cm^{-1} shows that there are very few *cis* vinylene units.

Fluorescence Spectroscopy

As we had hoped, the new dialkoxy-PNVs were highly fluorescent. Photoluminescence data is shown in Table 4 along with those of a few previously known PNVs and PPVs for comparison. When excited at its wavelength of maximum absorbance, 407 nm, polymer **4b** has a solution emission maximum at 534 nm, which is in the green part of the visible spectrum (Figure 14). The luminescence of this electron-rich PNV is blue shifted relative to **alkyl-PNV** emission, which occurs at 561 nm. This blue shift is contrary to the expected red shift based on theoretical calculations of polyarylenevinylenes containing electron-donating functional groups[51] and experimental evidence from dialkoxy-PPVs such as MEH-PPV (Table 4).[52,55] This effect is believed to be caused by the bulky ethylhexyloxy side groups which restrict certain geometrical conformations and prevent the polymer from becoming planar, thus decreasing the conjugation length (see Figure 15). A decreased π-conjugation length in organic molecules is well known to result in blue shifted emission.[53]

To test the hypothesis of the effect of bulky side groups, **4c** was prepared which has linear, less stericly demanding alkoxy groups. As expected, the emission wavelength (541 nm) is red shifted relative to **4b**, though only slightly. A better test would result if the alkoxy chains were even smaller, but as demonstrated with **4a**, if they are too small, the polymer will be insoluble. To circumvent this problem, conjugated block copolymer **16** was synthesized in which PNV with ethoxy side chains is solublized by covalent attachment to a block of **4b** (Figure 16).[54] Fluorescence from **16** (546 nm) is red shifted

slightly relative to both **4b** and **4c**, further supporting our premise that the steric influence of large alkoxy groups in the 5 and 8 positions of **4** can outweigh the electronic contributions.

Table 4. Luminescence data for conjugated polymers.

polymer	$\lambda_{max,ex}$ (nm)	solution $\lambda_{max,em}$ (nm)[a,b,c]	quantum yield (solution)[a,b]	film $\lambda_{max,em}$ (nm)
4b	407	534	15%	534
4c	407	541	7%	549
16	407	546	5%	546
17	475	598	8%	-
alkyl-PNV[25,28]	444	561[d]	0.5%[d]	593
PNV[19]	443	-	-	605
PPV[55]	442	-	-	558
MEH-PPV[56]	489	556[e]	20%[e]	600

[a] In CH_2Cl_2 solution unless otherwise noted. [b] Emission wavelengths and quantum yields were referenced to a $Ru(bpy)_3Cl_2$ emission standard. [c] For emission measurements, polymers were excited near the wavelength of maximum absorbance. [d] In $CHCl_3$ solution. [e] In *p*-xylene solution.

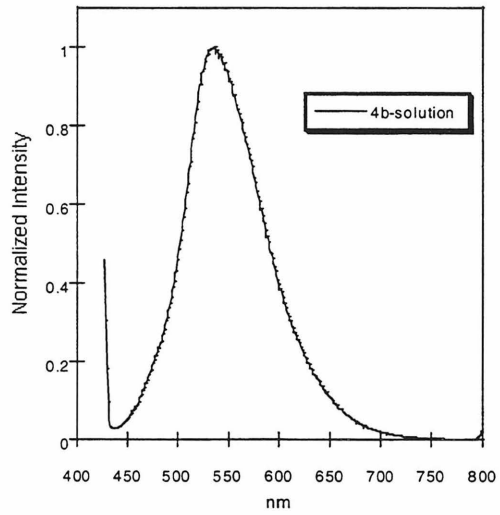

Figure 14a. Emission spectrum of **4b** in solution.

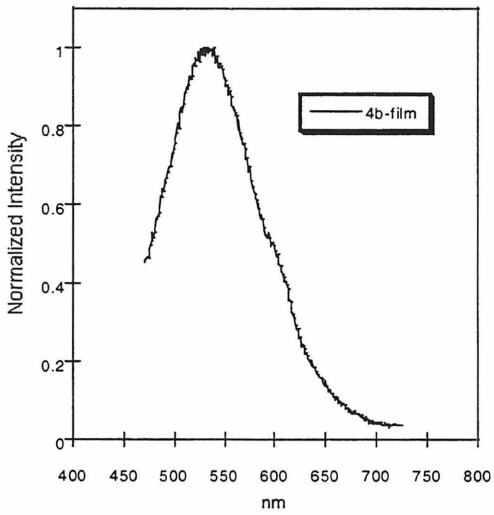

Figure 14b. Emission spectrum of a film of **4b**.

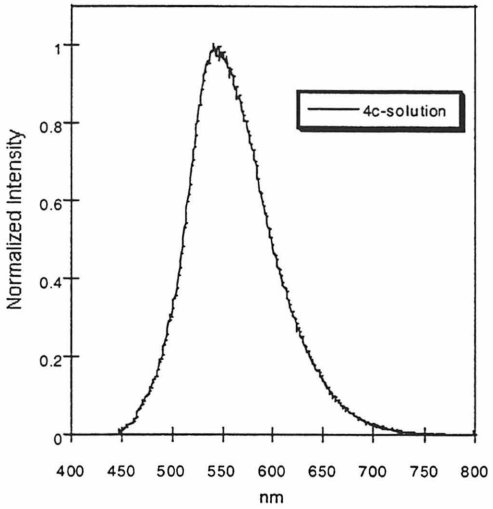

Figure 14c. Emission spectrum of **4c** in solution.

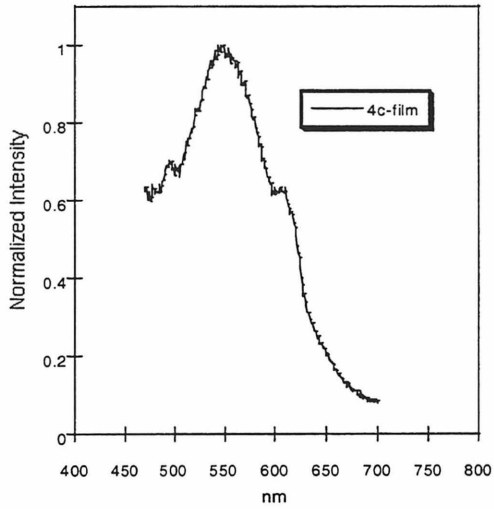

Figure 14d. Emission spectrum of film of **4c**.

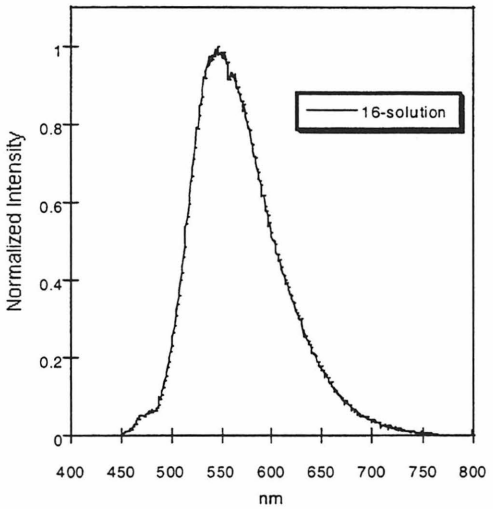

Figure 14e. Emission spectrum of **16** in solution

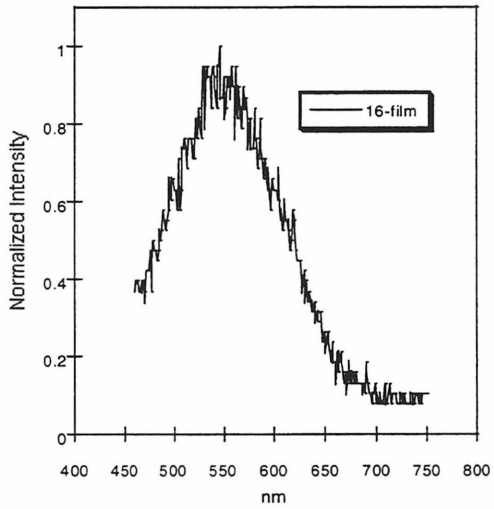

Figure 14f. Emission spectrum of film of **16**.

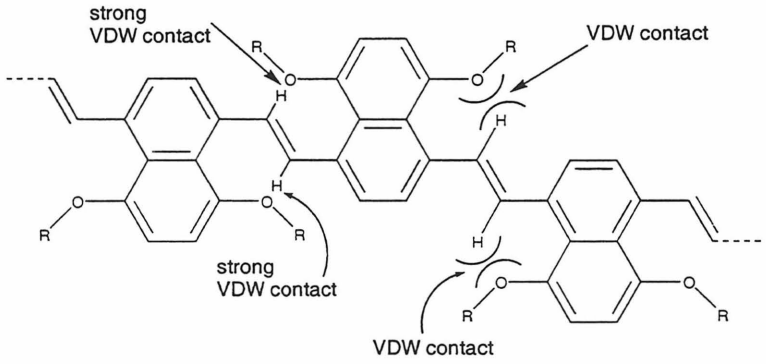

Figure 15. Model of 5,8-dialkoxy-PNV showing the sites of van der Waals (VDW) contact if the polymer is planar.

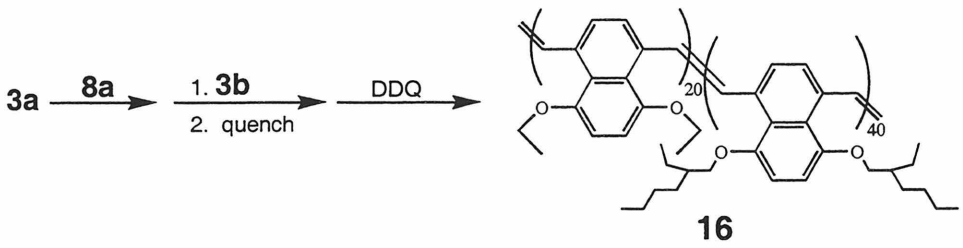

Figure 16. Synthesis scheme for block copolymer **16**.

Another consequence of the alkoxy groups in the 5 and 8 positions of **4** and **16** is that polymer reorganization and planarization in the solid state is less than what one typically observes for other PNVs and PPVs. Planarization increases in the solid state to increase packing density, and there is less freedom for the polymer backbone bonds to rotate. This increased planarization increases the π-conjugation length resulting in a red shift in the luminescence. Compare the solution and solid state photoluminescence wavelengths for **alkyl-PNV** and **MEH-PPV** in Table 4. $\lambda_{max,em}$ for **alkyl-PNV** increases by 32 nm in the solid state and $\lambda_{max,em}$ for **MEH-PPV** increases by 44 nm. However, $\lambda_{max,em}$ for **4b** and **16** do *not* change upon going to the solid state, and that of **4c** only increases a small amount, 8 nm.

The solvent effect on phololuminescence was examined, and data is shown in Table 5 for four solvents—C_6H_6, $CHCl_3$, THF, and CH_2Cl_2—in order of increasing dielectric constant. There is very little variation in wavelength of emission in these four solvents, only from 534 to 541 nm. There are also no new emission bands or shoulders. There is only slight variation in the quantum yield, from 14 to 20%. There seems to be no trend correlating increasing dielectric constant with $\lambda_{max,em}$ or quantum yield. Perhaps

the only consistency is that the solvent that results in the longest wavelength emission, THF, also gives the most efficient emission.

Emission spectra were also recorded of solid polymer films deposited from the same four solvents (Table 5). These samples had widely different emission maxima, varying by 45 nm. As with solution measurements, there was no correlation with dielectric constant. Emission maxima of films deposited from $CHCl_3$ and THF remarkably show blue shifts of 34 nm and 15 nm, respectively, relative to their solution values. The red shift observed with the film from C_6H_6 solution was smaller, only 13 nm. Currently we do not have a good explanation for the wide variation in emission wavelengths in the solid state. Perhaps dielectric constant or polarity is not the critical property to consider.

Conjugated arene polymers can frequently have serious aggregation problems resulting in eximer formation and luminescence quenching.[57] Bulky side chains or bulky end groups such as dendrons have been shown to diminish aggregation. The size of the alkoxy side groups of **4b** and **16** may also have a significant effect on polymer aggregation and quantum yield. Table 4 shows that as the alkoxy side chains decrease in size **4b** > **4c** > **16** the quantum yield decreases from 15% to 7% to 5%.

Table 5. Photoluminescence of **4b** in various solvents.

solvent	dielectric constant[58]	dipole moment (D)[58]	solution $\lambda_{max,em}$ (nm)[a,b]	quantum yield (solution)[a]	film $\lambda_{max,em}$ (nm)[c]
C_6H_6	2.28	0	535	19%	548
$CHCl_3$	4.81	1.04	537	14%	503
THF	7.6	1.75	541	20%	526
CH_2Cl_2	9.08	1.60	534	15%	534

[a] Emission wavelengths and quantum yields were referenced to a $Ru(bpy)_3Cl_2$ emission standard. [b] Polymers were excited at 407 nm. [c] Polymer films were cast on a glass slide by evaporation from the solvent shown.

Synthesis of 6,7-dialkoxy-PNV and ROMP-Aromatization

To further examine the interplay of sterics and electronics in **4**, a dialkoxy PNV whose alkoxy functional groups were farther removed from the polymer backbone was targeted. This 6,7-dialkoxy-PNV **17** may be synthesized by the ROMP-aromatization route from the appropriate benzobarrelene **18**.

Benzobarrelene **18** is synthesized as shown in Figure 17. This procedure follows the same general strategy outlined above for benzobarrelene synthesis. In the second step, **2** is the diene in a Diels-Alder reaction with a benzyne formed *in situ* at low temperature from the monolithiation of a 1,2-dibromobenzene. Unfortunately, product **19** was formed in very low yield and variations in organolithium reagent, dwell time for formation of the benzyne, and reactant ratios was unhelpful in increasing the yield. Using furan as a model diene under the same reaction conditions, GC/MS analysis was

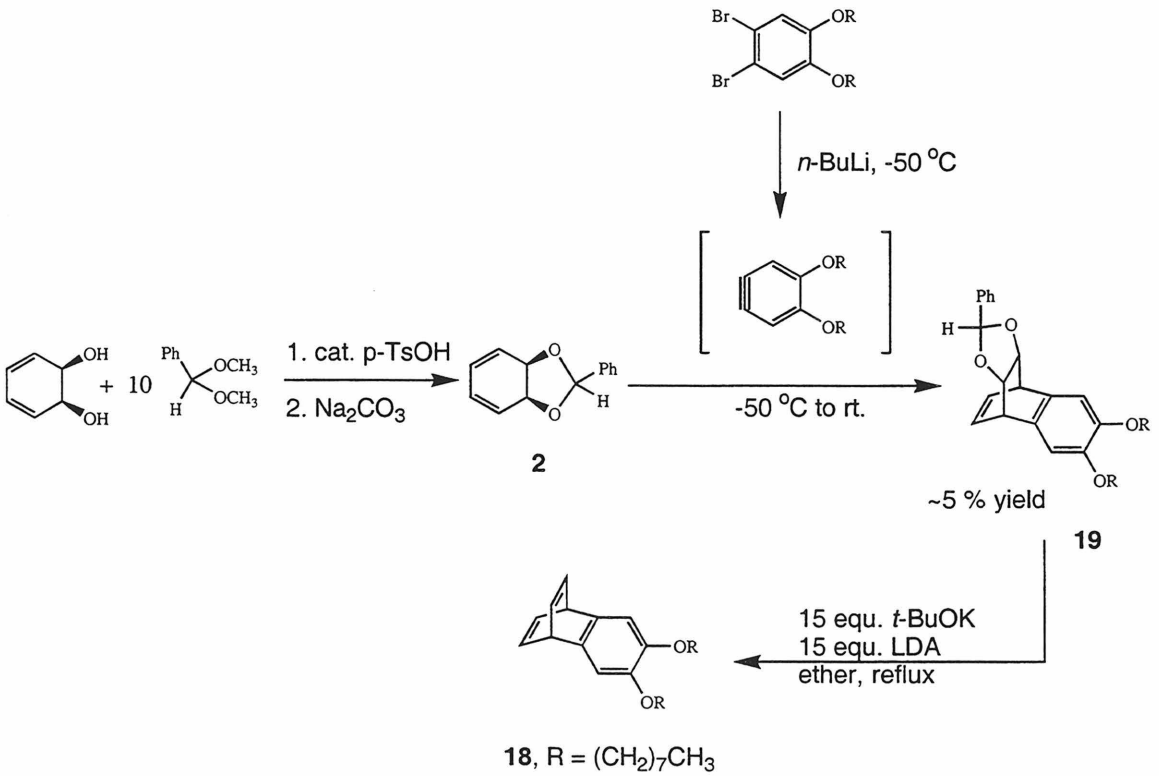

Figure 17. Synthesis of 4,5-dioctyloxy-benzobarrelene.

helpful in identifying some of the side reactions as alkylations, and mono- or di-dehalogenations. The final step was carried out as before and proceeded in similar yield.

Monomer **18** was polymerized by initiation with **8b** (Figure 18). Initiation reached completion within 10 minutes, and the propagating alkylidene (**20**) resonance was observed by NMR at 11.82 ppm (Figure 10 and Table 3). Propagation was also rapid, reaching completion in 35 minutes (Table 3). It is interesting that ROMP of **18** is faster than **3b** and **3c** but comparable to **3a**. This suggests that the alkyl groups of **3b** and **3c** may be interfering with olefin binding, thus slowing down propagation. Since the alkyl groups of **18** are farther away from the double bonds, they interfere less and propagation remains rapid. Polymer **21** is soluble in CH_2Cl_2, $CHCl_3$, and C_6H_6 and has a monomodal molecular weight distribution and a PDI of 1.60. Aromatization is effected with DDQ in CD_2Cl_2 and is rapid (10 minutes), but conjugation only reaches 80-90% because the polymer is sparingly soluble. This much-decreased solubility of **17** compared to **4b-c** is probably evidence of a more planar polymer backbone, which we had hoped for.

Despite incomplete aromatization, the polymer is highly fluorescent.[59] When excited at 434 nm, **17** fluoresces at 598 nm, red shifted relative to **4b**, **4c**, and **alkyl-PNV**; this wavelength is closer to what one might expect based only on an electron contribution of the alkoxy groups (Table 4, Figure 19). The quantum yield, 8%, is almost the same as

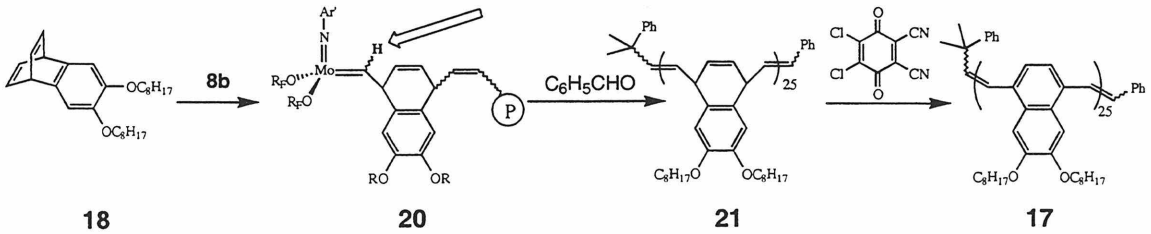

Figure 18. ROMP-Aromatization of **18**. The arrow points to the alkylidene proton monitored by ^1H NMR spectroscopy during polymerization.

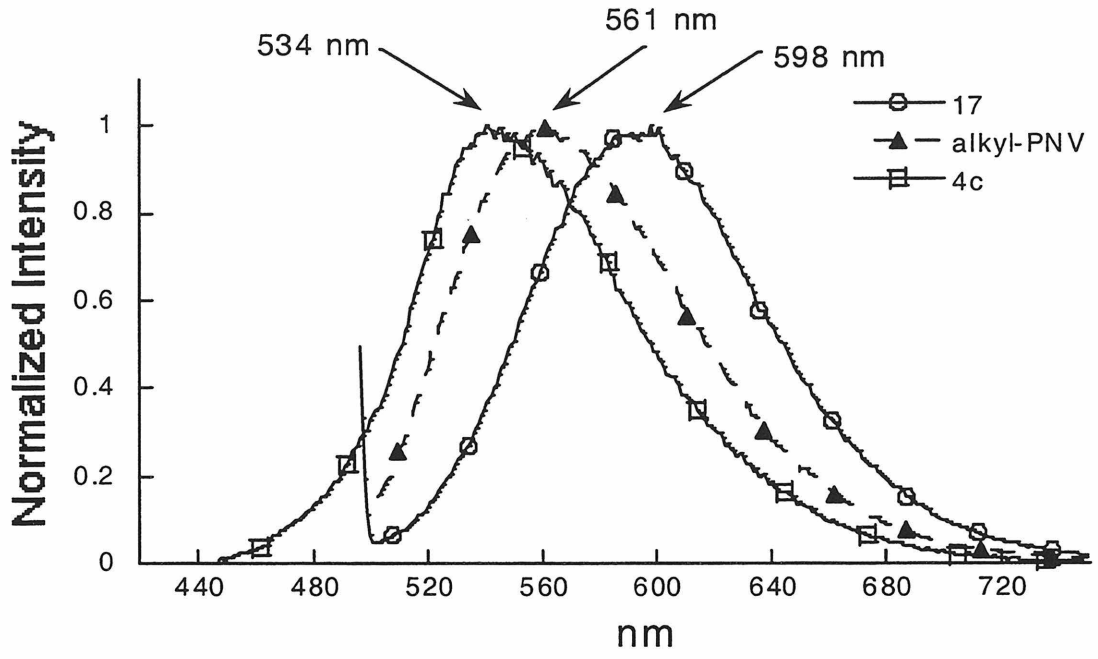

Figure 19. Emission spectra of **17** and **alkyl-PNV** and **4c** for reference.

that of **4c**. This supports our earlier hypothesis suggesting that alkoxy functional groups in the 5 and 8 positions of PNV interfere with the polymer backbone causing it to twist out of planarity, decreasing the effective length of conjugation, resulting in blue shifted emission.

Acknowledgments

I would like to thank Dr. Mike W. Wagaman for his immense help in planning the monomer synthesis, giving advice on polymer isolation procedures, and teaching me how to use the fluorescence spectrometer. I would like to thank Erika Bellmann for helpful discussions in all aspects of this project as well as the other members of the Center for Advanced Multifunctional Polymers and Non-Linear Optical Materials. Sean Shaheen, Kelly Killeen, Shannon Rice, and Jason Brooks are acknowledged for teaching me how to fabricate LEDs. I also thank ICI for donating a large amount of *cis*-3,5-cyclohexadiene-1,2-diol. The research group of Dr. J. K. Barton is gratefully

acknowledged for allowing us to use their fluorescence spectrometer, and particularly Chris S. Treadway for helpful discussions.

Experimental

General Considerations. Manipulations of air-sensitive materials were carried out using standard Schlenk techniques with an argon atmosphere or in a nitrogen filled Vacuum Atmospheres drybox. NMR spectra[60] were recorded with either a QE-300 Plus (300.10 MHz ^{1}H; 75.49 MHz ^{13}C) spectrometer, a JEOL GX-400 (399.65 MHz ^{1}H; 376.01 MHz ^{19}F; 100.50 MHz ^{13}C), or a Brucker AM500 or AMX500 (500.14 MHz ^{1}H; 470.56 MHz ^{19}F; 125.76 MHz ^{13}C). All chemical shifts are reported in parts per million (ppm) downfield from tetramethylsilane (TMS), and coupling constants are reported in Hz. Multiplicities are reported with the following abbreviations: s (singlet), d (doublet), t (triplet), q (quartet), m (multiplet), and br (broad). Gel permeation chromatograms were obtained in methylene chloride at a 1.0 mL/min flow rate on an AM Gel Linear 10 column with a Knauer differential refractometer detector. Molecular weights are calculated relative to polystyrene standards ranging from 2,950 to 2,400,000 daltons. Infrared spectra were recorded on a Perkin Elmer Paragon 1000 FT-IR spectrometer. Absorbance spectra were recorded on a HV Vectra ES/12 spectrometer with 2 nm resolution. Luminescence spectra were recorded on an SLM 8000 C spectrofluorometer at room temperature.

Materials. Benzene-d_6, tetrahydrofuran (THF), and ether were degassed by bubbling a stream of argon through the solvents and dried by passage through solvent purification columns.[61] Methylene chloride-d_2, was dried over CaH_2, vacuum transferred or distilled, then degassed by three freeze-pump-thaw cycles. Hexafluoro-*t*-butanol was

dried over activated $MgSO_4$, vacuum transferred, and degassed by three freeze-pump-thaw cycles. All other chemicals were obtained from EM Science; Lancaster Synthesis, Inc.; Aldrich Chemical Co.; or Strem Chemicals, Inc. and used as received unless otherwise noted. Alkylidenes **8a** and **8b**[36,37] and compound **2**[26,62,63] were prepared as previously reported.

General ROMP Procedure. In the drybox, a vial was charged with approximately 5 mmol of initiator **8b** (or **8a** and 15 equivalents hexafluoro-*t*-butanol) and dissolved in 0.1 mL C_6D_6. A second vial was charged with monomer **3** (typically 30-50 equivalents) and dissolved in 0.5 mL C_6D_6. The monomer solution was added *to* the catalyst solution via pipet and the vial was immediately swirled to ensure sufficient mixing during initiation. The solution was transferred to an NMR tube with a teflon valve seal (J-Young tube) and analyzed by NMR spectroscopy. (In scale up syntheses, non-deuterated benzene is used and the reaction is not monitored by NMR spectroscopy.) The solution became orange to brown during the course of the reaction. At the completion of the reaction, 0.1 mL dry, degassed benzaldehyde (~200 equivalents) was added in the drybox or in air then immediately sealed again by the teflon valve, and left for at least 30 min. The solution became green, a sign of complete catalyst quenching and conversion to $Mo(O)(NAr)(OR)_2$.[41,42] The solution was then diluted with 0.1-0.5 mL degassed benzene or CH_2Cl_2 as necessary to decrease viscosity, then poured into 40 mL degassed methanol to precipitate polymer. Polymer was left for ~10 h to precipitate fully, then centrifuged, and supernatant liquid removed by cannula transfer.[64] This methanol wash-centrifugation-solvent removal was repeated twice more to further purify the polymer. If colored, the polymer was redissolved in a minimal amount of benzene or

CH_2Cl_2 and reprecipitated into methanol followed by centrifugation and cannula transfer solvent removal. This reprecipitation was repeated two or three times until the polymer was nearly white. Though not necessary, polymer was typically freeze-dried from benzene *in vacuo*, resulting in fluffy solid, which was easier to work with in small quantities than the films or large solid chunks that often resulted otherwise. Drying *in vacuo* from any solvent was sufficient. All yields were 80% or greater.

General Procedure for Polymer Aromatization. In the drybox a vial was charged with the appropriate amount of **12** and dissolved in CD_2Cl_2, and a second vial was charged with a slight excess (1.2 equivalents) of 2,3-dichloro-5,6-dicyano-1,4-benzoquinone (DDQ) and slurried in CD_2Cl_2. The solutions were combined resulting in an instant color change to orange and formation of precipitate. The solution was transferred to an NMR tube with a teflon seal and analyzed by NMR spectroscopy. After reaction completion, the solution was poured into 40 mL degassed methanol[64] and left ~10 h to precipitate the polymer fully. The polymer slurry was centrifuged then the supernatant liquid removed by cannula transfer. The polymer was redissolved in a minimal amount of degassed benzene or CH_2Cl_2 and reprecipitated into methanol followed by centrifugation and cannula transfer solvent removal. This reprecipitation cycle was repeated twice more. Though not necessary, polymer was typically freeze-dried from benzene *in vacuo*, resulting in fluffy solid, which was easier to work with in small quantities than the films or large solid chunks that often resulted otherwise. Drying *in vacuo* from any solvent was sufficient.[64] Yields were nearly quantitative.

General Procedure for Photoluminescence Measurements. Measurements were performed with an SLM 8000 Spectrofluoremeter on solutions diluted to give a

polymer *repeat unit* concentration of 10^{-5} – 10⁻6 M. Quantum yields (Φ) were calculated relative to a $Ru(bpy)_3Cl_2$ (Ru) standard using the following equation:

$$\Phi_{poly} = \frac{I_{poly} \cdot \varepsilon_{Ru} \cdot c_{Ru}}{I_{Ru} \cdot \varepsilon_{poly} \cdot c_{poly}} \cdot \Phi_{Ru}$$

Emission intensity integration values, *I*, were measured on spectra that had been corrected for detector response. Extinction coefficients for the polymers were determined by absorbance spectroscopy and are shown in Table 6. Literature values for Φ_{Ru} (0.028) and ε_{Ru} (14,300) were based on excitation at 453 nm.[65]

3,6-diethoxy-tricyclo[6.2.2.0^{2,7}]dodecda-2(7),3,5,9,11-pentaene or 3,6-diethoxy-benzobarrelene (**3a**). lab notebook 4-069-2, 4-050-7. In the drybox, a flask was charged with 2.53 g (0.00752 mol) **6a** and 12.64 g (0.113 mol) potassium-*t*-butoxide and slurried in 50 mL ether. A second flask was charged with 12.1 g (0.113 mol) lithium diisopropylamide (LDA) in the drybox and slurried in 50 mL ether. After removal from the drybox, the first flask was heated to reflux and the LDA solution was added in 3.0 mL (0.0061 mol) aliquots carefully approximately every 15 min. CAUTION: the addition if LDA is very exothermic and should be handled slowly and with great care. After addition of 28.0 mL (7.5 equivalents) of the LDA solution, a 300 μL aliquot was taken out, quenched on ice, extracted into 300 μL ether, and dissolved in 300 μL C_6D_6 for ^1H NMR analysis. Comparing the bridgehead proton resonance of **6a** at 5.06 ppm (multiplet) to the bridgehead proton of **3a** at 5.54 ppm (multiplet), the reaction was deemed 90% complete. An additional 15.0 mL of the LDA solution (43.0 mL total, 0.0869 mol) was added in 3.0 mL aliquots over 1.3 h and allowed to reflux 15 more minutes. After cooling to room temp, 20 mL cold, dilute, aqueous HCl was added

slowly. The ether layer was separated then washed once more. The desired product could be isolated by concentrating the ether solution then subjecting to column chromatography eluting with 5% ethyl acetate in hexanes, however compound **7a** always remained in ~5% as an impurity (TLC in 10% ethyl acetate in hexanes shows that **7a** has an R_f of 0.45 and **3a** has an R_f of 0.34). A much more effective purification was achieved by crystallization from ether at –80 °C. Yield = 0.35-0.51 g (19-28%). **3a** ^{1}H NMR (C_6D_6, 300 MHz): δ 6.775 (d, J = 4 Hz, 1H), 6.772 (d, J = 4 Hz, 1H), 6.33 (s, 2H), 5.56 (m, 2H), 3.67 (q, J = 7 Hz, 4H), 1.26 (t, J = 7 Hz, 6H). ^{13}C NMR (C_6D_6, 75 MHz): δ 148.6, 140.9, 138.7, 109.4, 64.77, 43.83, 15.58. **7a** ^{1}H NMR (C_6D_6, 300 MHz): δ 8.55 (dd, J = 7, 3 Hz, 2H), 7.38, (dd, J = 7, 4 Hz, 2H), 6.49 (s, 2H), 3.78 (q, J = 7 Hz, 4H), 1.30 (t, J = 7 Hz, 6H).

3,6-bis(2-ethyl-hexyloxy)-tricyclo[6.2.2.0^{2,7}]dodecda-2(7),3,5,9,11-pentaene or 3,6-bis(2-ethyl-hexyloxy)-benzobarrelene **(3b)**. lab notebook 4-224-2, 4-120-9. Reaction carried out analogously to the synthesis of **3a** except using 2.90 g (0.00543 mol) **6b**, 11.5 g (0.102 mol) potassium-*t*-butoxide in 35 mL ether, and 41.0 mL (0.0849 mol) of a 2.07 M solution of LDA in ether. The LDA solution was added in 4-5 mL aliquots every 15-20 minutes. CAUTION: the addition if LDA is very exothermic and should be handled slowly and with great care. The product was isolated by column chromatography (12 in.) eluting with 4% ethyl acetate in hexanes. Yield: 1.57 g (70%). ^{1}H NMR (C_6D_6, 300 MHz): δ 6.81 (t, J = 4 Hz, 4H), 6.47 (s, 2H), 5.57 (m, 2H), 3.73 (d, J = 5 Hz, 4H), 1.70 (m, 2H), 1.48 (m, 8H), 1.28 (m, 8H), 0.91 (t, J = 7 Hz, 12H). ^{13}C NMR (C_6D_6, 300 MHz): d 148.7, 140.5, 138.4, 109.4, 71.85, 43.47, 40.05, 31.12, 29.47, 24.44, 23.46, 14.29, 11.39. A small impurity of **7b** was also present: ^{1}H NMR (C_6D_6, 300

MHz): δ 8.57 (dd, J = 7, 4 Hz, 2H), 7.39 (dd, J = 7, 4 Hz, 2H), 6.65 (s, 2H), 3.87 (d, J = 5 Hz, 4H), 1.76 (m, 2H), 1.51 (m, 8H), 1.29 (m, 8H), 0.92 (t, 12H).

3,6-bis(octyloxy)-tricyclo[6.2.2.0^{2,7}]dodecda-2(7),3,5,9,11-pentaene or 3,6-bis(octyloxy)-benzobarrelene **(3c).** lab notebook: 4-288-3, 4-290-7. Reaction carried out analogously to the synthesis of **3a** except in THF using 1.06 g (0.00191 mol) **6c**, 3.40 g (0.0303 mol) potassium-*t*-butoxide in 20 mL THF, and 19.1 mL (0.0210 mol) of a 1.1 M solution of LDA in THF. The LDA solution was added in 2.5-3.4 mL aliquots every 15-30 minutes. CAUTION: the addition if LDA is very exothermic and should be handled slowly and with great care. The product was isolated by two column chromatography purifications (12 in.) eluting with 10% ethyl acetate in hexanes and the second one with 5% ethyl acetate in hexanes. Yield: 0.8 g (99%); contains ~5% impurity of **7c**. **3c** ^{1}H NMR (C_6D_6, 300 MHz): δ 6.82 (m, 4H), 6.43 (s, 2H), 5.59 (m, 2H), 3.75 (t, 4H), 1.71 (m, 4H), 1.40 (m, 4H), 1.26 (br s, 16H), 0.91 (t, 6H). ^{13}C NMR (C_6D_6, 75 MHz): δ 148.8, 140.9, 138.7, 109.6, 69.60, 43.84, 32.68, 30.40, 30.27, 30.16, 26.98, 23.50, 14.80. **7c** ^{1}H NMR (C_6D_6, 300 MHz): δ 8.60 (m, 2H), 7.39 (m, 2H), 6.61 (s, 2H), 3.87 (m, 4H), 1.77 (m, 4H), 1.445 (m, 4H), 1.26 (br, 16H), 0.91 (m, 6H).

5,8-diethoxy-PNV (4a). lab notebook: 4-078-6. Polymer **12a** (0.0069 g, 0.0285 mmol per repeat unit) and 0.0115 g (0.0507 mmol) DDQ were reacted in 0.50 mL CD_2Cl_2 according to the General Aromatization Procedure. Polymer is insoluble in CH_2Cl_2 and even toluene-d_8 at 100 °C. ^{1}H NMR (toluene-d_8, 500 MHz): δ 8.7-7.6 (br, m), 6.7-6.4 (br), 4.1-3.3 (br, m), 1.5-1.0 (br, m), 1.0-0.7 (br, m).

5,8-bis(2-ethyl-hexyloxy)-PNV (4b). lab notebook: 4-234-1. Polymer **12b** (0.0.0488 g, 0.118 mmol per repeat unit) and 0.0355 g (0.156 mmol) DDQ were reacted

in 1.0 mL CD_2Cl_2 according to the General Aromatization Procedure. ^1H NMR (CD_2Cl_2, 500 MHz): δ 8.3-6.3 (br, m), 4.3 (br s), 1.91, 1.59, 1.41, 1.03, 0.96, 0.75 (br, m).

5,8-dioctyloxy-PNV (4c). lab notebook: 5-009-1. Polymer **12c** (0.0.0148 g, 0.0360 mmol per repeat unit) and 0.0093 g (0.0410 mmol) DDQ were reacted in 0.60 mL CD_2Cl_2 according to the General Aromatization Procedure. ^1H NMR (CD_2Cl_2, 500 MHz): δ 8.3-6.2 (br, m), 4.1 (br), 2.0-0.5 (br, m).

(5). lab notebook: 4-045-1. A flask was charged with 3.64 g (0.0182 mol) **2** and 2.10 g (0.0194 mol) freshly sublimed 1,4-benzoquinone and backfilled with argon. This was dissolved in THF and heated to reflux for 24 h. The solvent was removed *in vacuo*, then excess 1,4-benziquinone was removed by room temperature sublimation in a static vacuum of less than 100 mTorr leaving 5.38 g (~90% crude) **5** as a light yellow powder. ^1H NMR (C_6D_6, 300 MHz): δ 7.49 (d, J = 7 Hz, 2H), 7.13 (m, 3H), 6.02 (s, 2H), 5.87 (d, J = 4 Hz, 1H), 5.88 (d, J = 4 Hz, 1H), 5.48 (s, 1H), 3.72 (s, 2H), 3.60 (m, 2H), 2.01 (s, 2H). ^{13}C NMR ($CDCl_3$, 125 MHz): δ 197.2, 142.1, 142.1, 113.3, 129.9, 128.4, 127.5, 103.4, 78.15, 44.56, 39.59.

5,8-diethoxy-1,2,3,4-tetrahydro-2,3-(benzylidenedixoy)-1,4-ethenonaphthalene (6a). lab notebook: 4-047-2, 4-064-1. Prior to reaction, DMSO was dried over 4 Å molecular sieves and degassed; iodoethane was shaken twice with aqueous $Na_2S_2O_3$, dried over $CaCl_2$, and degassed; and KOH was powdered with mortar and pestle. A flask was charged with 5.37 g (0.0174 mol) **5**, backfilled with argon, dissolved in 70 mL DMSO, followed by the addition of 9.5 mL (0.119 mol) iodoethane. The flask was protected from direct light and after stirring for 25 min, 2.2 g (0.0392 mol) powdered KOH was added and the solution became immediately deep red. After 1 h, 5.0

mL (0.0625 mol) more iodoethane was added and stirring was continted for 23 h. To the solution was added 50 mL water then extracted with 6 x 30 mL CH_2Cl_2 then once with 30 mL water to remove DMSO from the organic layer. Both organic and aqueous layers were red due to the presence of iodine. The organic layer was concentrated under reduced pressure and the residue purified by chromatography (12 in.) eluting with 5% ethyl acetate in hexanes, affording 1.50-1.75 g (26-30%) of **6a** as a tan powder. ^{1}H NMR (C_6D_6, 300 MHz): δ 7.59 (dd, J = 8, 2 Hz, 2H), 7.15 (m, 3H), 6.49 (d, J = 1 Hz, 1H), 6.50 (d, J = 4 Hz, 1H), 6.45 (s, 2H), 5.63 (s, 1H), 5.06 (m, 2H), 4.27 (s, 2H), 3.72-3.57 (m, 4H), 1.14 (t, J = 7 Hz, 6H). ^{13}C NMR (C_6D_6, 75 MHz): δ 149.2, 138.0, 133.6, 131.0, 129.4, 128.2, 128.0, 110.6, 106.3, 79.72, 64.35, 39.18, 14.99.

5,8-bis(2-ethyl-hexyloxy)-1,2,3,4-tetrahydro-2,3-(benzylidenedixoy)-1,4-ethenonaphthalene (6b). Method A. lab notebook: 4-114-2. Prior to reaction, DMSO was dried over 4 Å molecular sieves and degassed; alkyliodide was washed three times with aqueous $Na_2S_2O_3$, dried over $CaCl_2$, filtered through alumina, and degassed; and KOH was powdered with mortar and pestle. The reaction was carried out as for **6a** except using 5.01 g (0.0162 mol) **5**, 20.0 mL (0.100 mol) 1-iodo-2-ethylhexane then 13.0 mL (0.0650 mol) more, and 2.04 g (0.0364 mol) KOH. After column chromatography, 1.51 g (17%) **6b** was obtained as a yellow viscous liquid. ^{1}H NMR (C_6D_6, 300 MHz): δ 7.60 (d, J = 7 Hz, 2H), 7.16 (m, 3H), 6.61 (s, 2H), 6.50 (m, 2H), 5.65 (s, 1H), 5.07 (s, 2H), 4.29 (s, 2H), 3.7 (m, 4H), 1.69 (m, 2H), 1.44 (m, 4H), 1.27 (m, 12H), 0.902 (t, 12 H).

Method B. lab notebook: 4-162-2. Reagents purified as mentioned for Method A. A flask was charged with 0.97 g (0.00313 mol) **5**, backfilled with argon, dissolved in

20 mL DMSO, then 4.20 mL (0.0210 mol) 1-iodo-2-ethylhexane was added. After 5 min, 0.049 g (0.873 mmol) KOH was added and the solution became red-orange. Additional aliquots of 0.20 g (0.00356 mol), 0.057 g (0.00102 mol), 0.113 g (0.00201 mol), and 0.080 g (0.00143 mol) KOH (0.499 g total, 0.00889 mol) were added at 0.5 h, 1.5 h, 2 h, and 4.9 h, respectively. After 5 hr, 3.0 mL (0.0150 mol) more 1-iodo-2-ethylhexane was added and stirring continued 11 more hours. The entire DMSO solution was loaded onto a silica gel column (12 in.), and the desired product was isolated by eluting with 5% ethyl acetate in hexanes. Yield: 0.49 g (29%).

Method C. lab notebook: 4-167-4. Reagents purified as mentioned for Method A. A flask was charged with 0.974 g (0.00316 mol) **5**, backfilled with argon, dissolved in 20 mL DMSO, then 4.20 mL (0.0210 mol) 1-iodo-2-ethylhexane was added. After 5 min, 0.025 g (0.00104 mol) LiOH (powdered) was added and the solution became red-brown. Additional aliquots of 0.030 g (0.00125 mol), 0.046 g (0.00192 mol), 0.057 g (0.00238 mol), and 0.035 g (0.00146 mol) LiOH (0.193 g total, 0.00806 mol) were added at 0.4 h, 0.9 h, 1.9 h, and 4.4 h, respectively, followed by stirring an additional 11 h at room temp. The entire DMSO solution was loaded onto a silica gel column (12 in.), and the desired product was isolated by eluting with 5% ethyl acetate in hexanes. Yield: 0.605 g (36%).

5,8-bis(octyloxy)-1,2,3,4-tetrahydro-2,3-(benzylidenedixoy)-1,4-ethenonaphthalene (6c). lab notebook: 4-274-3, 4-286-2. Prior to reaction, DMSO was dried over 4 Å molecular sieves and degassed, and bromooctane was dried over K_2CO_3, passed through a plug of silica gel, then degassed. A flask was charged with 0.90 g (0.00292 mol) **5**, backfilled with argon, dissolved in 20 mL DMSO, then 2.80 mL (0.0162 mol) 1-bromooctane was added. After 5 min, 0.022 g (0.000919 mol) LiOH

(powdered) was added and the solution became deep red within a minute. Additional aliquots of 0.023 g (0.000960 mol), 0.028 g (0.00117 mol), 0.042 g (0.00175 mol), 0.037 g (0.00154 mol), and 0.018 g (0.000752 mol) LiOH (0.170 g total, 0.00710 mol) were added at 0.3 h, 0.7 h, 2.5 h, 3.4, and 3.9 h, respectively. An additional 2.5 mL (0.0145 mol) 1-bromooctane was added 3.7 hr after starting the reaction, followed by stirring an additional 11 h at room temp. Water (20 mL) was added to the reaction, it was extracted with 5 x 15 mL CH_2Cl_2, and concentrated revealing the presence of a large amount of DMSO. The desired product was isolated by column chromatography, eluting with 5% ethyl acetate in hexanes. Yield: 1.189 g (74%). ^{1}H NMR (C_6D_6, 300 MHz): δ 7.57 (dd, *J* = 8, 2 Hz, 2H), 7.14 (m, 3H), 6.55 (s, 2H), 6.50, (d, *J* = 4 Hz, 1H), 6.49 (d, *J* = 4 Hz, 1H), 5.63 (s, 1H), 5.05 (s, 2H), 4.28 (s, 2H), 3.72 (m, 4H), 1.67 (m, 4H), 1.39 (m, 4H), 1.30 (s, 16 H), 0.90 (t, 6H). ^{13}C NMR ($CDCl_3$, 75 MHz): δ 149.9, 138.4, 134.0, 131.6, 129.7, 128.6, 128,3, 111.3, 106.8, 80.18, 69.59, 39.61, 32.59, 30.15, 30.15, 30.05, 26.89, 23.42, 14.71.

Poly(3,6-diethoxy-benzobarrelene) (12a). Method A. lab notebook: 4-141-2. Monomer **3a** (0.0527 g, 0.217 mmol) was reacted with 0.0033 g (0.00432 mmol) initiator **8a** in 0.50 mL C_6D_6 according to the General ROMP Procedure.

Method B. lab notebook: 4-056-3. Monomer **3a** (0.0588 g, 0.243 mmol) was reacted with 0.0038 g (0.00497 mmol) initiator **8a** and 0.0092 mL (0.0748 mmol) HFB in 0.50 mL C_6D_6 according to the General ROMP Procedure.

Method C. lab notebook: 4-072. Monomer **3a** (0.0551 g, 0.227 mmol) was reacted with 0.0033 g (0.00503 mmol) initiator **8b** in 0.50 mL C_6D_6 according to the General ROMP Procedure. ^{1}H NMR ($CDCl_3$, 500 MHz, all peaks are broad): δ 6.60

(2H), 5.81 (2H), 5.51, 5.40 (2H), 4.22 (2H), 3.90-3.33 (4H), 1.38-0.88 (6H). ^{13}C NMR ($CDCl_3$, 125 MHz, all peaks are broad): δ 150.7 (m), 132.2 (m), 128.9-127.4 (m), 109.5-109.1 (m), 64.15, 39.10 (m), 15.47-14.73 (m).

Poly(3,6-bis(2-ethyl-hexyloxy)-benzobarrelene) (12b). Method A. lab notebook: 4-142-3. Monomer **3b** (0.0689 g, 0.168 mmol) was reacted with 0.0031 g (0.00406 mmol) initiator **8a** in 0.50 mL C_6D_6 according to the General ROMP Procedure.

Method B. lab notebook: 4-123-6, 4-137-4. Monomer **3b** (0.0720 g, 0.175 mmol) was reacted with 0.0031 g (0.00406 mmol) initiator **8a** and 0.0075 mL (0.0610 mmol) HFB in 0.50 mL C_6D_6 according to the General ROMP Procedure. ^1H NMR (C_6D_6, 500 MHz, all peaks are broad): δ 6.78, 6.61, 5.98, 5.37 (6H), 4.60, 4.44, 3.94, 3.81 (6H), 2.09, 1.95-1.51, 1.40, 1.00 (30H). ^{13}C NMR ($CDCl_3$, 125 MHz, all peaks are broad): δ 150.8, 131.8 (m), 128.9, 127.8, 109.1, 108.5, 71.82, 70.50, 39.25, 38.79, 34.67, 30.31, 28.95, 23.78, 23.38,14.33, 10.90.

Method C. lab notebook: 4-148-4, 4-232-3. Monomer **3b** (0.0863 g, 0.210 mmol) was reacted with 0.0034 g (0.00518 mmol) initiator **8b** in 0.50 mL C_6D_6 according to the General ROMP Procedure.

Poly(3,6-bis(octyloxy)-benzobarrelene) (12c). Method B. lab notebook: 4-296-6. Monomer **3c** (0.0691 g, 0.168 mmol) was reacted with 0.0043 g (0.00497 mmol) initiator **8a** and 0.0102 mL (0.0829 mmol) HFB in 0.60 mL C_6D_6 according to the General ROMP Procedure. ^1H NMR ($CDCl_3$, 300 MHz): δ 6.60, 6.47, 6.36, 6.12, 6.04, 5.76, 5.64, 5.44, 5.28, 5.09, 4.98 (6H), 4.02, 3.83, 3.63 (6H), 1.81, 1.64, 1.25, 0.85, 0.83 (30H). ^{13}C NMR ($CDCl_3$, 75 MHz): δ 152.3 (br), 134.1 (br), 127.5 (br), 126.0 (br), 107.9 (br), 67.40 (br), 38.0 (br), 35.0 (br), 32.20, 29.68, 29.56, 26.45, 22.86, 14.37.

(powdered) was added and the solution became deep red within a minute. Additional aliquots of 0.023 g (0.000960 mol), 0.028 g (0.00117 mol), 0.042 g (0.00175 mol), 0.037 g (0.00154 mol), and 0.018 g (0.000752 mol) LiOH (0.170 g total, 0.00710 mol) were added at 0.3 h, 0.7 h, 2.5 h, 3.4, and 3.9 h, respectively. An additional 2.5 mL (0.0145 mol) 1-bromooctane was added 3.7 hr after starting the reaction, followed by stirring an additional 11 h at room temp. Water (20 mL) was added to the reaction, it was extracted with 5 x 15 mL CH_2Cl_2, and concentrated revealing the presence of a large amount of DMSO. The desired product was isolated by column chromatography, eluting with 5% ethyl acetate in hexanes. Yield: 1.189 g (74%). ^{1}H NMR (C_6D_6, 300 MHz): δ 7.57 (dd, *J* = 8, 2 Hz, 2H), 7.14 (m, 3H), 6.55 (s, 2H), 6.50, (d, *J* = 4 Hz, 1H), 6.49 (d, *J* = 4 Hz, 1H), 5.63 (s, 1H), 5.05 (s, 2H), 4.28 (s, 2H), 3.72 (m, 4H), 1.67 (m, 4H), 1.39 (m, 4H), 1.30 (s, 16 H), 0.90 (t, 6H). ^{13}C NMR ($CDCl_3$, 75 MHz): δ 149.9, 138.4, 134.0, 131.6, 129.7, 128.6, 128,3, 111.3, 106.8, 80.18, 69.59, 39.61, 32.59, 30.15, 30.15, 30.05, 26.89, 23.42, 14.71.

Poly(3,6-diethoxy-benzobarrelene) (12a). Method A. lab notebook: 4-141-2. Monomer **3a** (0.0527 g, 0.217 mmol) was reacted with 0.0033 g (0.00432 mmol) initiator **8a** in 0.50 mL C_6D_6 according to the General ROMP Procedure.

Method B. lab notebook: 4-056-3. Monomer **3a** (0.0588 g, 0.243 mmol) was reacted with 0.0038 g (0.00497 mmol) initiator **8a** and 0.0092 mL (0.0748 mmol) HFB in 0.50 mL C_6D_6 according to the General ROMP Procedure.

Method C. lab notebook: 4-072. Monomer **3a** (0.0551 g, 0.227 mmol) was reacted with 0.0033 g (0.00503 mmol) initiator **8b** in 0.50 mL C_6D_6 according to the General ROMP Procedure. ^{1}H NMR ($CDCl_3$, 500 MHz, all peaks are broad): δ 6.60

(2H), 5.81 (2H), 5.51, 5.40 (2H), 4.22 (2H), 3.90-3.33 (4H), 1.38-0.88 (6H). ^{13}C NMR ($CDCl_3$, 125 MHz, all peaks are broad): δ 150.7 (m), 132.2 (m), 128.9-127.4 (m), 109.5-109.1 (m), 64.15, 39.10 (m), 15.47-14.73 (m).

Poly(3,6-bis(2-ethyl-hexyloxy)-benzobarrelene) (12b). Method A. lab notebook: 4-142-3. Monomer **3b** (0.0689 g, 0.168 mmol) was reacted with 0.0031 g (0.00406 mmol) initiator **8a** in 0.50 mL C_6D_6 according to the General ROMP Procedure.

Method B. lab notebook: 4-123-6, 4-137-4. Monomer **3b** (0.0720 g, 0.175 mmol) was reacted with 0.0031 g (0.00406 mmol) initiator **8a** and 0.0075 mL (0.0610 mmol) HFB in 0.50 mL C_6D_6 according to the General ROMP Procedure. ^1H NMR (C_6D_6, 500 MHz, all peaks are broad): δ 6.78, 6.61, 5.98, 5.37 (6H), 4.60, 4.44, 3.94, 3.81 (6H), 2.09, 1.95-1.51, 1.40, 1.00 (30H). ^{13}C NMR ($CDCl_3$, 125 MHz, all peaks are broad): δ 150.8, 131.8 (m), 128.9, 127.8, 109.1, 108.5, 71.82, 70.50, 39.25, 38.79, 34.67, 30.31, 28.95, 23.78, 23.38,14.33, 10.90.

Method C. lab notebook: 4-148-4, 4-232-3. Monomer **3b** (0.0863 g, 0.210 mmol) was reacted with 0.0034 g (0.00518 mmol) initiator **8b** in 0.50 mL C_6D_6 according to the General ROMP Procedure.

Poly(3,6-bis(octyloxy)-benzobarrelene) (12c). Method B. lab notebook: 4-296-6. Monomer **3c** (0.0691 g, 0.168 mmol) was reacted with 0.0043 g (0.00497 mmol) initiator **8a** and 0.0102 mL (0.0829 mmol) HFB in 0.60 mL C_6D_6 according to the General ROMP Procedure. ^1H NMR ($CDCl_3$, 300 MHz): δ 6.60, 6.47, 6.36, 6.12, 6.04, 5.76, 5.64, 5.44, 5.28, 5.09, 4.98 (6H), 4.02, 3.83, 3.63 (6H), 1.81, 1.64, 1.25, 0.85, 0.83 (30H). ^{13}C NMR ($CDCl_3$, 75 MHz): δ 152.3 (br), 134.1 (br), 127.5 (br), 126.0 (br), 107.9 (br), 67.40 (br), 38.0 (br), 35.0 (br), 32.20, 29.68, 29.56, 26.45, 22.86, 14.37.

Method C. lab notebook: 4-294-4. Monomer **3c** (0.0675 g, 0.164 mmol) was reacted with 0.0036 g (0.00549 mmol) initiator **8b** in 0.60 mL C_6D_6 according to the General ROMP Procedure.

5,8-bis(2-ethyl-hexyloxy)-PNV-*block*-5,8-diethoxy-PNV (16). lab notebook: 4-272-5, 4-280-2. In the drybox, a vial was charged with 0.0033 g (0.00503 mmol) **8b** and dissolved in 0.10 mL C_6D_6. A second vial was charged with 0.0818 g (0.199 mmol) **3b**, dissolved in 0.50 mL C_6D_6, then added to the catalyst solution and swirled to ensure rapid mixing. The solution was transferred to an NMR tube with a teflon valve seal, and the reaction monitored by ^{1}H NMR. After 3.1 h, polymerization was complete. The NMR tube was taken back into the drybox and a small amount (~30 μL) was taken out, quenched with benzaldehyde, and after later precipitation into methanol, analyzed by GPC (M_n = 6,500; PDI = 1.34). The rest of the NMR solution was poured into a vial containing 0.0242 g (0.0999 mmol) **3a** dissolved in 0.10 mL C_6D_6 and swirled rapidly to ensure mixing. The solution was transferred back to the NMR tube and analyzed by NMR spectroscopy. The polymer was quenched, precipitated, and purified as outlined in the General ROMP Procedure above. ^{1}H NMR ($CDCl_3$, 500 MHz): δ 6.7-6.5 (br, m, 2H), 6.0-5.2 (br, m, 4H), 4.4-3.2 (br, m, 6H), 1.9-0.4 (br, m, 30H). ^{13}C NMR ($CDCl_3$, 125 MHz): δ 105.9 (br), 132.4 (br), 128.3 (br), 109.8-108.9 (br, m), 70.91 (br), 64.22 (br), 39.27 (br), 30.83 (br), 29.38 (br), 23.99 (br), 23.39, 15.19 (br, m), 14.28, 11.16 (br).

For aromatization, the polymer (0.0165 g, 0.0465 mmol per repeat unit) and 0.0123 g (0.0542 mmol) DDQ were reacted according to the General Procedure for Polymer Aromatization above. **16** ^{1}H NMR (CD_2Cl_2, 300 MHz): δ 8.5-7.2 (br, m), 7.0-6.4 (br, m), 4.00, 3.6 (br, m), 2.0-0.2 (br, m).

6,7-bis(octyloxy)-PNV (17). lab notebook: 5-078-2. Carried out according to General Procedure for Polymer Aromatization. Polymer **21** (0.0177 g, 0.0431 mmol per repeat unit) and 0.0104 g (0.0458 mmol) DDQ were reacted in 0.70 mL CD_2Cl_2. The solution became red, and polymer precipitated immediately; aromatization reached only 80-90% completion due to low solubility. ^{1}H NMR (CD_2Cl_2, 500 MHz, all peaks are broad): δ 8.0-7.0 (m), 6.60, 5.77, 4.15, 3.85, 2.1-0.6 (m).

4,5-bis(octyloxy)-tricyclo[6.2.2.0^{2,7}]dodeca-2,4,6,9,11-pentaene or 4,5-bis(octyloxy)-benzobarrelene **(18).** lab notebook: 5-066-5. Reaction carried out analogously to the synthesis of **3a** except using 0.179 g (0.335 mmol) **19**, 1.06 g (9.47 mmol) potassium-*t*-butoxide in 35 mL ether, and 31.0 mL (8.75 mmol) of a 0.282 M solution of LDA in ether. The LDA solution was added in 2-8 mL aliquots every 15-20 minutes. CAUTION: the addition if LDA is very exothermic and should be handled slowly and with great care. The product was isolated by column chromatography (12 in.) eluting with 5% ethyl acetate in hexanes. Yield: 0.090 g (65%). ^{1}H NMR (C_6D_6, 500 MHz): δ 6.83 (s, 2H), 6.76 (t, J = 4 Hz, 4H), 4.54 (m, 2H), 3.85 (t, J = 6 Hz, 4H), 1.71 (m, 4H), 1.44 (m, 4H), 1.25 (br, 20H), 0.90 (t, J = 7 Hz, 6H). ^{13}C NMR (C_6D_6, 125 MHz): δ 146.4, 141.8, 140.6, 112.8, 70.96, 49.66, 32.59, 30.64, 30.17, 30.08, 26.96, 23.40, 14.63.

6,7-bis(octyloxy)-1,2,3,4-tetrahydro-2,3-(benzylidenedixoy)-1,4-ethenonaphthalene (19). lab notebook: 5-060-7. Separate flasks were charged with 0.61 g (0.00305 mol) **2** and 1.518 g (0.00308 mol) 1,2-dibromo-4,5-dioctyloxybenzene and dried *in vacuo*. To the first flask was added 40 mL THF to dissolve the diene and this transferred to the second flask. After cooling to –78 °C, 2.1 mL (0.00378 mol) *n*-

butyllithium (1.8 M in hexanes) was added over 3 min. The solution became dark yellow and remained so during the next 2.7 h at –78 to –60 °C. At this time TLC (10% ethyl acetate in hexanes) showed there to be much starting material present. An additional 2.0 mL (0.00360 mol) butyllithium solution was added in spurts over 30 min. The –60 °C solution had become orangish and opaque. After 20 min, the cold bath was removed and the solution allowed to warm to room temperature. The solution became homogeneous, and 45 min after removing the cold bath, TLC showed decreased starting material (R_f = 0.39, 10% ethyl acetate in hexanes), but starting materials were also present, though in decreased content. The solution was cooled back to –60 °C, and 2.0 mL (0.00360 mol) more butyllithium was added dropwise over 5 min. The cold bath was removed and the solution allowed to warm to room temperature and stir a few hours. To the solution was added 30 mL water and 30 mL ether, and the organic layer was washed with 2 x 20 mL saturated aqueous NaCl, then the aqueous layer was washed with 20 mL ether. The combined organic layers were dried over $MgSO_4$, filtered, and concentrated. The desired product was isolated by column chromatography eluting with a solvent gradient of hexanes, 2% ethyl acetate in hexanes, 4% ethyl acetate in hexanes, then 6% ethyl acetate in hexanes. Yield: 0.099 g (6%). ^{1}H NMR (C_6D_6, 300 MHz): δ 7.68 (d J = 7 Hz, 2H), 7.23 (m, 3H), 6.69 (s, 2H), 6.53 (t, 2H), 5.77 (s, 1H), 4.25 (s, 2H), 4.06 (br, 2H), 3.80 (t, 4H), 1.75 (p, 4H), 1.48 (br, m, 4H), 1.27 (br, 16H), 0.91 (t, 6H). ^{13}C NMR (C_6D_6, 75 MHz): δ 148.6, 138.3, 134.0, 133.6, 129.8, 128.5, 128.3, 112.7, 106.9, 80.81, 70.04, 45.86, 32.72, 30.38, 30.17, 30.13, 26.96, 23.47, 14.75.

Poly(4,5-bis(octyloxy)-tricyclo[6.2.2.0^{2,7}]dodeca-2,4,6,9,11-pentaene) (21). lab notebook: 5-074-1. Carried out according to the General ROMP Procedure. Monomer

18 (0.0442 g, 0.108 mmol) was reacted with 0.0028 g (0.00427 mmol) initiator **8b** in 0.70 mL C_6D_6. ^1H NMR ($CDCl_3$, 500 MHz, all peaks are broad): δ 6.64 (2H), 5.76 (2H), 5.46 (2H), 3.92-3.87 (m, 6H), 1.77 (4H), 1.45 (4H), 1.29 (16 H), 0.88 (6H). ^{13}C NMR ($CDCl_3$, 125 MHz): δ 148.3, 134.2, 128.5, 128.1, 114.6, 69.69, 43.21, 32.12, 29.74, 29.56, 26.43, 22.90, 14.28.

Table 6. Absorbance spectroscopy data for conjugated polymers.[a]

polymer	solvent	λ_{max} (nm)	ε_{max} (M^{-1} cm^{-1}) (per repeat unit)	ε_{max} (M^{-1} cm^{-1}) (total)
4b	C_6H_6	352	7600	310,000
		390	7500	307,000
4b	$CHCl_3$	350	6500	265,000
		388	6100	252,000
4b	THF	356	8100	332,000
		396	9200	379,000
4b	CH_2Cl_2	338	9300	381,000
		386	8300	341,000
4c	CH_2Cl_2	354	5500	164,000
		408	5600	169,000
16	CH_2Cl_2	356	3700	221,000
		408	3900	233,000
17	CH_2Cl_2	372	7100	179,000
		434	9900	248,000

[a] Data recorded at room temperature.

References and Notes

1. Hörhold, H. H.; Opfermann, J. *Makromol. Chem.* **1970**, *131*, 105.
2. Kraft, A.; Grimsdale, A. C.; Holmes, A. B. *Angew. Chem., Int. Ed.* **1998**, *37*, 402.

3. Dodabalapur, A. *Solid State Commun.* **1997**, *102*, 259.

4. Lovinger, A. J. *J. Mater. Res.* **1996**, *11*, 3174.

5. a) Pei, Q.; Yu, G.; Zhang, C.; Yang, Y.; Heeger, A. J. *Science* **1995**, *269*, 108. b) Pei, Q.; Yang, Y.; Yu, G.; Zhang, C.; Heeger, A. J. *J. Am. Chem. Soc.* **1996**, *118*, 3922.

6. (a) Karasz, F. E.; Capistran, J. D.; Gagnon, D. R.; Lenz, R. W.; *Mol. Cryst. Liq. Cryst.* **1985**, *118*, 327. (b) Jin, J.-I.; Park, C.-K. *Macromolecules* **1993**, *26*, 1799.

7. Jullien, L.; Canceill, J.; Valeur, B.; Bardez, E.; Lefevre, J.-P.; Lehn, J.-M.; Marchi-Artzner, V.; Pansu, R. *J. Am. Chem. Soc.* **1996**, *118*, 5432.

8. a) Devadoss, C.; Bharathi, P.; Moore, J. S. *J. Am. Chem. Soc.* **1996**, *118*, 9635. b) Shortreed, M. R.; Swallen, S. F.; Shi, Z.-Y.; Tan, W.; Xu, Z.; Devadoss, C.; Moore, J. S.; Kopelman, R. *J. Phys. Chem. B* **1997**, *101*, 6318.

9. Swager, T. M.; Gil, C. J.; Wrighton, M. S. *J. Phys. Chem. B* **1995**, *99*, 4886.

10. Berggren, M.; Dodabalapur, A.; Slusher, R. E.; Bao, Z. *Nature* **1997**, *389*, 466.

11. Tasch, S.; List, E. J. W.; Hochfilzer, C.; Leising, G.; Schlichting, P.; Rohr, U.; Geerts, Y.; Scherf, U.; Müllen *Phys. Rev. B* **1997**, *56*, 4479.

12. Holzer, L.; Winkler, B.; Wenzl, F. P.; Tasch, S.; Dai, L.; Mau, A. W. H.; Leising, G. *Synth. Met.* **1999**, *100*, 71.

13. Kimura, M.; Horai, T.; Hanabusa, K.; Shirai, H. *Adv. Mater.* **1998**, *10*, 459.

14. a) Yoon, C. B.; Shim, H. K. *J. Mater. Chem.* **1998**, *8*, 913. b) Klarner, G.; Former, C.; Martin, K.; Rader, J.; Mullen, K. *Macromolecules* **1998**, *31*, 3571.

15. Hide, F.; Schwartz, B. J.; Diaz-Garcia, M. A.; Heeger, A. J. *Chem. Phys. Lett.* **1996**, *256,* 424.

16. Berggren, M.; Dodabalapur, A.; Slusher, R. E.; Bao, Z. *Synth. Met.* **1997**, *91,* 65.

17. Murase, I.; Ohnishi, T.; Noguchi, T.; Hirooka, M. *Polym. Commun.* **1984**, *25*, 327.

18. Onoda, M.; Morita, S.; Iwasa, T.; Nakayama, H.; Amakawa, K.; Yoshino, K. *J. Phys. D: Appl. Phys.* **1991**, *24*, 1152.

19. Onoda, M.; Uchida, M.; Ohmori, Y.; Yoshino, K. *Jpn. J. Appl. Phys.* **1993**, *32*, 3895.

20. Onoda, M.; Nakayama, H.; Ohmori, Y.; Yoshino, K. *IEICE Trans. Electron.* **1994**, *E77-C*, 672.

21. Onoda, M.; Ohmori, Y.; Kawai, T.; Yoshino K. *Synth. Met.* **1995**, *71*, 2181.

22. This nomenclature means that a 200 nm-thick layer of PNV is sandwiched between an ITO anode and magnesium-indium cathode.

23. For more on LEDs and conjugated polymer emitters, see Chapter 2.

24. The turn-on voltage of an LED is the minimum applied voltage required to induce light emission.

25. Tasch, S.; Graupner, W.; Leising, G.; Pu, L.; Wagaman, M. W.; Grubbs, R. H. *Adv. Mater.* **1995**, *7*, 903.

26. Pu, L.; Wagaman, M. W.; Grubbs, R. H. *Macromolecules* **1996**, *29*, 1138.

27. Wagaman, M. W.; Grubbs, R. H. *Synth. Met.* **1997**, *84*, 327.

28. Wagaman, M. W.; Bellmann, E.; Grubbs, R. H. *Phil. Trans. R. Soc. Lond. A* **1997**, *355*, 727.

29. Kido, J. *Trends Polym. Sci.* **1994**, *2*, 350.

30. Hide, F.; Días-García, M. A.; Schwartz, B. J.; Heeger, A. J. *Acc. Chem. Res.* **1997**, *30*, 430.

31. Wagaman, M. .W.; Bellmann, E.; Cucullu, M.; Grubbs, R. H. *J. Org. Chem.* **1997**, *62*, 9076.

32. Wagaman, M. W.; Grubbs, R. H. *Macromolecules* **1997**, *30*, 3978.

33. The net conversion is a Diels-Alder reaction of benzene with a benzyne (or alkyne). However, since benzene is not an active enough diene to react efficiently with most dieneophiles, *cis*-cyclohexadienediol is used with subsequent conversion of the vicinal diol to a double bond.

34. This product is unstable to silica gel chromatography. Wagaman, M. W.; Grubbs, R. H., unpublished results.

35. For a list of references see Larock, R. C. *Comprehensive Organic Transformations: A Guide to Functional Group Preparations*; VCH: New York, 1989; p 155.

36. Fox, H. H.; Lee, J.-K.; Park, L. Y.; Cai, S.; Schrock, R. R. *Organometallics* **1992**, *12*, 759.

37. Oskam, J. H.; Fox, H. H.; Yap, K. B.; McConville, D. H.; O'Dell, R.; Lichenstein, B. J.; Schrock, R. R. *J. Organomet. Chem.* **1993**, *459*, 185.

38. Wagaman, M. W.; Elder, D. L.; Grubbs, R. H. unpublished results.

39. All alkylidene resonances observed by ^{1}H NMR spectroscopy were broad, as is generally the case with macromolecules.

40. See Chapter 1 for more details.

41. Feldman, J.; Schrock, R. R. *Prog. Inorg.Chem.* **1991**, *39*, 1.

42. Ivin, K. J.; Mol, J. C. *Olefin Metathesis and Metathesis Polymerization*; Academic Press: San Diego, 1997.

43. (a) Fujimura, O.; Gu, G. C.; Grubbs, R. H. *J. Org. Chem.* **1994**, *59*, 4029. (b) Fujimura, O.; Fu, G. C.; Rothermung, P. W. K.; Grubbs, R. H. *J. Am. Chem. Soc.* **1995**, *117*, 2355.

44. We suggest that the more active one is in lower concentration because if that were not the case, very little low molecular weight polymer should be observed since the initiator responsible would be both slow and in lesser concentration.

45. We cannot rule out the possibility of overlapping alkylidene resonances.

46. Molecular weights and PDI are relative to polystyrene standards.

47. Schrock, R. R. *Polyhedron* **1995**, *14*, 3177.

48. Monomer **3c** was not polymerized without HFB present, but based on data with **3b**, the outcome would have been similar.

49. Wagaman, M. W. Ph.D. Thesis, California Institute of Technology, 1997.

50. (a) Jin, J.-I.; Park, C.-K.; Shim, H.-K. *Macromolecules* **1993**, *26*, 1799. (b) Jin, J.-I.; Lee, Y.-H.; Shim, H.-K. *Macromolecules* **1993**, *26*, 1805.

51. Meyers, F.; Heeger, A. J.; Bredas, J. L. *J. Chem. Phys.* **1992**, *97*, 2750.

52. Burn, P. L.; Kraft, A.; Baigent, D. R.; Bradley, D. D. C.; Brown, A. R.; Friend, R. H.; Gymer, R. W.; Holmes, A. B.; Jackson, R. W. *J. Am. Chem. Soc.* **1993**, *115*, 10117.

53. Silverstein, R. M.; Bassler, G. C.; Morrill, T. C. *Spectrometric Identification of Organic Compounds*, 5th ed., John Wiley & Sons: New York, 1991; pp 289-315.

54. For more details on block copolymer synthesis, see Chapter 4.

55. Baigent, D. R.; Greenham, N. C.; Gruner, J.; Marks, R. N.; Friend, R. H. *Synth. Met.* **1994**, *67*, 3.

56. Gettinger, C. L.; Heeger, A. J. *J. Chem. Phys.* **1994**, *101*, 1673.

57. (a) Kreyenschmidt, M.; Klaerner, G.; Fuhrer, T.; Ashenhurst, J.; Karg, S.; Chen, W. D.; Lee, V. Y.; Scott, J. C.; Miller, R. D. *Macromolecules* **1998**, *31*, 1099. (b) Klaerner, G.; Davey, M. H.; Chen, W. D.; Scott, J. C.; Miller, R. D. *Chem. Mater.* **1998**, *10*, 993.

58. See Lide, D. R.; Frederikse, H. P. R. *CRC Handbook of Chemistry and Physics*; CRC Press: Boca Raton, 1995, and references therein.

59. Actually, quantum yield is often larger in conjugated polymers with partial unsaturation than in fully conjugated ones.[32,52]

60. The following reference was used for help with NMR spectra interpretation: Silverstein, R. M.; Bassler, G. C.; Morrill, T. C. *Spectrometric Identification of Organic Compounds*, 5th ed., John Wiley & Sons: New York, 1991; pp 165-265.

61. Pangborn, A. B.; Giardello, M. A.; Grubbs, R. H.; Rosen, R. K.; Timmers, F. J. *Organometallics* **1996**, *15*, 1518.

62. Pu, L.; Grubbs, R. H. *J. Org. Chem.* **1994**, *59*, 1351.

63. Cotterill, I. C.; Roberts, S. M.; Williams, J. O. *J. Chem. Soc., Chem. Commun.* **1988**, 1628.

64. Polymers are very slightly air-sensitive, and care is taken to not expose them to large amounts of air during work-up. Thus degassed solvents are used and polymer is kept under argon during purification. Also, polymer is kept under argon for long-term storage.

65. (a) Nakamaru, K. *Bull. Chem. Soc. Jpn.* **1982**, *55*, 2697. (b) Juris, A.; Balzani, V. *Coord. Chem. Rev.* **1988**, *84*, 85.

Chapter 4

Synthesis of PPV/PNV Block Copolymers and Random Copolymers and Observations of Photoluminescence Quantum Yield Enhancements by an Energy Transfer Mechanism

Abstract

Poly(*p*-phenylenevinylene)/poly(1,4-naphthalenevinylene) (PPV/PNV) block copolymers 2,3-di-*tert*-butylester-PPV-*block*-5,8-dialkoxy-PNV (**24-block**) and 5,8-dialkoxy-PNV-*block*-6-alkyl-PNV (**33**) and random copolymers 2,3-di-*tert*-butylester-PPV-*random*-5,8-dialkoxy-PNV (**24-rand**) have been synthesized by living ring-opening metathesis polymerization (ROMP), using the initiator $Mo(CHCMe_2Ph)(N\text{-}2,6\text{-}C_6H_3\text{-}{}^{i}Pr_2)(OCMe_2(CF_3))_2$ (**19b**), followed by DDQ aromatization. This ROMP-Aromatization Route is a mild synthesis procedure and provides polymers of controlled molecular weight that are low in polydispersity and soluble in common organic solvents such as methylene chloride and chloroform. The diester-PPV segments ($\lambda_{max,em}$ = 490 nm) have a larger HOMO-LUMO gap than the dialkoxy-PNV segments ($\lambda_{max,em}$ = 534-546 nm) allowing the polymer to be able to execute through bond (non-Förster) energy transfer. Upon photoexcitation of the large band gap segments, the block copolymers **24b-block**, **24c-block**, and **28** however do not display energy transfer, but the random copolymers **24a-c-rand** do display energy transfer of 50% to greater than 98% efficiency. Remarkably, in the case of **24c-rand**, the photoluminescence efficiency from the dialkoxy-PNV segments is increased by a factor of 2 over that of the parent homopolymer, to 18%. Block copolymer **33** also displays efficient energy transfer upon photoexcitation of the larger band gap dialkoxy-PNV block, and emission from the alkyl-PNV block occurs with an efficiency of 5%, a 10-fold enhancement over the alkyl-PNV homopolymer. This copolymer strategy should be a general technique to increase the quantum efficiency of polyarylenevinylenes.

Introduction

One of the issues facing luminescent polymers for light-emitting diode (LED) applications is their emission efficiency (quantum yield), or how much light is given off relative to the energy put in.[1,2,3] The highest LED external quantum efficiencies reported are 4-5% (at 100 cd/m^2 brightness[4]), and 2% or greater has been reported for red,[5] green,[6,7] and blue[8] emitters suitable for color mixing to give a full-color display.[3] However, improvements are still necessary and are being sought vigorously in order to discover materials with improved film-forming properties, long-term stability, and which are cheaper to fabricate. For more information on LEDs and light-emitting polymers, see Chapter 2.

Researchers have worked on methods to increase the efficiency of conjugated polymers, particularly poly(*p*-phenylenevinylene) (PPV) derivatives. One of these methods involves decreasing luminescence quenching by decreasing the conjugation length of the polymer.[9,10] For example Friend and coworkers have shown that the partially conjugated random copolymer **1** has a twofold greater electroluminescence efficiency than PPV, and random copolymer **2** has a 30-fold improvement in efficiency (Figure 1).[9] This enhancement is presumably due to prevention of exitons (conjugated polymer excited states) from migrating and accessing the entire polymer backbone (since it is not conjugated) and locating potential quenching sites. Though significantly

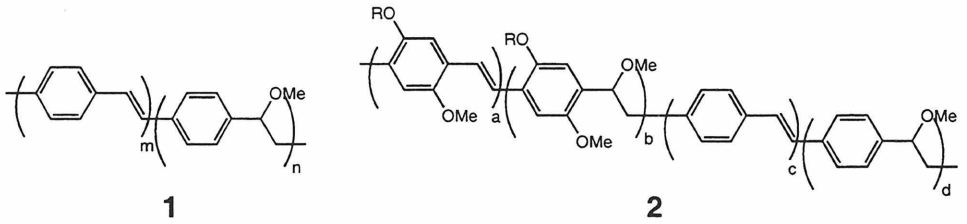

1 **2**

Figure 1. Partially conjugated PPV derivatives.

increasing the emission quantum yield, this method is somewhat disadvantageous in that it increases the content of insulating material in the polymer, thus higher voltages will be required to transport charges (for electroluminescence).

The second example increases enhancement by introducing disorder in PPV by increasing the number of *cis* vinylene units producing a polymer such as **3**.[11] Polymer **3** is produced by a thermal elimination at 170 °C from a particular precursor polymer that yields a high ratio of *cis* double bonds (Figure 2). The *cis* units decrease the conjugation length of the polymer, thereby preventing exitons from locating quenching sites, and increasing the electroluminescence efficiency by a factor of two. However, the efficiency is very sensitive to *cis* content and drops below that of PPV if the temperature of xanthane elimination is more than 10 °C above or below 170 °C.[11]

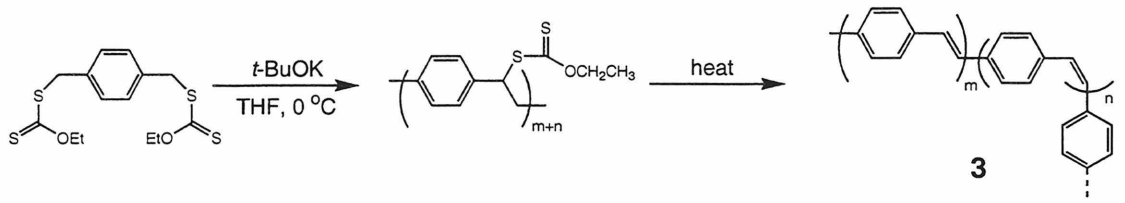

Figure 2. Synthesis of PPV with a high content of *cis* vinylene units.

The third example involves the use of polymer multilayers in the LED device.[12,13,14,15] Rubner, Schrock, and coworkers fabricated LEDs by dip-coating alternately water-soluble, cationic PPV precursor polymer **4** and anionic polymer **5** or **6** from aqueous solutions onto ITO (indium tin oxide) coated glass slides (Figures 3 and 4). Approximately 20 polymer bilayers (or multiple bilayers) were deposited, followed by thermal conversion of the precursor polymer **4** to PPV. On top of this was spin cast emissive polymer **7**, **8**, or **9**, then a metal cathode layer was deposited by vacuum evaporation. LEDs fabricated in this fashion behave (current-Voltage characteristics for

example) just as LEDs with spin-coated polymers. The PPV/polyanion structure (LED type B, Figure 4) enhances the electroluminescence emission of **7** by a factor of 47 and decreases the turn on voltage from 22 to 12 V.[16] The type B LED also enhances the emission of random copolymer **8** by a factor of 18 and decreases the turn on voltage from 21 to 8 V, and enhances the emission of random copolymer **9** by a factor of 11 and decreases the turn on voltage from 13 to 6 V (Table 1).[15] Though there have been a few examples displaying the benefits of polymer multilayer structures in LEDs, why it is beneficial is not well-understood. Also, this strategy does not alter the intrinsic emissive ability of the luminescing polymer, rather it applies only to LED fabrication.

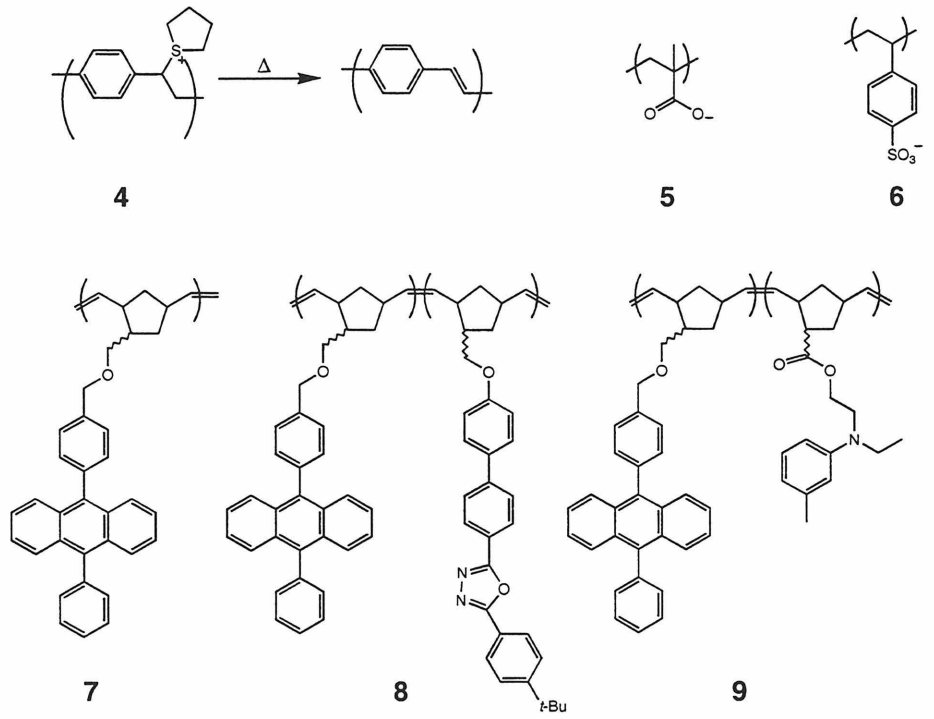

Figure 3. Water-soluble PPV precursor (**4**), anionic polymers (**5** and **6**), and emissive polymers (**7**, **8**, and **9**) used in the multi-bilayer LEDs of Figure 4.

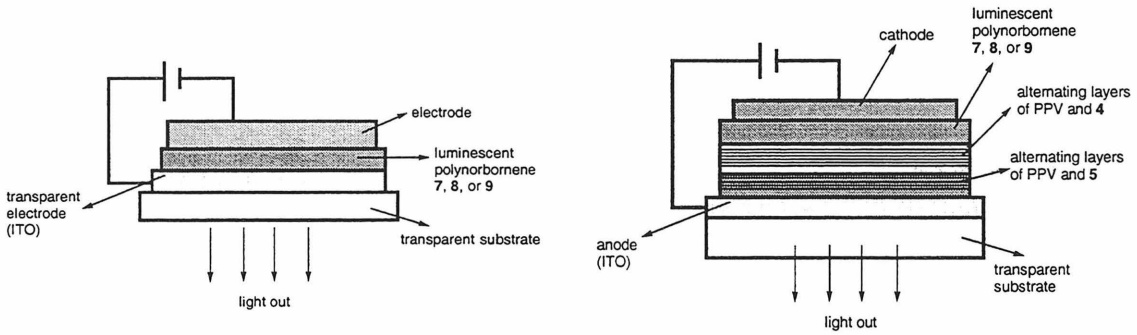

Figure 4. Single layer LED (Type A) and a multiple bilayer LED (Type B).

Table 1. LED performance of type A or type B LEDs using emissive polymers **7**, **8**, or **9**.

emissive polymer	device type	% external quantum yield (x 10^{-4})	turn on voltage (V)
7	type A	0.0034	22
7	type B	0.16	12
8	type A	0.19	21
8	type B	3.5	8
9	type A	0.48	13
9	type B	5.4	6

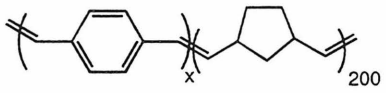

x = 10, 20, 30, 40

10

Figure 5. PPV/polynorbornene block copolymer.

The fourth strategy reveals that quantum yield may be increased by dispersing the emitting material—polymer or small molecule—in a non-conjugated polymer matrix.[17,50] An example by Bazan and coworkers measures the efficiency of PPV/polynorbornene block copolymers (**10**) as a function of the relative length of the polynorbornene block (Figure 5). As the ratio of norbornene to PPV repeat units is increased from 5:1 to 6.7:1 to 10:1 to 20:1 (varying the length of the PPV segment and holding the norbornene block constant at a much longer 200 repeat units), the solid state photoluminescence quantum

yield increases from 8% to 30% to 45% to 51%.[17] The luminescence increases because the polynorbornene segments prevent the emissive PPV segments from aggregating and forming non-emissive or weakly emissive eximers. Alternatively, bulky polymer side chains or end groups have been incorporated successfully to prevent polymer aggregation and increase efficiency.[18,19,20] One drawback of this method is that it incorporates a large amount of non-conjugated polymer, which results in low charge mobilities and high drive voltages in electroluminescent devices.

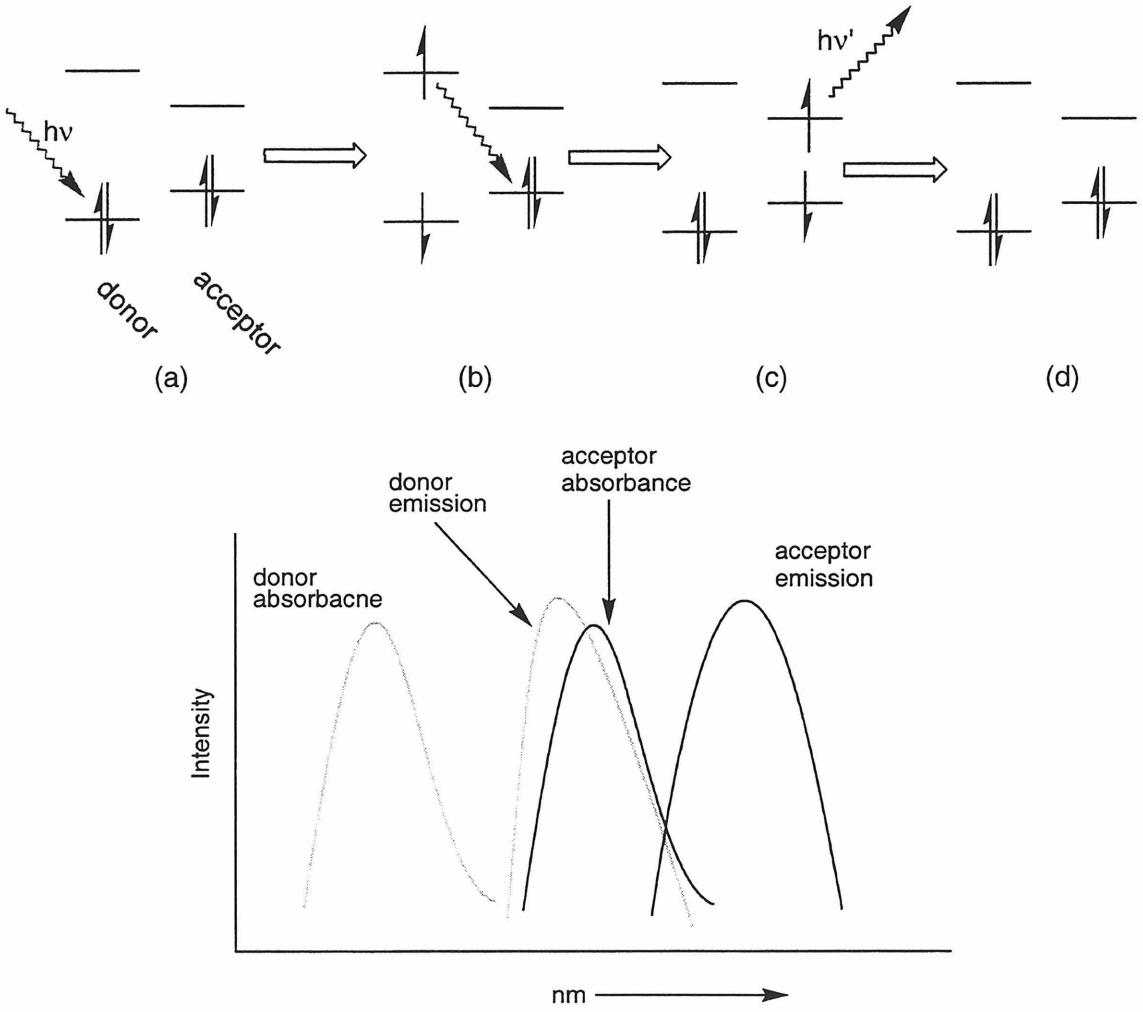

Figure 6. (a) Excitation, (b) energy transfer, (c) emission, (d) ground state. (e) Plot showing the overlap of donor emission spectra and acceptor spectra required for Förster energy transfer.

One of the most widely used and most successful approaches to efficiency enhancement depends on energy transfer.[21,22,23,24,25] In energy transfer, two (or more) emissive components are utilized: One component (donor) is excited, then emits and the second molecule (acceptor) absorbs that radiation, as long as the absorbance band overlaps with the emission band of the donor (Figure 6).[26,27] This is called Förster energy transfer. The second acceptor becomes excited and emits. Förster energy transfer is distance dependant but can be quite efficient for distances from 10–60 Å.[28,29,30] One important requirement is that the acceptor molecule should have a smaller HOMO-LUMO gap[31] than the donor so that the energy transfer will be thermodynamically downhill. Emission from polymers or small molecules using the energy transfer strategy can be more efficient than exciting the acceptor alone due to elimination of concentration quenching and elimination of limitations due to low absorption extinction coefficients.[60]

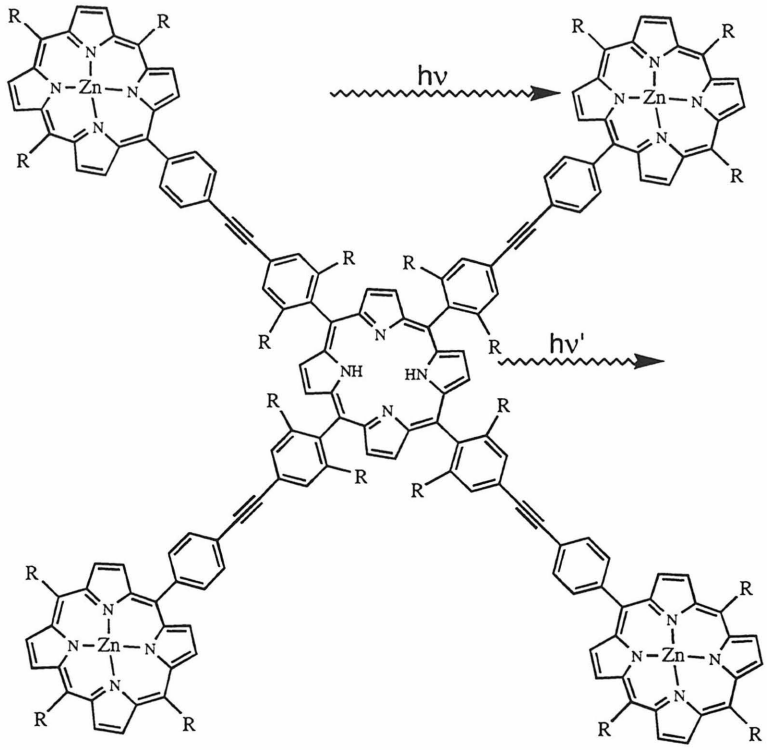

Figure 7. Light harvesting porphyrin array. Excitation of the periphery Zn porphyrins results in energy transfer and emission from the central core.

Researchers have long sought after ways to design molecular light harvesting assemblages for artificial photosynthesis systems that utilize energy transfer mechanisms.[32,33] Lindsey and coworkers synthesized the light harvesting porphyrin array shown in Figure 7 and showed that solution photoexcitation of the periphery Zn porphyrins results in 90% efficient energy transfer to and almost exclusive emission from the central free base porphyrin.[34] Kopelman, Moore, and coworkers observed the same phenomenon in a fourth generation phenylene ethynylene dendron containing a perylene dye at the core (Figure 8).[35] Upon exciting the phenylene ethynylene backbone, energy transfer occurs with greater than 98% efficiency, and emission is observed from the perylene chromophore. Remarkably, the quantum yield is increased by a factor of three over that of the perylene alone. Many others have observed similar energy funneling effects in dendrimeric systems.[32b,36,37,38,39,40]

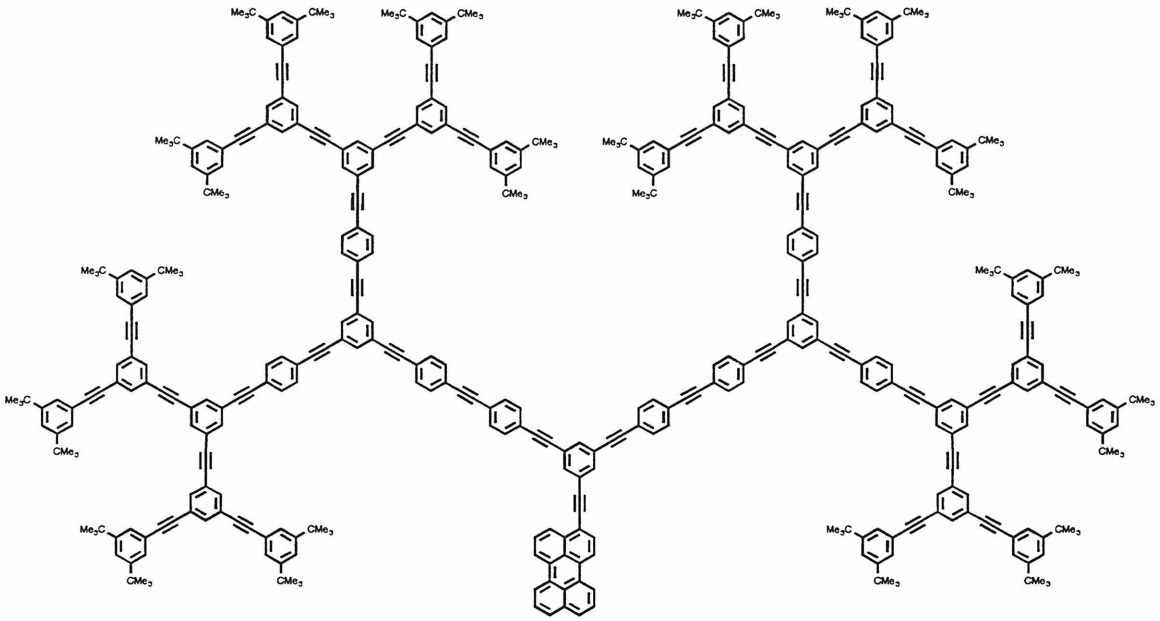

Figure 8. Dendrimer "energy funnel." Excitation of the phenylene ethynylene backbone results in emission from the core chromophore.

Wrighton, Swager, and coworkers reported similar results in the *linear* conjugated polymer shown in Figure 9. Photolysis of the phenylene ethynylene backbone at 450 nm results in > 95% efficient energy transfer to the anthracenyl end groups and emission at 524 nm.[41]

The above three examples are of photoinduced energy transfer, but the same effect has been observed in electroexcited systems.[42] In LEDs, instead of having a single layer[43] device (Figure 10a), the donor and acceptor components are often in separate layers (Figures 10b and 10c).[44] PPVs tend to be better at transporting holes than electrons,[45] so materials with high electron affinities such as Alq or an oxadiazole compound such as PBD are often used as the electron transport layer (ETL) (Figures 10b and 11). In this configuration, charge is injected from the cathode to the ETL, and at the ETL/emitter interface, energy transfer occurs, exciting the PPV, and stimulating emission.[46] This double layer configuration can typically result in quantum efficiency

enhancements of an order of magnitude or more than observed from a single layer device.[2,3,42,47]

If an emitter is used which is a good electron transporter, a hole transport layer (HTL) is used to balance charge injection (Figure 10c). Aryl amines such as TPD and the polymer PVK are often used (Figure 11).[7,42,48] The energy transfer mechanism is similarly operative at the HTL/emitter interface. Three layer devices—containing a HTL, emitter, and ETL—have also been successfully utilized (Figure 10d), again with efficiency enhancements of an order of magnitude or more.[42,49]

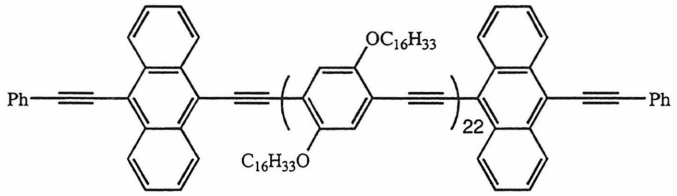

Figure 9. Poly(phenyleneethynylene) with anthracenyl end groups. Excitation of the phenylene ethynylene backbone results in energy transfer and emission from the end groups.

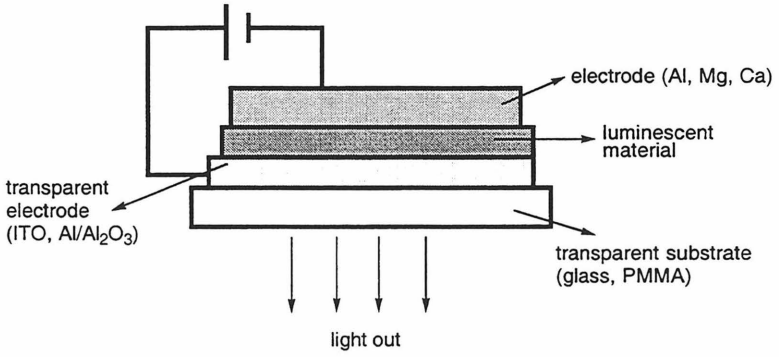

Figure 10a. Single layer LED.

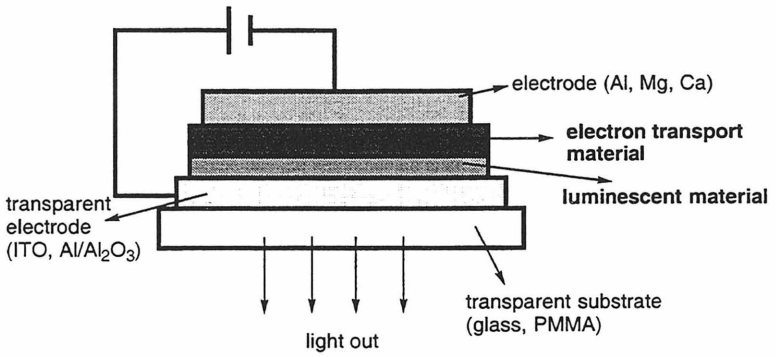

Figure 10b. Double layer LED with an electron transport layer.

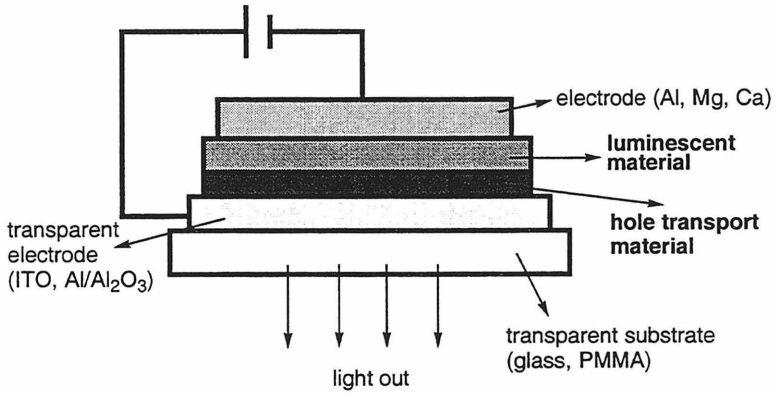

Figure 10c. Double layer LED with a hole transport layer.

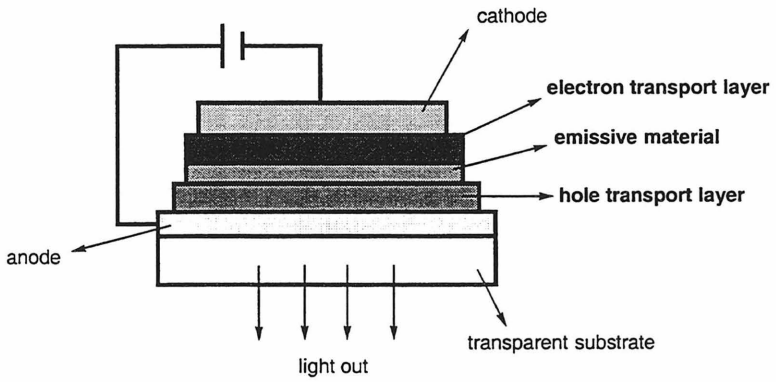

Figure 10d. Triple layer LED.

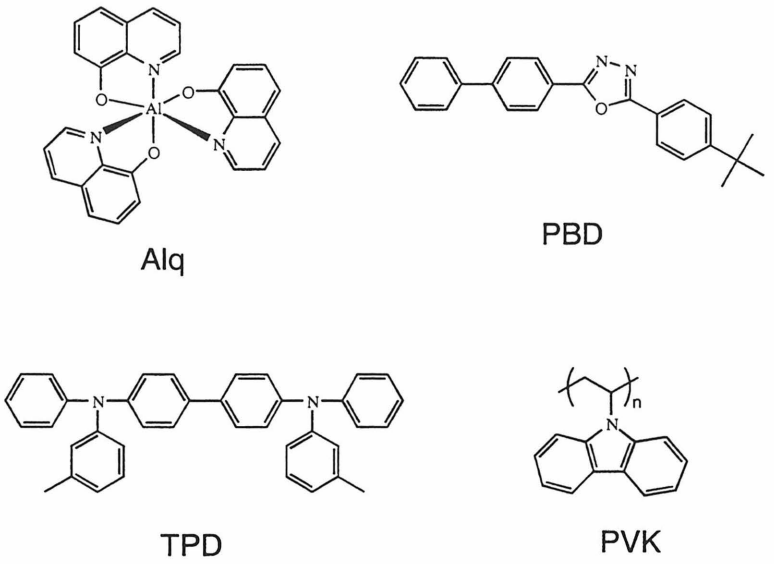

Figure 11. Electron transport materials (Alq and PBD) and hole transport materials (TPD and PVK).

Researchers have explored combining the transport materials and emitters into a single layer.[50,51,52,53] As an example, the emissive layer may be a spin cast film made up of a dye molecule such as C6 dispersed (0.2 wt%) in a matrix of electron transport material (PBD, 28.5 wt%) and hole transport polymer (PVK, 71.3 wt%) (Figure 12).[52] The ratios of components can be easily varied to optimize electron and hole recombination events (which occur by energy transfer just as in the multilayer devices) at the dye molecules leading to emission.[46] Multicomponent single layer LEDs of this type can be orders of magnitude more efficient than single component, single layer LEDs, and as efficient as multilayer LEDs.

Multicomponent single layer LEDs are not limited to dispersion of small molecules in polymer matricies, indeed, polymer emitters and transport materials work as well.[54,55] However, problems can arise with phase separation in the polymer components. To circumvent this problem, the transport material may be covalently attached to the emissive polymer.[56,57,58] For example polymers **11** and **12** containing oxadiazole electron

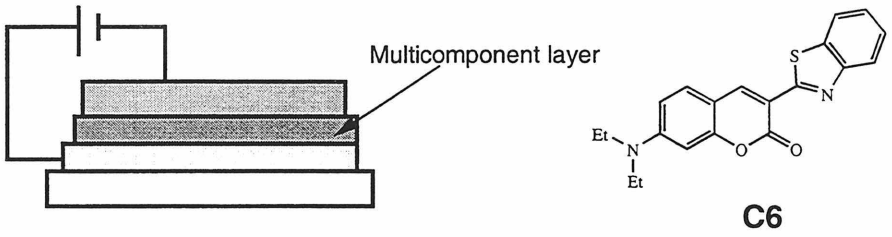

C6

Figure 12. Multicomponent single layer LED. Layer contains emissive material as well as transport molecules.

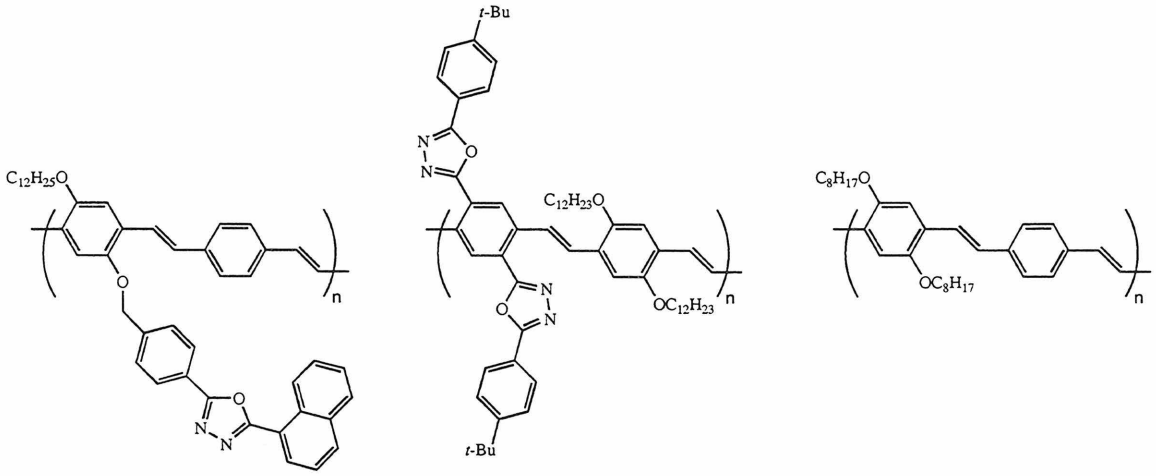

11 **12** **13**

Figure 13. PPVs with covalently attached electron transport moieties (**11**-**13**) and the parent polymer (**13**).

transport moieties as side groups displayed external quantum efficiencies of 0.020% and 0.045%, and turn on voltages of 9.8 V and 8 V, respectively, in single layer LEDs compared to the 0.002% efficiency and 14 V turn on voltage of the parent polymer **13** (Figure 13).[56,58] It has been confirmed that PPV excitation is occurring by an energy transfer mechanism in these materials.[56]

These examples show that conjugated macromolecules able to display energy transfer do have advantages in luminescence applications, however, these materials can be improved upon. Though energy transfer is very efficient, the porphyrin array in

Figure 7 and the anthracene terminated poly(phenyleneethynylene) in Figure 9, they do not yield efficiency enhancements over what is observed with the chromophores alone.[34,41] The perylene-cored dendrimer in Figure 8 does display efficiency enhancement, but we would like to be able to display such enhancements in the more popular and successful arylenevinylene polymers.

Considering all of this as background and motivation for our work, we wanted to focus on the possibility of boosting efficiency through energy transfer in arylenevinylene polymers *in which the donor and acceptor moieties are in conjugation with one another* (Figure 14).[59] Our plan is different from most of those previously mentioned in that energy transfer does not occur in a Förster transfer-type mechanism which is a "through space" incident and depends on overlap of the donor emission band and the acceptor absorption band.[30] Rather, if the donor and acceptor are in conjugation, as in the macromolecules shown in Figures 7-9, energy transfer may occur by exiton migration "through bond," and this type of excitation can be more efficient over long distances.[60,61]

We should emphasize that construction of the copolymer **14** in Figure 14 should be a *general* strategy to increase the quantum yield of any polyarylenevinylene as long as a sufficient large band gap (donor) polyarylenevinylene can be identified. Furthermore, we would like to investigate random- and block-copolymers of **14** and compare their

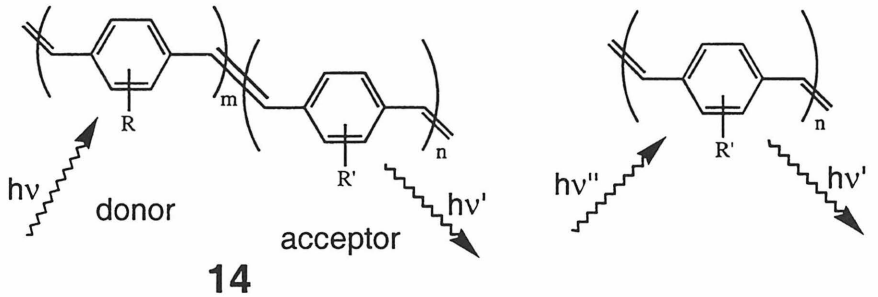

Figure 14. Donor and acceptor segments in a polyarylenevinylene copolymer.

energy transfer and efficiency enhancement abilities. This is notable because to our knowledge, no one has employed diblock arylenevinylene copolymers in LEDs. The routes typically used to synthesize PPVs (see Chapter 2) cannot produce block copolymers. However, the polymerization method we use, ring-opening metathesis polymerization (ROMP)[62] is a living[63] polymerization procedure and can readily produce block copolymers by sequential addition of monomers (Figure 15).[64]

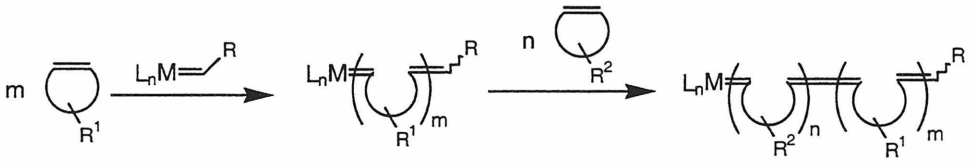

Figure 15. Synthesis of block copolymers by ROMP.

Results and Discussion

Copolymer Synthesis

Careful design of the copolymer components was necessary to be able to show unambiguous energy transfer and still have the system be general and applicable to future development. One would like the emission bands of the two polyarylenevinylene (PAV) components to occur at widely different wavelengths so that it is easy to distinguish which block is emmitting. Also, one would like the large band gap segment to be a blue emitter to accommodate a variety of PAVs which may emit anywhere from the blue to red parts of the visible spectrum (energy transfer will occur efficiently only to smaller band gap segments, that is, from blue shifted emitters to red shifter emitters). Since we are using the living ROMP polymerization method, we must select from the PAVs previously synthesized by ROMP, which are shown in Figure 7 of Chapter 2.[10,65,66,67,68] The diester-PPV (**16**) is the best choice in that it is a blue emitter ($\lambda_{max,em}$ = 490 nm), has

a very strong solution photoluminescence quantum efficiency (~100%), and is more soluble in common organic solvents than the other blue emitting PPVs containing fluoroalkyls (Figure 16).[10]

For the small band gap emitter, we wanted an electron-rich PAV, as it is known that electron donating substituents decrease the HOMO-LUMO gap in PAVs, red shifting the emission.[69] We chose the recently developed dialkoxy poly(1,4-naphthalenevinylene)s (PNVs) (**18**) to fulfill this role (Figure 17).[70] Besides having red shifted emission ($\lambda_{max,em}$ = 534-541 nm), the quantum yields are moderately low (7-15%), leaving room for significant enhancements.

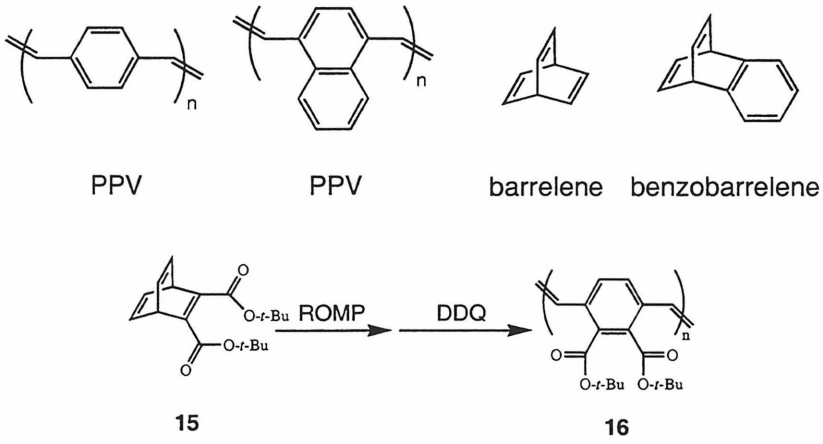

Figure 16. ROMP-Aromatization synthesis of diester-PPV.

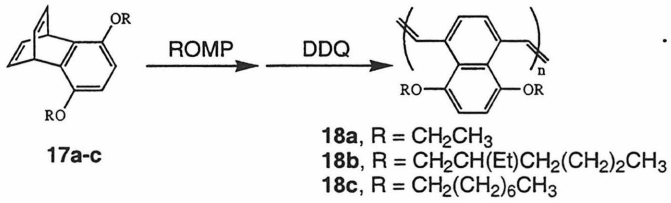

Figure 17. ROMP-Aromatization synthesis of dialkoxy-PNV.

A number of well-defined, single component ROMP initiators are available for use, principally the more popular **19** and **20** (Figure 18),[71,88,89] and we have chosen the

molybdenum complex **19b** for two particular reasons. One of the thermodynamic driving forces for ROMP is the relief of ring strain,[62] and we have discovered that **20** is not active enough to polymerize low strain monomers such as **15** and **17** effectively. Initiator **19b** is used instead of the more common **19a** because **19a**, for reasons which are still not completely understood, always produces two propagating alkylidenes in solution when polymerizing **17a-c**, leading to **18a-c** with bimodal molecular weight distributions (see Chapter 3).[72] Polymerizations with initiator **19b** are well behaved and produce monomodal molecular weight distributions and low polydispersity indices (PDIs) in the ROMP of **15** and **17a-c**.

Block copolymers are synthesized as shown in Figure 19. Monomer **15** is polymerized first because it initiates better than **17**.[73] Reactions are carried out on a small scale in C_6D_6 solvent and monitored by ^1H NMR. Initiation is rapid and complete in less than 10 minutes, and propagation takes about 2 h to reach completion for 20 equivalents of monomer. A few drops of solution are removed for GPC analysis before addition of the second monomer. Low PDIs of 1.14 – 1.15 in CH_2Cl_2 (1.17 – 1.20 in THF) relative to polystyrene standards were observed for **21** in all cases (Table 2). ROMP of 20

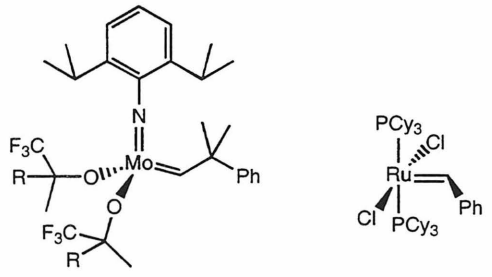

19a, R = CF_3
19b, R = CH_3

20

Figure 18. Popular single-component ROMP initiators.

equivalents of **17a** is rapid and complete within 15 min. Initiation is also relatively rapid,[74] as the PDI of copolymer **22a** was found to be 1.3. ROMP of **17b** and **17c** was slower, requiring 2-3 h for 20-30 equivalents and 7 h for 60 equivalents of **17b**. In all cases, initiation reached completion in 20 minutes or less. PDIs of **22b** and **22c** were in all cases slightly lower (1.12 - 1.21) than achieved in **22a** (Table 2). Prior to polymer purification by precipitation into methanol, the metal complexes were quenched and cleaved from the polymers through reaction with benzaldehyde.[62] All polymerization yields were quantitative by NMR spectroscopy and polymers were soluble in common organic solvents such as C_6H_6, CH_2Cl_2, $CHCl_3$, and THF. Polymers were treated as if slightly oxygen sensitive, degassed solvents were used for washing and dissolving, and polymers were kept in nitrogen or argon environments for long-term storage.

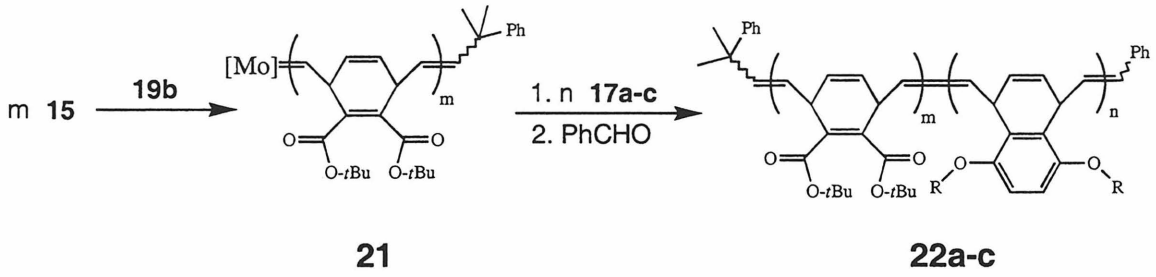

Figure 19. Block copolymer synthesis by ROMP.

Table 2. Polymerization data for block copolymers.

polymer	m [a]	n [b]	PDI [c] (block 1)	PDI [c] (copolymer)	M_n [c]	MW (theory)
22a	20	20	1.14	1.30	16,600	10,900
22b	30	30	1.15	1.17	14,300	21,500
22b2	30	60	1.14	1.12	26,800	33,800
22b3	40	20	-	1.16	22,700	20,400
22c	20	20	1.15	1.21	11,700	14,300
22c2	10	20	1.20[d] (1.18)[e]	1.19	8600	11,300
22c3	5	20	1.17[d] (1.15)[e]	1.23	8300	9730
27	10	20	-	1.44	11,000	19,400
32	50	100	1.47	2.09	71,000	51,000

[a] Number of repeat units diester-PPV segments in copolymers. [b] Number of repeat units of dialkoxy-PNV isegments in copolymers. [c] PDI and molecular weight data are relative to polystyrene standards and were measured by GPC in CH_2Cl_2 unless mentioned otherwise. [d] Measured in THF relative to polystyrene standards. [e] Measured in THF relative to poly(methylmethacrylate) standards.

Random copolymers **23a-c** were synthesized by polymerizing 1:1 ratios of monomers simultaneously (Figure 20).[75] Polymerizations were monitored by NMR revealing that initiation was rapid, and **15** and **17** were consumed at similar rates. This (along with the NMR evidence in the next paragraph) gives us confidence that the repeat units are distributed fairly randomly. Reactions were completed within 4 h then quenched as mentioned above for the block copolymers. Solubilities of **23** were the same as **22**.

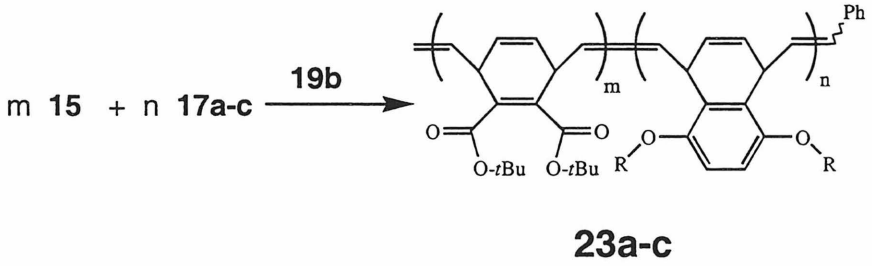

23a-c

Figure 20. Random copolymer synthesis by ROMP.

Table 3. Polymerization data for random copolymers.

polymer	m, n	PDI [a]	M_n [a]	MW (theory)
23a	25	-[b]	-[b]	13,700
23b	35	1.16	23,100	25,000
23c	20	1.18	12,900	14,300

[a] PDI and molecular weight data are relative to polystyrene standards and were measured in CH_2Cl_2. [b] The polymer was insoluble in GPC solvents so the PDI and molecular weight was not determined.

The random and block copolymers can be distinguished by ^{1}H NMR as illustrated by the spectra of **22c** and **23c** ($CDCl_3$ solvent) in Figure 21. The chemical shift differences are slight, however, what is most notable is the peak width. In the block copolymer, resonances from the poly(**15**) block are sharp, while those of poly(**17c**) are broader.[76] In the random copolymer, resonances from both segments are similarly broadened. This contrast suggests that the monomer incorporation in the random copolymers is random or consists of short blocks of varying lengths, and the broadness of the signals is evidence against an alternating copolymer: One would expect sharper signals if a regular chemical and magnetic environment was maintained. A similar conclusion can be deduced by analysis of the ^{13}C NMR spectra of **22c** and **23c** (Figure 22): The block copolymer spectrum displays narrow peaks for poly(**15**) and broad ones for poly(**17c**), while the random copolymer spectrum shows broad peaks for both units.[76]

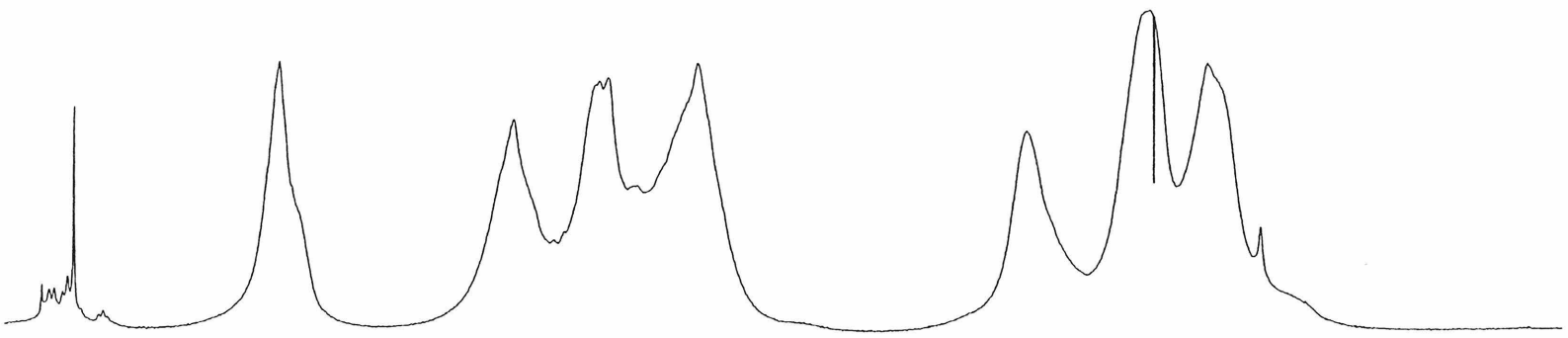

Figure 21a. ^{1}H NMR Spectrum of random copolymer **23c**.

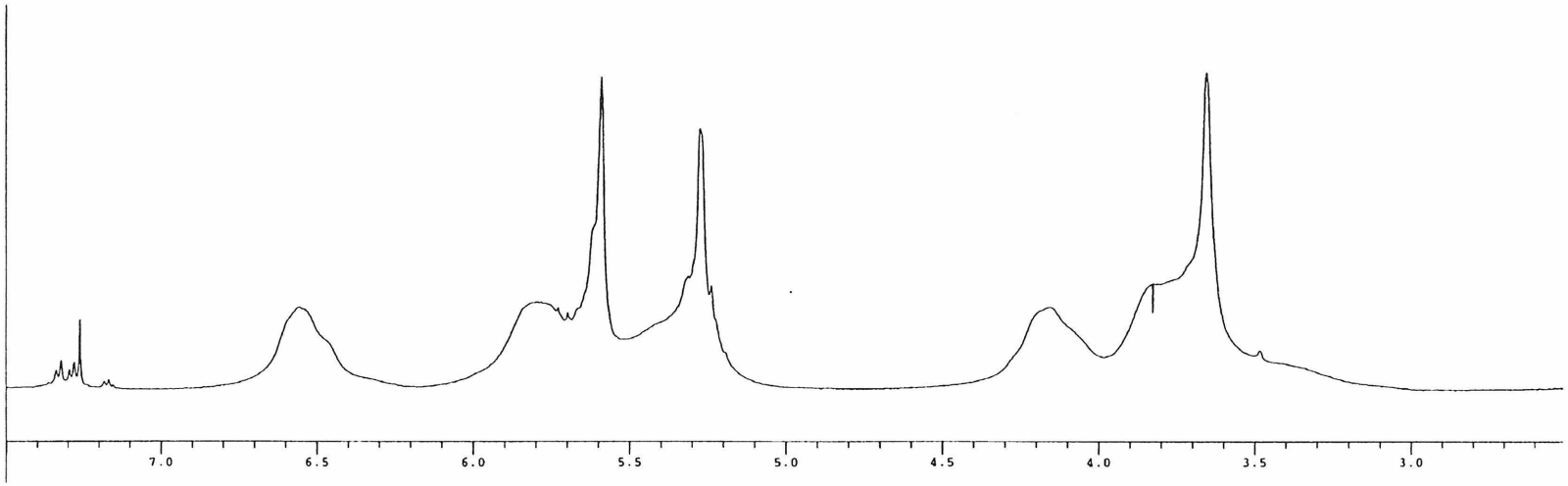

Figure 21b. ^{1}H NMR Spectrum of block copolymer **22c**.

Figure 22a. ^{13}C NMR Spectrum of random copolymer **23c**.

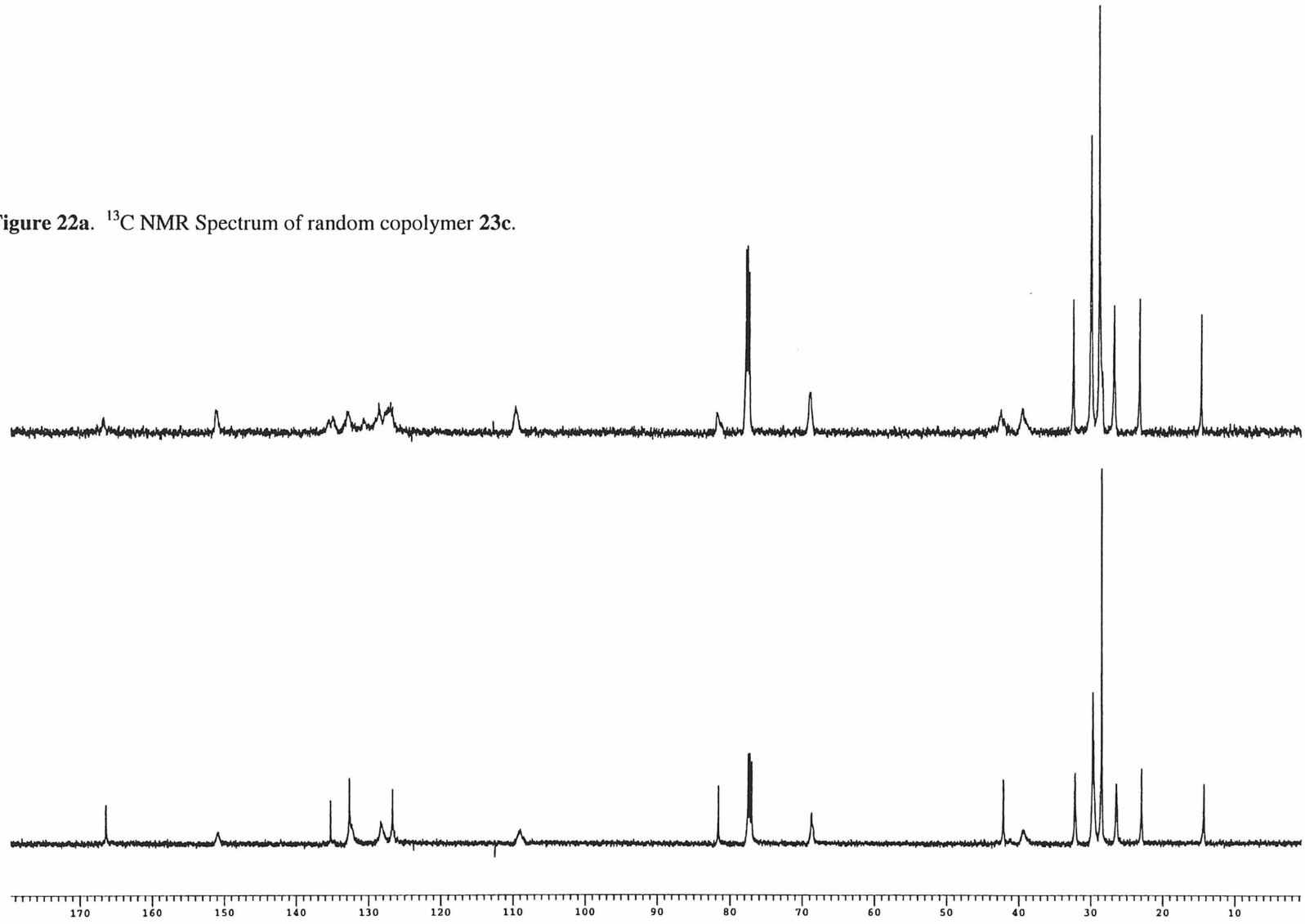

Figure 22b. ^{13}C NMR Spectrum of block copolymer **22c**.

The final step of PAV synthesis, aromatization, is carried out in the same fashion for block- and random copolymers (Figure 23). The oxidant 2,3-dichloro-5,6-dicyano-1,4-benzoquinone (DDQ) is used, and it operates by abstracting two hydrogen radicals from each polymer repeat unit. The reaction was carried out in CD_2Cl_2 and monitored by ^1H NMR for disappearance of olefin signals. Excess DDQ was used (1.2 – 2 equivalents) to ensure complete aromatization. When 2 equivalents were used, the reaction was rapid and complete within 10 min. When 1.2 equivalents were used, the more electron-rich dialkoxy segments aromatized rapidly (10 min), but the electron-poor diester segments took 2 - 6 h to reach full aromatization. Polymers **24a-block** and **24a-rand** crashed out of solution during aromatization and were only sparingly soluble in other solvents such as C_6H_6, $C_6H_5CH_3$, $CHCl_3$, and THF. To bypass this solubility problem, **26-block** was synthesized as shown in Figure 24. This triblock copolymer is meant to emulate **24a-block**, and the terminal dioctyloxy-PNV block serves only to aid solubility.[77] The other polymers (**24b-c-block** and **24b-c-rand**), containing longer alkoxy side chains, remained soluble, and even after precipitation could be readily redissolved in the solvents

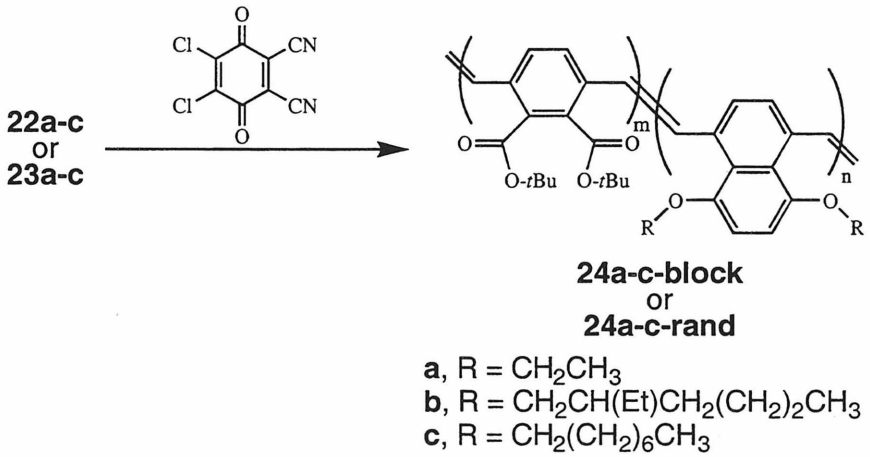

Figure 23. Aromatization of block and random copolymers.

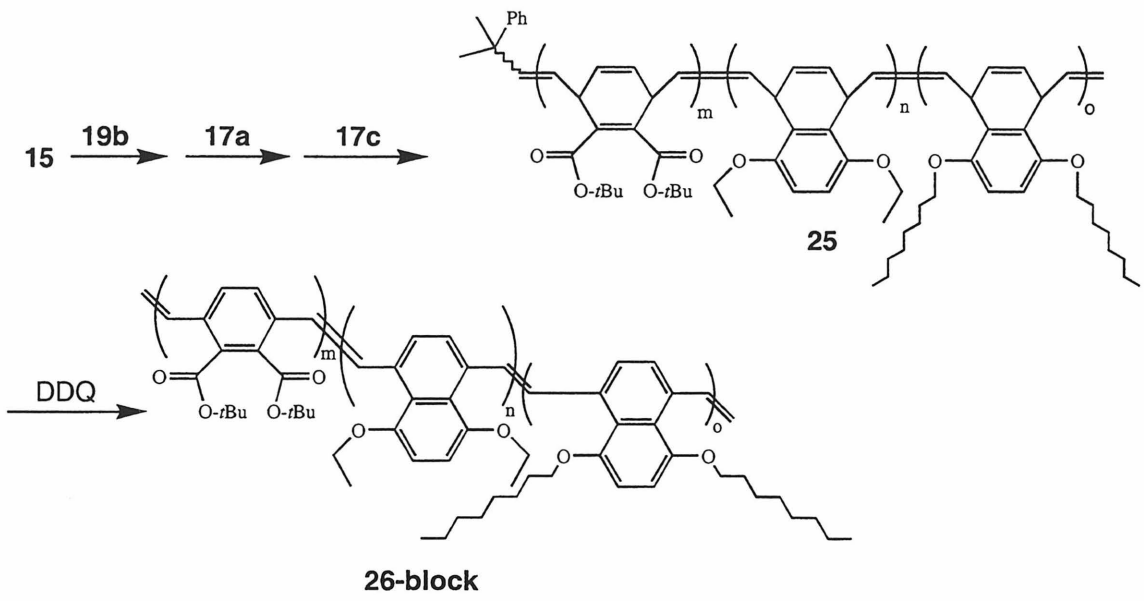

Figure 24. ROMP-Aromatization yielding triblock copolymer **26-block**.

mentioned above.

Polymers **24-block** and **24-rand** have almost exclusively *trans* vinylene units as determined by IR spectroscopy. As a representative example, the IR spectrum of **24c-block** is shown in Figure 25. The peak at 965.7 cm^{-1} is representative of the *trans* C-H out of plane bending mode. The absence of a peak at 882 cm^{-1} shows that there are very few *cis* vinylene units. [78]

Fluorescence Spectroscopy

To determine the energy transfer efficiency and quantum yield ehnacement in the copolymer systems, one needs to photoexcite the large band gap segment at its wavelength of maximum absorbance (determined by UV/vis absorbance spectroscopy and excitation spectra) then determine which segments are emitting. Figure 26 shows a schematic representation of the HOMO and LUMO levels in these conjugated copolymers and the action of through bond energy transfer; this should be contrasted with the Förster energy transfer schematic shown in Figure 6. Solution photoluminescence

spectra of diester-PPV (**16**) and dialkoxy-PNV (**18b**) homopolymers are shown in Figure 27. Polymer **16**, the larger band gap polymer, emits at 490 nm, and **18a-c** emit at 534-546 nm (Table 4). If efficient energy transfer occurs in the copolymers, excitation of the diester-PPV segments should result in no emission at 490 nm, rather exclusive emission from the dialkoxy-PNV segments would be observed.

However, upon exciting the diester-PPV block ($\lambda_{max,ex}$ = 420 nm) of **26-block**, **24b-block**, and **24c-block**, no energy transfer emission is observed; all of the emission surprisingly occurred from the same block that is excited (Table 4, Figure 29). However, the emission efficiencies (15%, 40%, and 15%) were much lower that that of the diester-PPV homopolymer, so either energy transfer is occurring and the dialkoxy-PNV block is not emitting, or the dialkoxy-PNV block is simply partially quenching the emission in another way.

The effect of changing the block lengths was examined. To compare with **24b-block**, **24b2-block** was prepared with a dialkoxy-PNV block that was twice as long (60 repeat units), and **24b3-block** was prepared which had a longer diester-PPV block length (40 repeat units). Neither of these displayed energy transfer either, emitting only from the large band gap block (Table 4 and Figure 29). Of the three, the one with the longest diester-PPV block emitted the strongest (Φ = 91%),[79] comparable to the diester-PPV homopolymer, and the one with the longest dialkoxy-PNV block emitted the weakest (Φ = 23%).

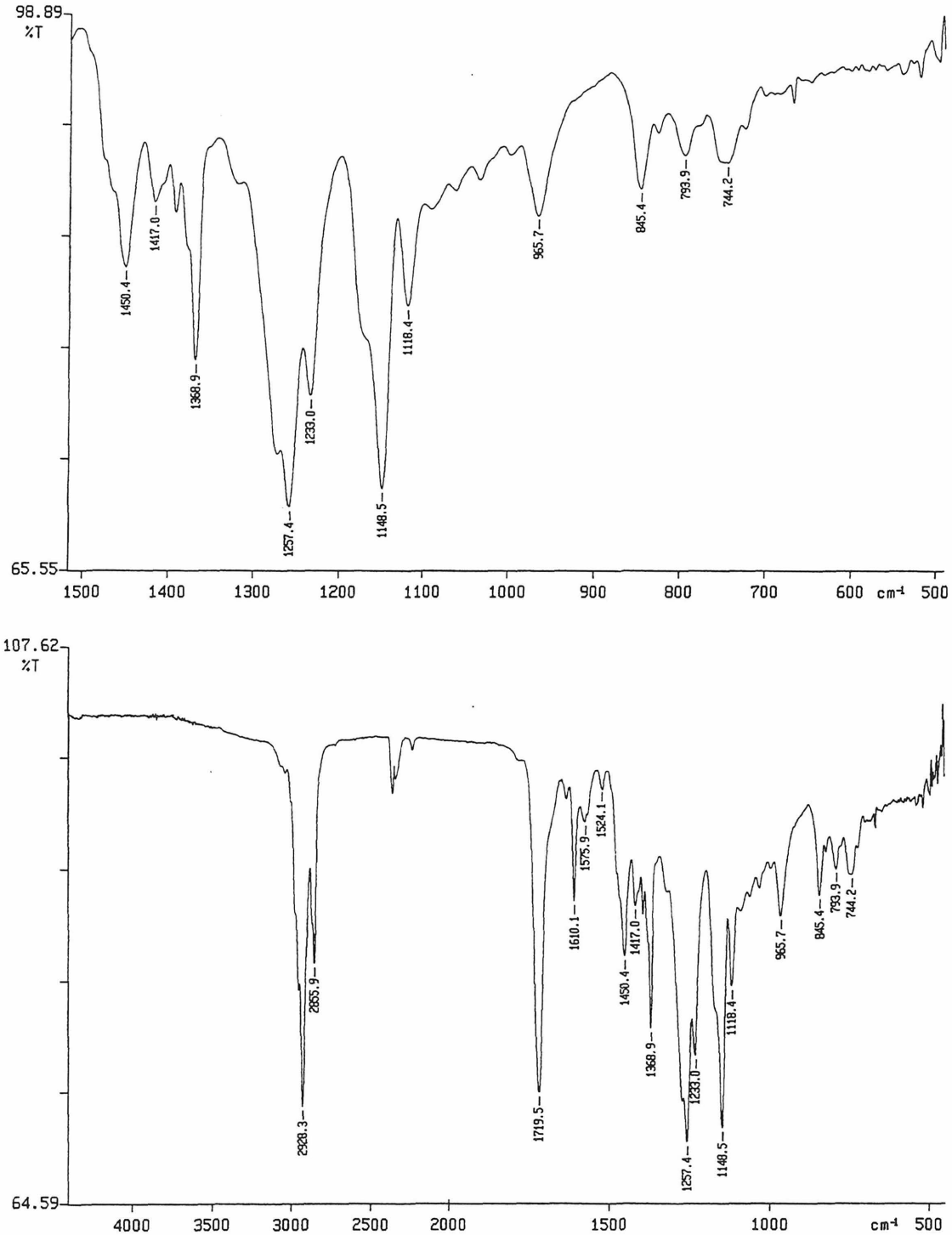

Figure 25. IR spectrum of **24c-block**.

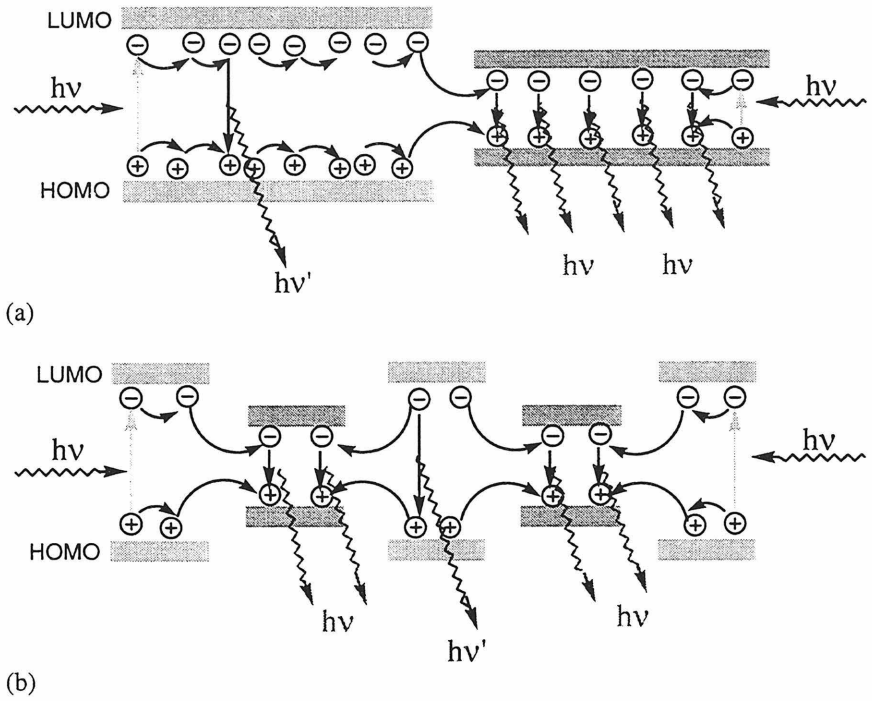

Figure 26. Energy transfer scheme showing charge migration in the HOMO and LUMO levels of (a) a block copolymer and (b) a random (or blocky) copolymer.

Phololuminescence spectra of the random copolymers **24-rand** were also recorded using the same procedure. But unlike the blocks, the random copolymers displayed moderate to very efficient energy transfer. Excitation of the diester-PPV segments of **24a-rand** at 420 nm resulted in 90% of the light being emitted from the dialkoxy-PNV segments (585 nm) and only 10% from diester-PPV segments (Table 4 and Figure 29). Unfortunately, due to the low solubility of **24a-rand**, the quantum yield could not be quantitated reliably, thus we were unable to determine whether or not there was an efficiency enhancement.

Polymer **24b-rand** also displayed good energy transfer, but not as good as **24a-rand**. Upon excitation of the diester-PPV fragments, luminescence was observed from both segments of **24b-rand** (492 nm and 571 nm) in a 50:50 ratio (Table 4 and Figure

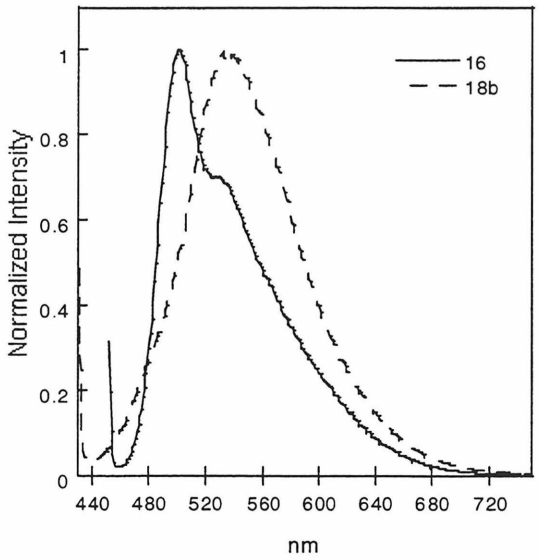

Figure 27. Fluorescence spectra of **16** and **18b**.

29). This polymer was soluble, and the quantum yield (from both bands) was calculated to be 52%. Considering that half comes from the dialkoxy-PNV segments, its emission efficiency in the copolymer is 1.7 times what is observed from the homopolymer (**18b**).

Though broadband emission from **24b-rand** was not the goal, this could be a useful feature since the emission intensity is nearly uniform from 480 – 610 nm. Uniform intensity over the entire visible range is required for white LEDs and this range of colors is often achieved with blends of emissive polymers or small molecules,[54,80,81] or complex LED architectures.[82] Here we demonstrate the same effect with copolymers.

Polymer **24c-rand** displays the most efficient energy transfer of the three random copolymers. Excitation in to the diester-PPV region yields almost exclusive emission from the dialkoxy-PNV at 581 nm (Table 4 and Figure 29). Based on the almost completely quenched diester-PPV emission, the energy transfer efficiency is estimated to be > 98%. Remarkably, the quantum yield is 18%, which is more than a 2-fold

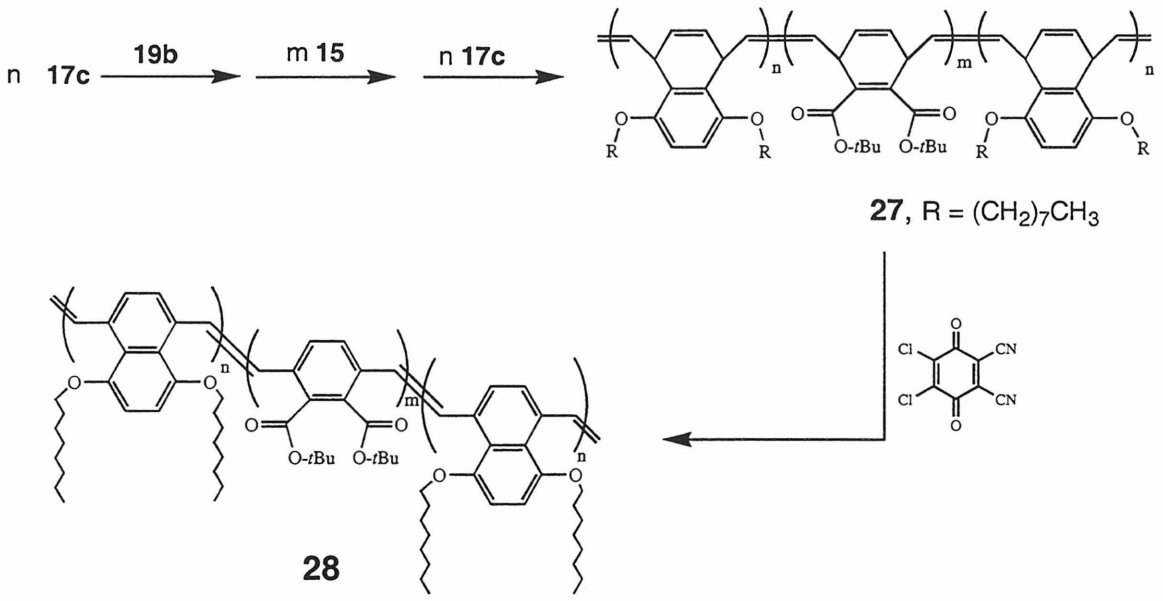

Figure 28. ROMP-Aromatization synthesis of ABA triblock copolymer.

enhancement over that of the homopolymer **18c** (7%). Emission from the copolymers **24a-c-rand** occurs at red shifted values (571-585 nm) compared to the dialkoxy-PNV homopolymers **18a-c** (534-546 nm). This is likely a result of increased planarity (increased π-conjugation length) of the dialkoxy-PNV repeat units as a result of decreased steric interactions with adjacent repeat units which may be the less bulky diester-PPV units rather than the dialkoxy-PNVs.[83] It is well accepted in polymers of this type that decreased steric interactions and twisting of the polymer backbone increases the wavelength of emission.

The question remains as to why the random copolymers display efficient energy transfer, but the block copolymers do not. The fact that **24b-rand** emits evenly from both segments suggests that energy transfer and emission occur on similar timescales. The fact that **24b3-block**, with the longest diester-PPV block (40 repeat units), does not permit energy transfer yet still emits efficiently, suggests that emission is in this case faster. To address this issue, **24c2-block** and **24c3-block** were synthesized with short

diester-PPV blocks of 10 and 5 repeat units, respectively. Comparing these two and **24c-block** (Table 4) one can see that as the diester-PPV block becomes shorter, the quantum yield continues to decrease from 15% to 10% to 4%. Like the block copolymers with longer diester-PPV blocks, polymer **24c2-block** displays no noticeable energy transfer. However, **24c3-block** does show partial energy transfer emission from the dialkoxy-PNV block at 570 nm (Figure 29). Approximately 60% of the emission intensity is from the diester-PPV and 40% is from the dialkoxy-PNV, but unlike with the random copolymers, no efficiency enhancement is observed.

A dialkoxy-PNV/diester-PPV ABA triblock copolymer, with the diester-PPV segment as the central block, was synthesized, and its fluorescence properties compared to the diblock copolymers. This was to see if having acceptor blocks at *both* ends of the donor block resulted in more efficient energy transfer than having it at just one end, eliminating any potential end group effects on the diester-PPV block. The triblock copolymer **27**, with a diester-PPV block 10 repeat units long and the dialkoxy-PNV blocks 20 repeat units long, was synthesized by sequential monomer addition using ROMP initiator **19b**, as shown in Figure 29 (Table 2). DDQ aromatization to yield **28** followed the same procedure as for the diblock copolymers (Figure 29). Upon excitation of the diester-PPV block at 420 nm, emission was observed only from that same block (492 nm) with a quantum efficiency of 18% (Table 4 and Figure 28). This efficiency is comparable to but greater than the diblock copolymers **24c-block**, showing that, for this system, there is no real advantage to using ABA triblock copolymers rather than diblocks.

Table 4. Photoluminescence data.

polymer	m [a]	n [b]	$\lambda_{max,ex}$	solution [c] $\lambda_{max,em}$	quantum [c] yield	film [d] $\lambda_{max,em}$
16 [10]	-	40	420	490	~100%	553
18a [84]	-	20	407	546	5%	546
18b	-	41	407	534	15%	534
18c	-	30	407	541	7%	549
31 [65]		45	485	561	0.5%	593
26-block	20	20	421	491	15%	545
24b-block	30	30	416	491	40%	550
24b2-block	30	60	421	492	23%	554
24b3-block	40	20	419	491	91%	-
24c-block	20	20	420	487	15%	545
24c2-block	10	20	420	491	10%	-
24c3-block	5	20	420	490	4%	-
28	10	20	420	492	18%	558
24a-rand	25	25	420	585	-	-
24b-rand	35	35	421	492, 571	52%	550
24c-rand	20	20	420	581	18%	571
33	50	100	430	558	5.0%	610 [e]

[a] Number of repeat units diester-PPV segments in copolymers. [b] Number of repeat units of dialkoxy-PNV isegments in copolymers. [c] Measurements obtained in CH_2Cl_2 solution. [d] Films deposited from CH_2Cl_2 solutions. [e] Polymer was excited at 407 nm.

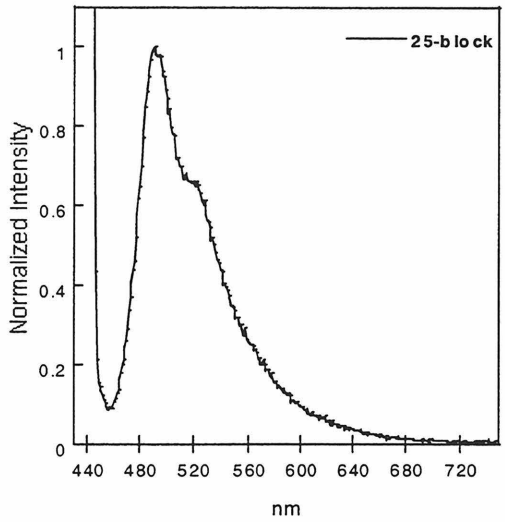

Figure 29a. Solution photoluminescence spectrum of **25-block**.

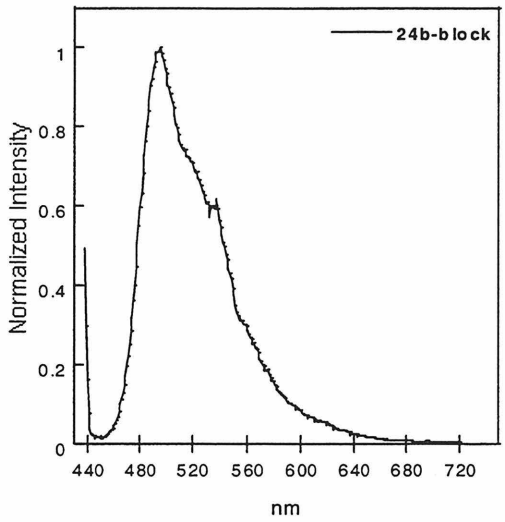

Figure 29b. Solution photoluminescence spectrum of **24b-block**

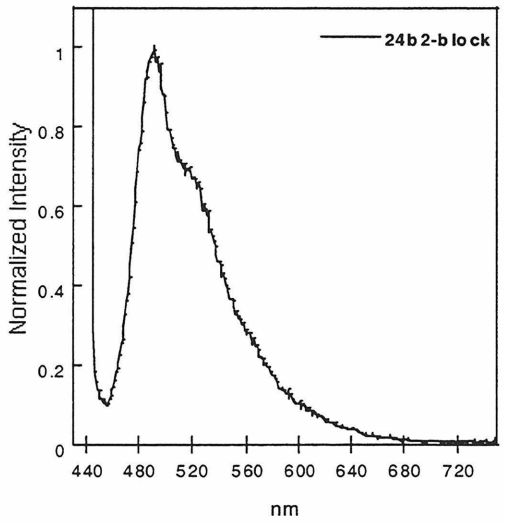

Figure 29c. Solution photoluminescence spectrum of **24b2-block**

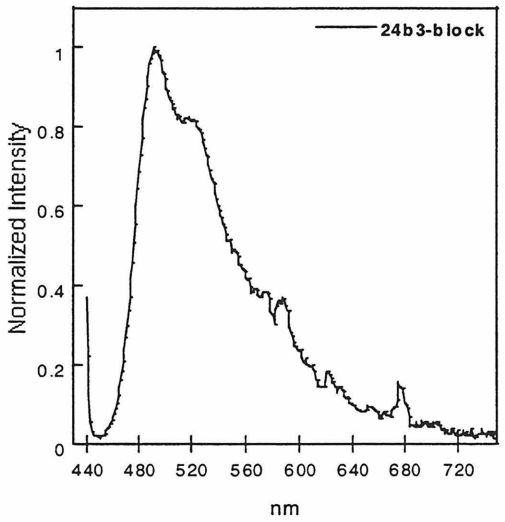

Figure 29d. Solution photoluminescence spectrum of **24b3-block**

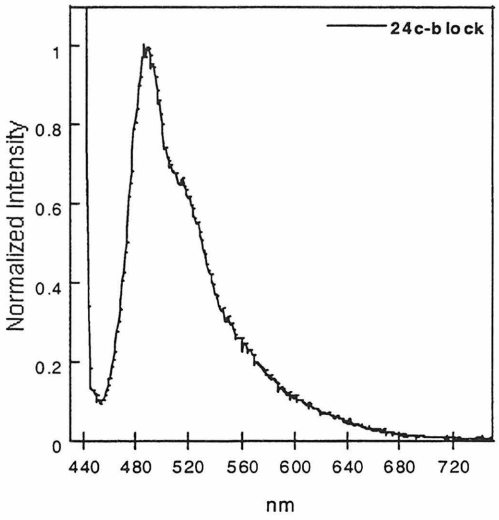

Figure 29e. Solution photoluminescence spectrum of **24c-block**

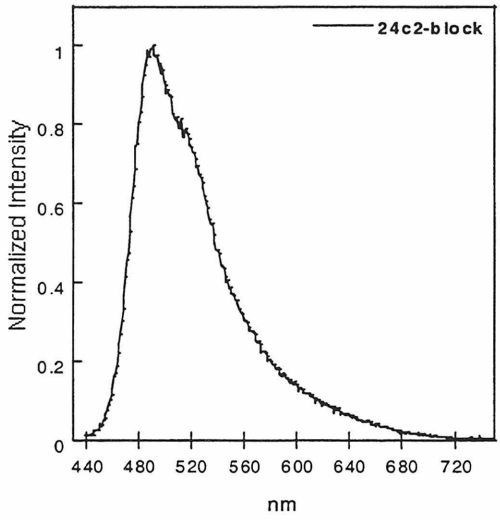

Figure 29f. Solution photoluminescence spectrum of **24c2-block**

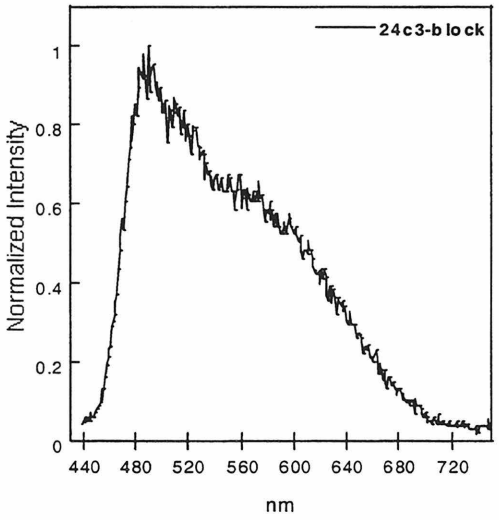

Figure 29g. Solution photoluminescence spectrum of **24c3-block**

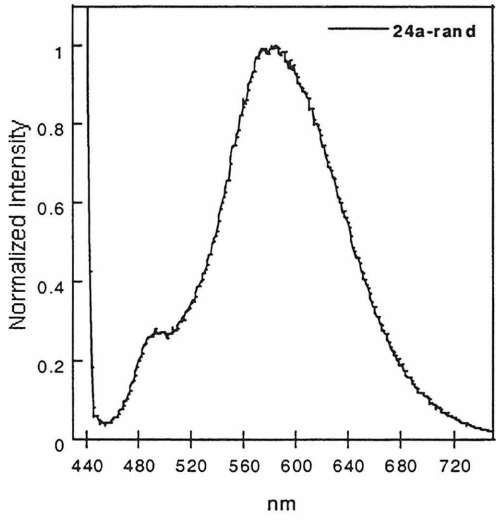

Figure 29h. Solution photoluminescence spectrum of **24a-rand**

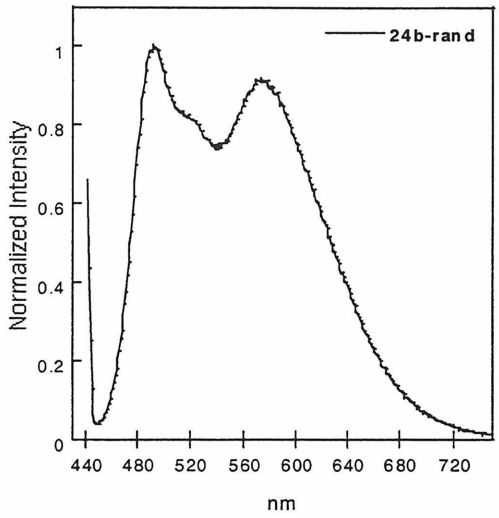

Figure 29i. Solution photoluminescence spectrum of **24b-rand**

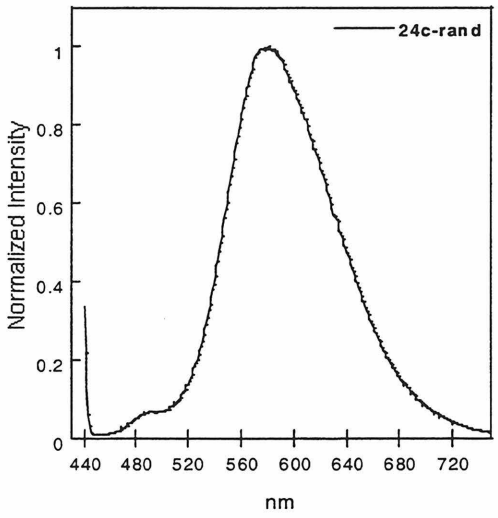

Figure 29j. Solution photoluminescence spectrum of **24c-rand**

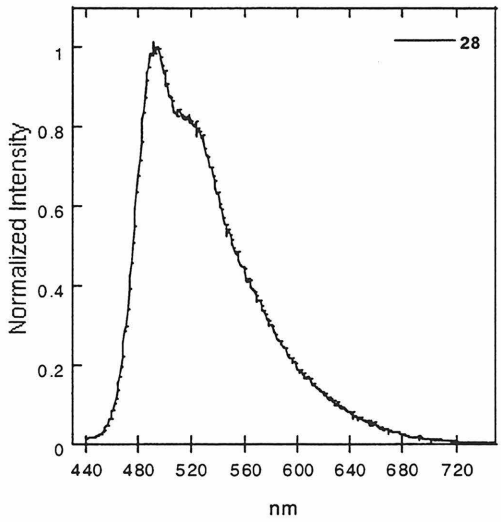

Figure 29k. Solution photoluminescence spectrum of **28**

Synthesis and Energy Transfer Luminescence Spectroscopy of a Dialkoxy-PNV/Alkyl-PNV Block Copolymer

To demonstrate the generality of this efficiency enhancement by energy transfer strategy, a PAV copolymer was synthesized having a different donor segment than diester-PPV and a different acceptor segment that dialkoxy-PNV. Dialkoxy-PNV was used as the large band gap block segment and alkyl-PNV (**31**, Figure 30) was used as the small band gap segment.[65,66,67] The diblock copolymer **33** was synthesized following the same ROMP-Aromatization route and is shown in Figure 31. The rate of initiation relative to propagation is low for the ROMP of alkyl-benzobarrelene **29**. For example, reaction of 30 equivalents of **29** with alkylidene **19b** results in only 30% initiation (dialkoxy-benzobarrelenes **17a-c** achieve full initiation at this monomer/catalyst ratio). In the presence of Lewis bases such as THF or 1,2-dimethoxyethane, 50 equivalents of **29**

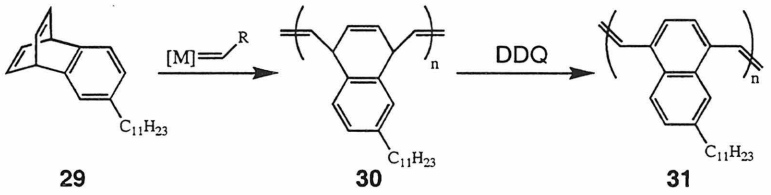

Figure 30. ROMP-Aromatization synthesis of alkyl-PNV

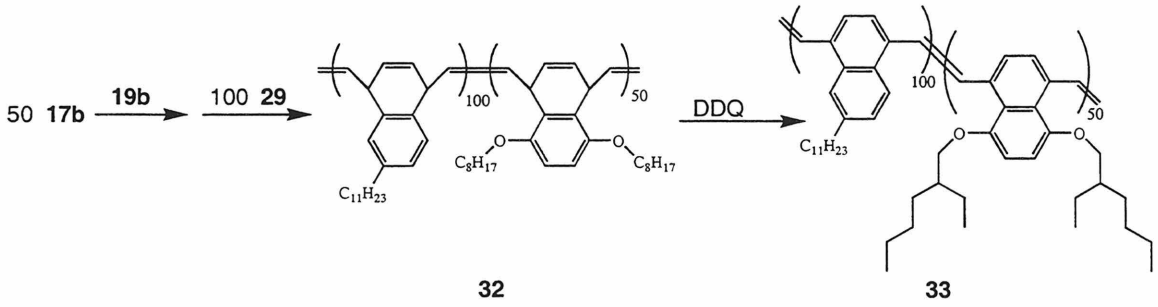

Figure 31. ROMP-Aromatization synthesis of dialkoxy-PNV/alkyl-PNV block copolymer.

yields only 40% or 44% initiation, respectively. Therefore, large amounts of **29**—100 equivalents—were required to achieve full initiation in block copolymer **32** (Table 2). Aromatization of **32** proceeded rapidly to **33** in the presence of excess DDQ, but the polymer was only slightly soluble in halogenated solvents such as CH_2Cl_2.

As mentioned above, the large band gap segment (dilakoxy-PNV) luminesces at 534 nm, and alkyl-PNV emits at 561 nm (Table 4).[67] Luminescence analysis of **33** was performed in CH_2Cl_2 solution exciting into the dialkoxy-PNV block ($\lambda_{max,ex}$ = 430 nm), and good energy transfer was observed resulting in emission from the alkyl-PNV block at 558 nm (Table 4 and Figure 32). This is much more efficient energy transfer than in the previously mentioned block copolymers **24** and **25**. The quantum yield is 5.0% which is an order of magnitude greater than that of the alkyl-PNV homopolymer **31** (0.5%).

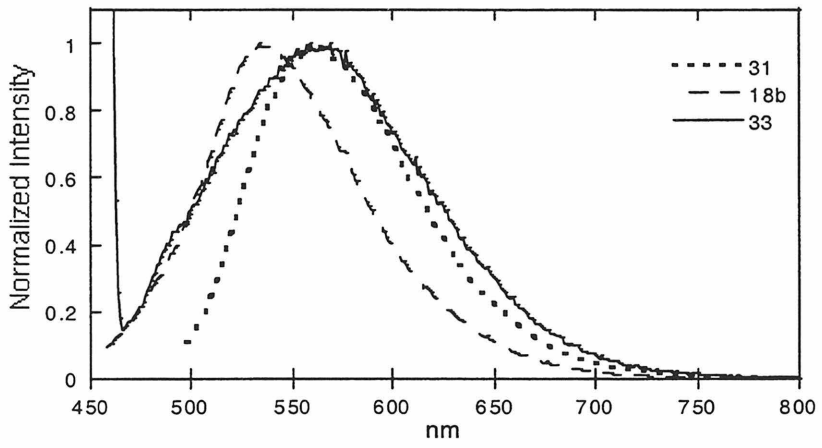

Figure 32. Solution photoluminescence spectrum of **31**, **18b**, and **33**.

It should be noted that the emission wavelength of **33** is the same as that of the small band gap homopolymer (**31**). That was not observed with random copolymers **24a-c-rand**, rather, we recorded a red shift in the emission. The color homogeneity between

33 and **31** is advantageous because one would like to be able to predict the color of emission of the copolymer based on the homopolymer. This represents an advantage to using block copolymers for energy transfer quantum yield enhancements rather than random copolymers.[85]

Luminescence Studies of Polymer Films

Thus far we have focused only on solution photoluminescence though solid state luminescence should be more important for applications such as LEDs and lasers. Energy transfer is expected to be much more efficient in the solid state because Förster energy transfer, which may occur intermolecularly, is distance dependent and may play a larger role sinceby romp

the polymer chains are closely packed. Unfortunately, it is difficult to determine the degree of energy transfer in most of the **24-block** copolymers because both of the segments emit at nearly the same wavelength: **16** emits at 553 nm in the solid state and **18a-c** emit at 534-549 nm (Table 4). Block copolymers **24b-block**, **24b2-block**, **24c-block**, and **26-block** emit in the 545 – 554 nm range in the solid state (upon excitation of the large band gap segment) which overlaps the region of both diester-PPV and dilakoxy-PNVs, so we cannot be sure which is emitting (Table 4 and Figure 33). The random copolymer **24b-rand** is also ambiguous, emitting at 550 nm. However **24c-rand** emits at 571 nm which is significantly red shifted relative to diester-PPV and is close to the solution emission wavelength, so we conclude that the emission is coming from the dialkoxy-PNV segments and energy transfer is very efficient. Copolymer **33** also displays efficient energy transfer in the solid state, emitting at 610 nm from the alkyl-PNV block. We have not been able to quantitate the luminescence quantum yield in the

solid state, so we are unable to compare the effect of block lengths on intensity or quenching.

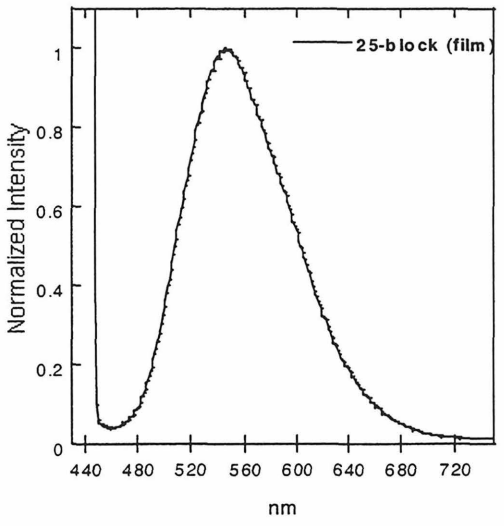

Figure 33a. Photoluminescence spectrum of a film of **25-block**.

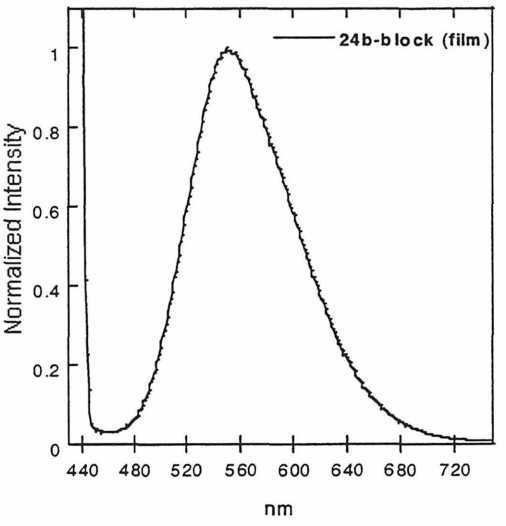

Figure 33b. Photoluminescence spectrum of a film of **24b-block**.

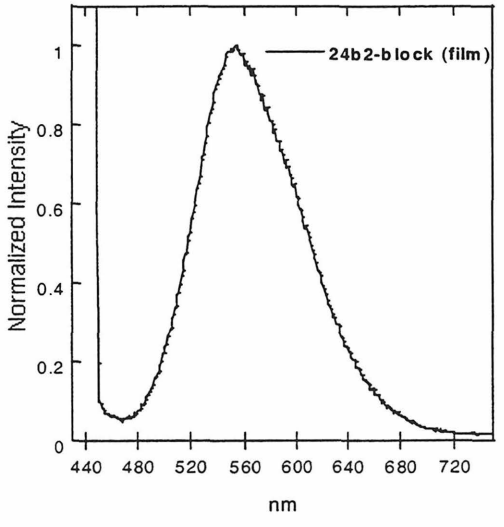

Figure 33c. Photoluminescence spectrum of a film of **24b2-block**.

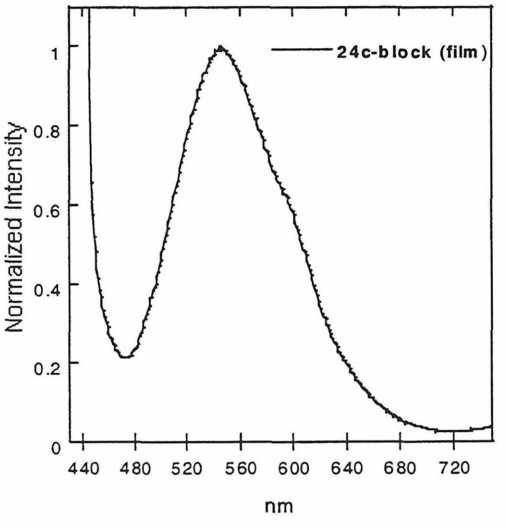

Figure 33d. Photoluminescence spectrum of a film of **24c-block**.

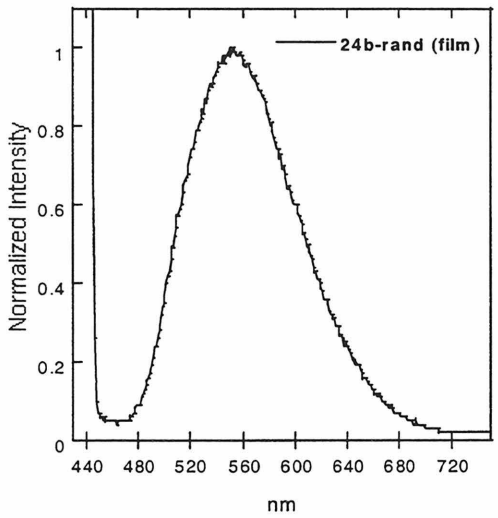

Figure 33e. Photoluminescence spectrum of a film of **24b-rand**.

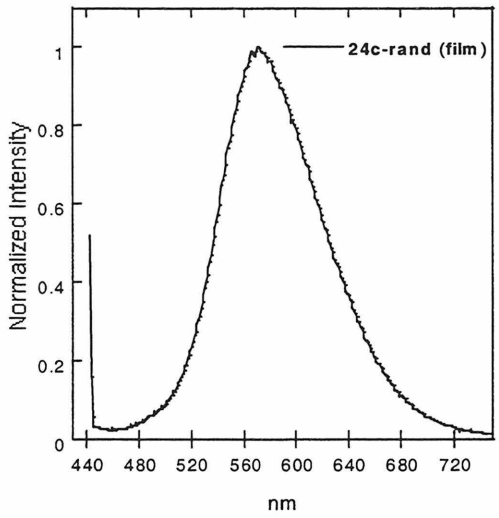

Figure 33f. Photoluminescence spectrum of a film of **24c-rand**.

Acknowledgments

I would like to thank Dr. Mike W. Wagaman for his immense help in planning the monomer synthesis, giving advice on polymer isolation procedures, and teaching me how to use the fluorescence spectrometer. I would like to thank Erika Bellmann for helpful discussions in all aspects of this project as well as the other members of the Center for Advanced Multifunctional Polymers and Non-Linear Optical Materials. Sean Shaheen, Kelly Killeen, Shannon Rice, and Jason Brooks are acknowledged for helping me to fabricate and test LEDs. The research group of Dr. J. K. Barton is gratefully acknowledged for allowing us to use their fluorescence spectrometer, and particularly Chris S. Treadway for helpful discussions.

Experimental

General Considerations. Manipulations of air-sensitive materials were carried out using standard Schlenk techniques with an argon atmosphere or in a nitrogen filled Vacuum Atmospheres drybox. NMR spectra[86] were recorded with either a QE-300 Plus (300.10 MHz ^{1}H; 75.49 MHz ^{13}C) spectrometer, a JEOL GX-400 (399.65 MHz ^{1}H; 376.01 MHz ^{19}F; 100.50 MHz ^{13}C), or a Brucker AM500 or AMX500 (500.14 MHz ^{1}H; 470.56 MHz ^{19}F; 125.76 MHz ^{13}C). All chemical shifts are reported in parts per million (ppm) downfield from tetramethylsilane (TMS), and coupling constants are reported in Hz. Multiplicities are reported with the following abbreviations: s (singlet), d (doublet), t (triplet), q (quartet), m (multiplet), and br (broad). Gel permeation chromatograms were obtained in methylene chloride at a 1.0 mL/min flow rate on an AM Gel Linear 10 column with a Knauer differential refractometer detector. Molecular weights are calculated relative to polystyrene standards ranging from 2,950 to 2,400,000 daltons. Infrared spectra of polymer films were recorded on a Perkin Elmer Paragon 1000 FT-IR spectrometer. Absorbance spectra were recorded on a HV Vectra ES/12 spectrometer with 2 nm resolution. Luminescence spectra were recorded on an SLM 8000 C spectrofluorometer at room temperature.

Materials. When dry solvents, when required, were prepared as follows: benzene-d_6, tetrahydrofuran (THF), and ether were degassed by bubbling a stream of argon through the solvents and dried by passage through solvent purification columns.[87] Methylene chloride-d_2, was dried over CaH_2, vacuum transferred or distilled, then degassed by three continuous freeze-pump-thaw cycles. Hexafluoro-*t*-butanol was dried over activated $MgSO_4$, vacuum transferred, and degassed by three freeze-pump-thaw

cycles. All other chemicals were obtained from EM Science; Lancaster Synthesis, Inc.; Aldrich Chemical Co.; or Strem Chemicals, Inc. and used as received unless otherwise noted. Alkylidenes **19a** and **19b**[88,89] and monomers **15**,[10] **17a-c**,[90] and **29**[65,66,67] were prepared as previously reported.

General Procedure for Block Copolymer Synthesis by ROMP. In the drybox, a vial was charged with approximately 5 mmol (~0.0035 g) of initiator **19b** and dissolved in 0.1 mL C_6D_6. A second vial was charged with the first monomer (typically 20-40 equivalents) and dissolved in 0.5 mL C_6D_6. The monomer solution was added *to* the catalyst solution via pipet and the vial was immediately swirled to ensure sufficient mixing during initiation. The solution was transferred to an NMR tube with a teflon valve seal (J-Young tube) and analyzed by NMR spectroscopy. (In scale up syntheses, reactions were carried out in a capped vial in the drybox.) During ROMP of **15**, the solution became red during propagation and yellow-orange when all monomer had been consumed. During polymerization of all other monomers, the solutions were orange to brown and there were no color changes when propagation was complete. When the first block was complete, the NMR tube was taken into the drybox, and a few drops removed for GPC analysis: (First benzaldehyde was added to quench the catalyst, and after 30 min, methanol was added to precipitate the polymer. After centrifugation, methanol was decanted, and the polymer was dried *in vacuo* for five min before dissolving for GPC analysis.) To grow the second block, the second monomer, dissolved in 0.1 – 0.2 mL C_6D_6 was added to the solution containing the first block in the NMR tube with immediate shaking to ensure sufficient mixing during initiation. (To prepare a triblock copolymer, a third monomer in 0.1 – 0.2 mL C_6D_6 was added to the reaction solution

after completion of the second block and propagation monitored by NMR.) ROMP of 30 equivalents of **15** and **17b-c** took ~2 h under these conditions, while ROMP of **17a** reached completion within 15 min. At the completion of the reaction, 0.1 mL dry, degassed benzaldehyde (~200 equivalents) was added in the drybox or in air then immediately sealed again by the teflon valve, and left for at least 30 min. The solution became green, a sign of complete catalyst quenching and conversion to $Mo(O)(NAr)(OR)_2$.[62,91] The solution was then diluted with 0.1-0.5 mL degassed benzene or CH_2Cl_2 as necessary to decrease viscosity, then poured into 40 mL degassed methanol[92] to precipitate polymer. Polymer was left for ~10 h under argon to precipitate fully, then centrifuged, and supernatant liquid removed by cannula transfer.[92] This methanol wash-centrifugation-solvent removal was repeated twice more to further purify the polymer. If colored, the polymer was redissolved in a minimal amount of benzene or CH_2Cl_2 and reprecipitated into methanol followed by centrifugation and cannula transfer solvent removal. This reprecipitation was repeated two or three times until the polymer was nearly white. Though not necessary, polymer was typically freeze-dried from benzene *in vacuo*, resulting in a fluffy solid, which was easier to work with in small quantities than the films or large solid chunks that often resulted otherwise. Drying *in vacuo* from any solvent was sufficient. All yields were 80% or greater.

Poly(2,3-di-*tert*-butylester-barrelene)$_{20}$-*block*-poly(3,6-diethoxy-benzobarrelene)$_{20}$ (22a). lab notebook: 4-275. Reaction was carried out according to the General Procedure using 0.0348 g (0.114 mmol) **15**, 0.0250 g (0.103 mmol) **17a**, and 0.0035 g (0.00533 mmol) initiator **19b**. ^{1}H NMR (C_6D_6, 500 MHz, all peaks are broad): δ 6.54, 6.07, 5.65, 5.45, 4.56, 3.79, 1.52, 1.20, 0.98.

Poly(2,3-di-*tert*-butylester-barrelene)$_{30}$-*block*-poly(3,6-bis-(2-ethyl-hexyloxy)-benzobarrelene)$_{30}$ (22b). lab notebook: 4-235. Reaction was carried out according to the General Procedure using 0.0502 g (0.1649 mmol) **15**, 0.0664 g (0.162 mmol) **17b**, and 0.0036 g (0.00549 mmol) initiator **19b**. ^{1}H NMR (C_6D_6, 500 MHz, all peaks are broad): δ 6.57, 5.95, 5.65, 5.56, 5.45, 4.40, 3.77, 1.53, 1.36, 0.98. ^{13}C NMR (C_6D_6, 125 MHz): δ 166.6, 152.0 (br), 135.9, 133.1 (br), 127.2, 109.1 (br), 81.4, 71.4 (br), 42.8, 40.0 (br), 31.4, 29.9, 28.8, 25.0 24.0, 14.8, 11.6 (br).

Poly(2,3-di-*tert*-butylester-barrelene)$_{30}$-*block*-poly(3,6-bis-(2-ethyl-hexyloxy)-benzobarrelene)$_{60}$ (22b2). lab notebook: 4-237. Reaction was carried out according to the General Procedure using 0.0482 g (0.158 mmol) **15**, 0.135 g (0.321 mmol) **17b**, and 0.0035 g (0.00533 mmol) initiator **19b**. ^{1}H NMR (C_6D_6, 500 MHz, all peaks are broad): δ 6.55, 5.98, 5.62, 5.54, 5.42, 4.39, 3.77, 1.52, 1.35, 0.95. ^{13}C NMR (C_6D_6, 125 MHz): δ 166.6, 152.2 (br), 133.1, 128.6 (br), 127.3, 109.0, 81.4, 71.4 (br), 42.8, 40.1 (br), 31.9, 29.9, 28.8, 25.0, 24.0, 14.8, 11.6 (br)

Poly(2,3-di-*tert*-butylester-barrelene)$_{40}$-*block*-poly(3,6-bis-(2-ethyl-hexyloxy)-benzobarrelene)$_{20}$ (22b3). lab notebook: 4-152. Reaction was carried out according to the General Procedure using 0.0594 g (0.195 mmol) **15**, 0.0363 g (0.0884 mmol) **17b**, and 0.0032 g (0.00488 mmol) initiator **19b**. ^{1}H NMR (C_6D_6, 400 MHz, all peaks are broad): δ 6.58, 6.00, 5.63, 5.54, 5.43, 4.40, 3.77, 1.53, 1.36, 0.99.

Poly(2,3-di-*tert*-butylester-barrelene)$_{20}$-*block*-poly(3,6-bis-octyloxy-benzobarrelene)$_{20}$ (22c). lab notebook: 5-012. Reaction was carried out according to the General Procedure using 0.0329 g (0.108 mmol) **15**, 0.0444 g (0.108 mmol) **17c**, and 0.0035 g (0.00533 mmol) initiator **19b**. ^{1}H NMR ($CDCl_3$, 500 MHz, all peaks are broad):

δ 6.56, 5.78, 5.59, 5.27, 4.15, 3.83, 3.65, 1.47, 1.28, 0.89. ^{13}C NMR ($CDCl_3$, 125 MHz): δ 166.4, 150.9 (br), 135.2, 132.6 (br), 128.3 (br), 126.7, 108.9 (br), 81.6, 68.7 (br), 42.1, 39.4 (br), 32.2, 29.6, 28.5, 26.4, 22,9, 14.3.

Poly(2,3-di-*tert*-butylester-barrelene)$_{10}$-*block*-poly(3,6-bis-octyloxy-benzobarrelene)$_{20}$ (22c2). lab notebook: 6-157. Reaction was carried out according to the General Procedure using 0.0389 g (0.128 mmol) **15**, 0.105 g (0.257 mmol) **17c**, and 0.0131 mmol initiator **19b**. ^{1}H NMR ($CDCl_3$, 300 MHz, all peaks are broad): δ 6.68, 6.06, 5.88, 5.61, 4.64, 4.40, 4.26, 2.05, 1.89, 1.56. ^{13}C NMR ($CDCl_3$, 125 MHz): δ 166.4, 150.8 (br), 135.2, 132.6 (br), 127.9 (br), 126.6, 108.6 (br), 81.6, 68.46, 42.1, 29.3 (br), 32.2, 29.7, 28.4, 26.4, 23.0, 14.3.

Poly(2,3-di-*tert*-butylester-barrelene)$_5$-*block*-poly(3,6-bis-octyloxy-benzobarrelene)$_{20}$ (22c3). lab notebook: 6-159. Reaction was carried out according to the General Procedure using 0.0255 g (0.0838 mmol) **15**, 0.138 g (0.336 mmol) **17c**, and 0.0108 g (0.01646 mmol) initiator **19b**. ^{1}H NMR ($CDCl_3$, 300 MHz, all peaks are broad): δ 6.56, 5.80, 5.60, 5.28, 4.16, 3.77, 3.66, 1.70, 1.48, 1.27, 0.89. ^{13}C NMR ($CDCl_3$, 125 MHz): δ 166.4, 150.7 (br), 135.0, 132.4 (br), 127.8 (br), 126.3, 108.5 (br), 81.6, 75.0 (br), 68.4, 42.1, 39.1 (br), 32.2, 29.7, 28.4, 26.3, 22.9, 14.3.

Poly(2,3-di-*tert*-butylester-barrelene)$_{25}$-*random*-poly(3,6-diethoxy-benzobarrelene)$_{25}$ (23a). lab notebook: 4-081. Reaction was carried out according to the General Procedure for block copolymer synthesis except both monomers were added to the initiator simultaneously: 0.0352 g (0.116 mmol) **15**, 0.0277 g (0.114 mmol) **17a**, and 0.0035 g (0.00458 mmol) initiator **19a** along with 0.0691 mmol hexafluoro-*t*-butanol and 0.123 mmol THF.[93] ^{1}H NMR ($CDCl_3$, 400 MHz, all peaks are broad): δ 6.26, 6.16, 5.86,

5.60, 5.31, 5.10, 5.00, 4.89, 4.63, 4.43, 4.21, 3.93, 3.63, 1.48, 0.92. ^{13}C NMR ($CDCl_3$, 125 MHz, all peaks are broad): δ 150.5, 134.5, 132.2, 128.1, 109.1, 81.6, 64.0, 42.1, 39.1, 34.6, 28.4, 15.1.

Poly(2,3-di-*tert*-butylester-barrelene)$_{35}$-*random*-poly(3,6-bis-(2-ethyl-hexyloxy)-benzobarrelene)$_{35}$ (23b). lab notebook: 4-227. Reaction was carried out according to the General Procedure for block copolymer synthesis except both monomers were added to the initiator simultaneously: 0.052 g (0.171 mmol) **15**, 0.072 g (0.175 mmol) **17b**, and 0.0032 g (0.00488 mmol) initiator **19b**. ^1H NMR (C_6D_6, 400 MHz, all peaks are broad): δ 6.64, 6.04, 5.69, 5.42, 4.52, 3.84, 3.76, 3.66, 1.52, 1.36, 0.96.

Poly(2,3-di-*tert*-butylester-barrelene)$_{25}$-*random*-poly(3,6-bis-octyloxy-benzobarrelene)$_{25}$ (23c). lab notebook: 5-011. Reaction was carried out according to the General Procedure for block copolymer synthesis except both monomers were added to the initiator simultaneously: 0.0309 g (0.101 mmol) **15**, 0.0418 g (0.102 mmol) **17c**, 0.0034 g (0.00518 mmol) initiator **19b**. ^1H NMR ($CDCl_3$, 500 MHz, all peaks are broad): δ 6.60, 5.86, 5.57, 5.27, 4.23, 3.84, 3.66, 1.77, 1.47, 1.29, 0.89. ^{13}C NMR ($CDCl_3$, 125 MHz): δ 166.4 (br), 150.7 (br), 135.2 (br), 134.5 (br), 132.6 (br), 130.9 (br), 128.3 (br), 126.9 (br), 109.3 (br), 81.5 (br), 68.6 (br), 42.1 (br), 39.0 (br), 32.1, 29.6, 26.6, 22.9, 14.1.

General Procedure for Polymer Aromatization. In the drybox a vial was charged with the appropriate amount of **22**, **23**, or **32** and dissolved in 0.2 mL CD_2Cl_2, and a second vial was charged with a slight excess (1.2 - 2 equivalents) of 2,3-dichloro-5,6-dicyano-1,4-benzoquinone (DDQ) and slurried in 0.6 mL CD_2Cl_2. The solutions were combined resulting in an instant color change to orange-brown and formation of precipitate. The solution was transferred to an NMR tube with a teflon seal and analyzed

by NMR spectroscopy. After reaction completion (1 – 6 h), the solution was poured into 40 mL degassed methanol and left ~10 h to precipitate the polymer fully. The polymer slurry was centrifuged then the supernatant liquid removed by cannula transfer. The polymer was redissolved in a minimal amount of degassed benzene or CH_2Cl_2 and reprecipitated into methanol followed by centrifugation and cannula transfer solvent removal. This reprecipitation cycle was repeated twice more. Though not necessary, polymer was typically freeze-dried from benzene *in vacuo*, resulting in a fluffy solid, which was easier to work with in small quantities than the films or large solid chunks that often resulted otherwise. Drying *in vacuo* from any solvent was sufficient.[92] Yields were nearly quantitative.

2,3-di-*tert*-butylester-PPV$_{25}$-*random*-5,8-diethoxy-PNV$_{25}$ (24a-rand). lab notebook: 4-094. Reaction was carried out according to the General Procedure for aromatization using 0.0087 g (0.0383 mmol) DDQ and 0.0095 g (0.0348 mmol repeat units) **23a**.

2,3-di-*tert*-butylester-PPV$_{30}$-*block*-5,8-bis(2-ethyl-hexyloxy)-PNV$_{30}$ (24b-block). lab notebook: 4-249. Reaction was carried out according to the General Procedure for aromatization using 0.0274 g (0.121 mmol) DDQ and 0.0202 g (0.0565 mmol repeat units) **22b**. ^{1}H NMR (CD_2Cl_2, 400 MHz, all peaks are broad): δ 8.4-6.3 (m), 4.05, 2.2-0.0 (m).

2,3-di-*tert*-butylester-PPV$_{30}$-*block*-5,8-bis(2-ethyl-hexyloxy)-PNV$_{60}$ (24b2-block). lab notebook: 4-250. Reaction was carried out according to the General Procedure for aromatization using 0.0262 g (0.115 mmol) DDQ and 0.0217 g (0.0578

mmol repeat units) **22b2**. ^{1}H NMR (CD_2Cl_2, 400 MHz, all peaks are broad): δ 8.4-6.3 (m), 4.05, 2.2-0.0 (m).

2,3-di-*tert*-butylester-PPV$_{40}$-*block*-5,8-bis(2-ethyl-hexyloxy)-PNV$_{20}$ (24b3-block). lab notebook: 4-156. Reaction was carried out according to the General Procedure for aromatization using 0.0152 g (0.0670 mmol) DDQ and 0.0110 g (0.0324 mmol repeat units) **22b3**. ^{1}H NMR (CD_2Cl_2, 300 MHz, all peaks are broad): δ 8.3-6.4 (m), 4.04, 2.0 - -0.5 (m).

2,3-di-*tert*-butylester-PPV$_{35}$-*random*-5,8-bis(2-ethyl-hexyloxy)-PNV$_{35}$ (24b-rand). lab notebook: 4-231. Reaction was carried out according to the General Procedure for aromatization using 0.0592 g (0.261 mmol) DDQ and 0.0463 g (0.129 mmol repeat units) **23b**. ^{1}H NMR ($CDCl_3$, 500 MHz, all peaks are broad): δ 8.5-6.3 (m), 4.00, 3.90, 3.50, 1.67, 1.4-0.5 (m). ^{13}C NMR ($CDCl_3$, 100 MHz): δ 167.8, 151.6 (br), 136.2 (br), 133.7 (br), 128.6, 127.1, 126.4, 109.8 (br) 83.3, 72.3 (br), 39.9, 31.1, 30.4, 29.3, 28.5, 28.2, 24.4, 23.9, 23.2, 14.3, 11.0.

2,3-di-*tert*-butylester-PPV$_{20}$-*block*-5,8-dioctyloxy-PNV$_{20}$ (24c-block). lab notebook: 5-022, 6-093. Reaction was carried out according to the General Procedure for aromatization using 0.0111 g (0.0489 mmol) DDQ and 0.015 g (0.0420 mmol repeat units) **22c**. ^{1}H NMR (CD_2Cl_2, 500 MHz, all peaks are broad): δ 8.3-6.4 (m), 4.12, 2.3-0.5 (m).

2,3-di-*tert*-butylester-PPV$_{10}$-*block*-5,8-dioctyloxy-PNV$_{20}$ (24c2-block). lab notebook: 6-161. Reaction was carried out according to the General Procedure for aromatization using 0.0419 g (0.1846 mmol) DDQ and 0.0575 g (0.153 mmol repeat units) **22c2**. ^{1}H NMR ($CDCl_3$, 300 MHz, all peaks are broad): δ 8.4-6.5 (m), 3.99, 2.0-0.3

(m). ^{13}C NMR ($CDCl_3$, 125 MHz): δ 167.3, 151.9 (br), 133.0 (br), 128.0, 126.6 (br), 107.5 (br), 83.3, 70.4, 32.1, 29.7, 29.5, 29.3, 28.5, 26.7, 22.8, 14.3.

2,3-di-*tert*-butylester-PPV$_5$-*block*-5,8-dioctyloxy-PNV$_{20}$ (24c3-block). lab notebook: 6-162. Reaction was carried out according to the General Procedure for aromatization using 0.0420 g (0.185 mmol) DDQ and 0.0588 g (0.151 mmol repeat units) **22c3**. ^1H NMR ($CDCl_3$, 300 MHz, all peaks are broad): δ 8.5-6.3 (m), 3.98, 2.1-0.2 (m). ^{13}C NMR ($CDCl_3$, 125 MHz): δ 151.7 (br), 133.0 (br), 126.5 (br), 107.4 (br), 83.4, 70.4, 32.1, 29.9, 29.7, 29.3, 29.5, 26.7, 22.8, 14.3.

2,3-di-*tert*-butylester-PPV$_{20}$-*rand*-5,8-dioctyloxy-PNV$_{20}$ (24c-rand). lab notebook: 5-021. Reaction was carried out according to the General Procedure for aromatization using 0.0151 g (0.0670 mmol) DDQ and 0.0193 g (0.0540 mmol repeat units) **23c**. ^1H NMR ($CDCl_3$, 500 MHz, all peaks are broad): δ 8.39, 8.0-6.3 (m), 4.03, 2.2-0.5 (m).

Poly(2,3-di-*tert*-butylester-barrelene)$_{20}$-*block*-poly(3,6-diethoxy-benzobarrelene)$_{20}$-*block*-poly(3,6-bis-(2-ethyl-hexyloxy)-benzobarrelene)$_{20}$ (25). lab notebook: 4-275. Reaction was carried out according to the General Procedure for block copolymer synthesis using 0.0348 g (0.114 mmol) **15**, 0.0250 g (0.103 mmol) **17a**, 0.0442 g (0.108 mmol) **17b**, and 0.0035 g (0.00533 mmol) initiator **19b**. ^1H NMR ($CDCl_3$, 500 MHz, all peaks are broad): δ 6.60, 5.81, 5.17, 5.28, 4.19, 3.87, 3.66, 1.80, 1.47, 1.27, 0.89. ^{13}C NMR ($CDCl_3$, 125 MHz): δ 166.4, 150.9 (br), 135.3, 132.6 (br), 128.3 (br), 126.8, 109.5 (br) 81.6, 71.0 (br), 64.2, 42.2, 39.2 (br), 31.0, 30.3, 29.4, 28.5, 24.3, 23.4, 15.2 (br), 14.3, 11.2.

2,3-di-*tert*-butylester-PPV$_{20}$-*block*-5,8-diethoxy-PNV$_{20}$-*block*-5,8-dioctyloxy-PNV$_{20}$ (26-block). lab notebook: 4-276. Reaction was carried out according to the General Procedure for aromatization using 0.0229 g (0.101 mmol) DDQ and 0.0207 g (0.0649 mmol repeat units) **25**. ^{1}H NMR (CD_2Cl_2, 300 MHz, all peaks are broad): δ 8.3-6.4 (m), 4.02, 2.2-0.3 (m).

Poly(3,6-bis-octyloxy-benzobarrelene)$_{20}$-*block*-poly(2,3-di-*tert*-butylester-barrelene)$_{10}$-*block*-poly(3,6-bis-octyloxy-benzobarrelene)$_{20}$ (27). lab notebook: 6-185. In the dry box, a vial was charged with 0.0049 g (0.00747 mmol) **19b** and dissolved in 0.1 mL C_6D_6. A second vial was charged with 0.0622 g (0.151 mmol) **17c** and 0.5 mL C_6D_6, and this solution was added to the first. The solution was stirred for 3 h then added to a solution of the second monomer: 0.0232 g (0.0762 mmol) **15** in 0.1 mL C_6D_6. The solution became red within 10 min (a sign of complete initiation) and returned to yellow-orange after 40 min (a sign of complete propagation).[10] After 5 additional min, the solution was added to a 0.1 mL C_6D_6 solution of 0.0606 g (0.148 mmol) **17c** and stirred for 3 h before adding 0.1 mL benzaldehyde to quench the catalyst. After 30 min, the solution was removed from the dry box and poured into 40 mL degassed methanol to precipitate the polymer. The rest of the purification and isolation procedure was carried out as shown in the General Procedure for Block Copolymer Synthesis section.

5,8-dioctyloxy-PNV$_{20}$-*block*-2,3-di-*tert*-butylester-PPV$_{10}$-*block*-5,8-dioctyloxy-PNV$_{20}$ (28). lab notebook: 6-187. In the dry box, a vial was charged with 0.0345 g (0.0886 mmol repeat units) **27** and dissolved in 0.5 mL CH_2Cl_2. Another vial was charged with 0.0377 g (0.166 mmol) DDQ and 1.5 mL CH_2Cl_2. The solutions were combined with an immediate color change to red-brown and accompanying formation of

precipitate. After stirring for 6 h, the solution was removed from the dry box and poured into 40 mL degassed methanol to precipitate the polymer. The rest of the purification and isolation procedure was carried out as shown in the General Procedure for polymer aromatization section. ^{1}H NMR ($CDCl_3$, 300 MHz): δ 8.75-6.3 (m, br), 4.4-3.5 (m, br), 2.0-0.2 (m, br), 1.63 (s). ^{13}C NMR ($CDCl_3$, 125 MHz): δ 167.3, 151.6 (br), 149.9 (br), 135.0 (br), 133.5 (br), 128.5, 127.0, 126.5, 111.7 (br), 107.0 (br), 83.4, 70.1 (br), 32.0, 29.5, 28.5, 26.5, 22.8, 14.3.

Poly(3,6-bis-(2-ethyl-hexyloxy)-benzobarrelene)$_{50}$-*block*-poly(4-undecyl-benzobarrelene)$_{100}$ (32). 4-248. Reaction was carried out according to the General Procedure for block copolymer synthesis using 0.0973 g (0.237 mmol) **17b**, 0.147 (0.476 mmol) **29**, and 0.0031 g (0.00472 mmol) **19b**. ^{1}H NMR (C_6D_6, 400 MHz, all peaks are broad): δ 7.08, 7.01, 6.55, 5.91, 5.59, 4.37, 3.91, 2.52, 1.58, 1.29, 0.92. ^{13}C NMR (C_6D_6, 100 MHz, all peaks are broad): δ 151.9 (br), 136.8, 134.4, 129.7, 127.4, 108.9 (br), 71.2 (br), 44.5, 44.2, 40.0 (br), 36.5, 32.8, 32.4, 30.5, 30.3, 24.0, 23.5, 14.8, 11.6 (br).

5,8-bis(2-ethyl-hexyloxy)-PNV$_{50}$-*block*-4-undecyl-PNV (33). lab notebook: 4-281, 5-023. Reaction was carried out according to the General Procedure for aromatization using 0.0094 g (0.0414 mmol) DDQ and 0.0172 g (0.0502 mmol repeat units) **32**. ^{1}H NMR (CD_2Cl_2, 300 MHz, all peaks are broad): δ 8.6-6.3 (m), 4.00, 2.83, 2.0 - -0.5 (m).

General Procedure for Photoluminescence Measurements. Measurements were performed with an SLM 8000 Spectrofluoremeter on solutions diluted to give a polymer *repeat unit* concentration of 10^{-5} – 10^{-6} M. Quantum yields (Φ) were calculated relative to a $Ru(bpy)_3Cl_2$ (*Ru*) standard using the following equation:

$$\Phi_{poly} = \frac{I_{poly} \cdot \varepsilon_{Ru} \cdot c_{Ru}}{I_{Ru} \cdot \varepsilon_{poly} \cdot c_{poly}} \cdot \Phi_{Ru}$$

Emission intensity integration values, *I*, were measured on spectra that had been corrected for detector response. Extinction coefficients for the polymers were determined by absorbance spectroscopy and are shown in Table 5. Literature values for Φ_{Ru} (0.028) and ε_{Ru} (14,300) were based on excitation at 453 nm.[94] The energy transfer efficiency in a donor-acceptor system may be estimated by considering the degree of quenching of the donor in concert with comparison of the emission intensity of the acceptor with and without energy transfer taking place.[29,30]

or electrons (electroluminescence) injected into the sample.

2. Bradley, D. *Curr. Opin. Solid State Mater. Sci.* **1996**, *1*, 789.

3. Dodabalapur, A. *Solid State Commun.* **1997**, *102*, 259.

4. The brightness level of 100 cd/m^2 is generally accepted to be suitable for most targeted display applications and is as bright as current computer screens.

5. (a) Yu, G. *Synth. Met.* **1996**, *80*, 143. (b) Braun, D.; Staring, E. G. J.; Demandt, R. C. J. E.; Rikken, G. L. J.; Kessener, Y. A. R. R.; Venhuizen, A. H. J. *Synth. Met.* **1994**, *66*, 75. (c) Staring, E. G. J. *Philos. Trans. R. Soc. Math. Phys. Eng. Sci.* **1996**, *80*, 111. (d) Salbeck, J. *Ber. Bunsenges. Phys. Chem.* **1996**, *100*, 1666.

6. Andersson, M. R.; Yu, G.; Heeger, A. J. *Synth. Met.* **1997**, *85*, 1275.

7. Bellmann, E.; Shaheen, S. E.; Thayumanavan, S.; Barlow, S.; Grubbs, R. H.; Marder, S. R.; Kippelen, B.; Peyghambarian, N. *Chem. Mater.* **1998**, *10*, 1668.

8. (a) Yang, Y.; Pei, Q.; Heeger, A. J. *J. Appl. Phys.* **1996**, *79*, 934. (b) Birgerson, J.; Kaeriyama, K.; Barta, P.; Broms, P.; Fahlman, M.; Granlund, T.; Salaneck, W. R. *Adv. Mater.* **1996**, *8*, 982.

9. (a) Burn, P. L.; Holmes, A. B.; Kraft, A.; Bradley, D. D. C.; Brown, A. R.; Friend, R. H. *J. Chem. Soc., Chem Commun.* **1992**, 32. (b) Burn, P. L.; Kraft, A.; Baigent, D. R.; Bradley, D. D. C.; Brown, A. R.; Friend, R. H.; Gymer, R. W.; Holmes, A. B.; Jackson, R. W. *J. Am. Chem. Soc.* **1993**, *115*, 10117.

10. Wagaman, M. W.; Grubbs, R. H. *Macromolecules* **1997**, *30*, 3978.

11. Son, S.; Dodabalapur, A.; Lovinger, A. J.; Galvin, M. E. *Science* **1995**, *269,* 376.

12. Onitsuka, O.; Fou, A. C.; Ferreira, M.; Hsieh, B. R.; Rubner, M. F. *J. Appl. Phys.* **1996**, *80*, 4067.

13. Fou, A. C.; Onitsuka, O.; Ferreira, M.; Rubner, M. F. *J. Appl. Phys.* **1996**, *79*, 7501.

14. (a) Ferreira, M.; Rubner, M. F. *Macromolecules* **1995**, *28*, 7107. (b) Ferreira, M.; Cheung, J. H.; Rubner, M. F. *Thin Solid Films* **1994**, *244*, 806.

15. Boyd, T. J.; Geerts, Y.; Lee, J.-K.; Fogg, D. E.; Lavoie, G. G.; Schrock, R. R.; Rubner, M. F. *Macromolecules* **1997**, *30*, 3553.

16. In the type B LED, PPV is not emitting, rather is acts as a transport layer for the diphenylanthracene chromophore.

17. Bazan, G. C.; Miao, Y. J.; Renak, M. L.; Sun, B. J. *J. Am. Chem. Soc.* **1996**, *118*, 2618.

18. Klärner, G.; Davey, M. H.; Chen, W.-D.; Scott, J. C.; Miller, R. D. *Adv. Mater.* **1998**, *10*, 993.

19. Bao, Z.; Amundson, K. R.; Lovinger, A. J. *Macromolecules* **1998**, *31*, 8647.

20. (a) Malenfant, P. R. L.; Groenendaal, L.; Fréchet, J. M. J. *J. Am. Chem. Soc.* **1998**, *120*, 10990. (b) Karakaya, B.; Claussen, W.; Schafer, A.; Lehmann, A.; Schluter, A. D. *Acta Polymerica* **1996**, *47*, 79.

21. Wagner, R. W.; Lindsey, J. S. *J. Am. Chem. Soc.* **1994**, *116*, 9759.

22. Tasch, S.; List, E. J. W.; Hochfilzer, C.; Leising, G.; Schlichting, P.; Rohr, U.; Geerts, Y.; Scherf, U.; Müllen, K. *Phys. Rev. B* **1997**, *56*, 4479.

23. Berggren, M.; Dodabalapur, A.; Slusher, R. E. *Appl. Phys. Lett.* **1997**, *71*, 2230.

24. Okamoto, Y.; Ueba, Y.; Dzhanibekov, N. F.; Banks, E. *Macromolecules* **1981**, *14*, 17.

25. Murray, C. B.; Kagan, C. R.; Bawendi, M. G. *Science* **1995**, *270*, 1335.

26. Blasse, G.; Grabmaier, B. C. *Luminescent Materials*; Springer-Verlag: Berlin, 1994.

27. Bourson, J.; Mugnier, J.; Valeur, B. *Chem. Phys. Lett.* **1982**, *92*, 430.

28. Förster energy transfer efficiency decreases with inverse distance to the sixth power.

29. Stryer, L. *Ann. Rev. Biochem.* **1978**, *47*, 819.

30. Valeur, B. in *Molecular Luminescence Spectroscopy: Methods and Applications*; Ed.: Schulman, S. G., Wiley: New York, 1985; Part 3, Vol. 77.

31. HOMO-LUMO gap and band gap are used interchangeably here.

32. See the following references and references therein. (a) Jullien, L.; Canceill, J.; Valeur, B.; Bardez, E.; Lefèvre, J.-P.; Lehn, J.-M.; Marchi-Artzner, V.; Pansu, R. *J. Am. Chem. Soc.* **1996**, *118*, 5432. (b) Jiang, D.-L.; Aida, T. *Nature* **1997**, *388*, 454. (c) Kaschak, D. M.; Lean, J. T.; Waraksa, C. C.; Saupe, G. B.; Usami, H.; Mallouk, T. E. *J. Am. Chem. Soc.* **1999**, *121*, 3435. (d) Gust, D.; Moore, T. A.; Moore, A. *Acc. Chem. Res.* **1993**, *26*, 198.

33. (a) McDermott, G.; Prince, S. M.; Freer, A. A.; Hawthornthwaite-Lawless, A. M.; Papiz, M. Z.; Cogdell, R. J.; Isaacs, N. W. *Nature* **1995**, *374*, 517. (b) Kühlbrandt, W. *Nature* **1995**, *374*, 497.

34. Prathapan, S.; Johnson, T. E.; Lindsey, J. S. *J. Am. Chem. Soc.* **1993**, *115*, 7519.

35. Shortreed, M. R.; Swallen, S. F.; Shi, Z.-Y.; Tan, W.; Xu, Z.; Devadoss, C.; Moore, J. S.; Kopelman, R. *J. Phys. Chem. B* **1997**, *101*, 6318.

36. (a) Kawa, M.; Fréchet, J. M. J. *Chem. Mater.* **1998**, *10*, 286. (b) Kawa, M.; Frechet, J. M. J. *Thin Solid Films* **1998**, *331*, 259.

37. Gilat, S. L.; Adronov, A.; Fréchet, J. M. J. *Polym. Mater. Sci. Eng.* **1997**, *77*, 91.

38. Adronov, A.; Gilat, S. L.; Malenfant, P.; Fréchet, J. M. J. *Polym. Mater. Sci. Eng.* **1999**, *80*, 114.

39. Devadoss, C.; Bharathi, P.; Moore, J. S. *J. Am. Chem. Soc.* **1996**, *118*, 9635.

40. Gilat, S. L.; Adronov, A.; Fréchet, J. M. J. *Angew. Chem., Int. Ed.* **1999**, *38*, 1422.

41. Swager, T. M.; Gil, C. J.; Wrighton, M. S. *J. Phys. Chem.* **1995**, *99*, 4886.

42. Rothberg, L. J.; Lovinger, A. J. *J. Mater. Res.* **1996**, *11*, 3174.

43. This refers to the number of layers *between* the electrodes.

44. Tang, C. W.; VanSlyke, S. A. *Appl. Phys. Lett.* **1987**, *51,* 913.

45. This refers to the *rates* of electron and hole mobilities.

46. For a comparison of emission in electroluminescence and photoluminescence, see Chapter 2.

47. Kraft, A.; Grimsdale, A. C.; Holmes, A. B. *Angew. Chem., Int. Ed.* **1998**, *37*, 402.

48. Kido, A. *Trends Polym. Sci.* **1994**, *2*, 350.

49. Tang, C. W.; VanSlyke, S. A.; Chen, C. H. *J. Appl. Phys.* **1989**, *65,* 3610.

50. Kido, J.; Kohda, M.; Okuyama, K.; Nagai, K. *Appl. Phys. Lett.* **1992**, *61*, 761.

51. Wen, W.-K.; Jou, J.-H.; Wu, H.-S.; Cheng, C.-L. *Macromolecules* **1998**, *31*, 6515.

52. Wu, C.-C.; Sturm, J. C.; Register, R. A.; Tian, J.; Dana, E. P.; Thompson, M. E. *IEEE Trans. Electron Devices* **1997**, *44*, 1269.

53. Zhang, C.; von Seggern, H.; Kraabel, B.; Schmidt, H.-W.; Heeger, A. J. *Synth. Met.* **1995**, *72*, 185.

54. Granström, M.; Inganäs, O. *Appl. Phys. Lett.* **1996**, *68,* 147.

55. Berggren, M.; Dodabalapur, A.; Slusher, R. E.; Bao, Z. *Nature* **1997**, *389*, 466.

56. Bao, Z.; Peng, Z.; Galvin, M. E.; Chandross, E. A. *Chem. Mater.* **1998**, *10*, 1201.

57. Chung, S.-J.; Kwon, K.-Y.; Lee, S.-W.; Jin, J.-I.; Lee, C. H.; Lee, C. E.; Park, Y. *Adv. Mater.* **1998**, *10*, 1112.

58. Peng, Z.; Zhang, J. *Chem. Mater.* **1999**, *11*, 1143.

59. For examples of non-arylenevinylene polymers which display energy transfer see (a) Jenekhe, S. A.; Chen, X. L. *Macromolecules* **1996**, *29*, 6189. (b) Jenekhe, S. A.; Chen, X. L. *Appl. Phys. Lett.* **1997**, *70*, 487. (c) Jenekhe, S. A.; Chen, X. L. *Synth. Met.* **1997**, *85*, 1431.

60. Krasovitskii, B. M.; Bolotin, B. M. *Organic Luminescent Materials*; VCH: Weinheim, 1988.

61. Through space and through bond energy transfer are also be referred to as the inductive-resonance and the exchange-resonance energy transfer mechanism, respectively.[60]

62. Ivin, K. J.; Mol, J. C. *Olefin Metathesis and Metathesis Polymerization*; Academic Press: San Diego, 1997.

63. A living polymerization is one without chain transfer and termination. Odian, G. *Principles of Polymerization*; Wiley: New York, 1991; p 389.

64. (a) Grubbs, R. H.; Tumas, W. *Science* **1989**, *243*, 907. (b) Schrock, R. R. *Acc. Chem. Res.* **1990**, *23*, 158.

65. Tasch, S.; Graupner, W.; Leising, G.; Pu, L.; Wagaman, M. W.; Grubbs, R. H. *Adv. Mater.* **1995**, *7*, 903.

66. Pu, L.; Wagaman, M. W.; Grubbs, R. H. *Macromolecules* **1996**, *29*, 1138.

67. Wagaman, M. W.; Bellmann, E.; Grubbs, R. H. *Phil. Trans. R. Soc. Lond. A* **1997**, *355*, 727.

68. Wagaman, M. W.; Grubbs, R. H. *Synth. Met.* **1997**, *84*, 327.

69. Meyers, F.; Heeger, A. J.; Bredas, J. L. *J. Chem. Phys.* **1992**, *97*, 2750.

70. For more on the synthesis and emission spectroscopy of dialkoxy-PNVs, see Chapter 3.

71. (a) Schwab, P.; Grubbs, R. H.; Ziller, J. W. *J. Am. Chem. Soc.* **1996**, *118*, 100. (b) Schwab, P.; France, M. B.; Ziller, J. W.; Grubbs, R. H. *Angew. Chem. Int. Ed. Engl.* **1995**, *34*, 2039.

72. Bimodal molecular weight distributions are not commonly observed in the polymerizations of other barrelenes or benzobarrelenes initiated by **19a**.

73. Fast initiation relative to propagation is important to achieve low PDIs. The sterically bulky ligands surrounding Mo, including the tertiary center α to the alkylidene carbon, slow down initiation, so it is best to use the faster initiating monomer first. Once initiated, the carbon α to the alkylidene carbon is a secondary center, less bulky, so initiation may be fast even with the worse initiating monomer.

74. Broader PDI values are often observed for more rapid polymerizations.

75. Monomer **17a**, when purified by *crystallization,* is very pure and actually polymerizes much faster than **15** precluding the formation of a 1:1 random copolymer. When **17a** is purified by *chromatography*, a slight impurity remains that slows the polymerization rate comparable that of **15**. This "slightly impure" **17a** was used to produce **23a**, but initiator **19a** was used and a bimodal molecular weight distribution was obtained. However, there is no correlation between molecular weight distribution and monomer distribution, so the polymer should be a random copolymer like **23b** and **23c**.

76. Analyzing the homopolymers of **15** and **17c** (Chapter 3) assisted peak assignment.

77. Though other cheaper, commercially available monomers—such as norbornene or cyclooctene—could have been polymerized as the terminal block to aid solubility, these monomers initiate more than 100 time slower (relative to propagation) than **17** (see Chapter 1), so a large amount of monomer would be required to ensure that every polymer chain had a third block.

78. (a) Hörhold, H. H.; Opfermann, J. *Makromol. Chem.* **1970**, *131*, 105. (b) Jin, J.-I.; Park, C.-K.; Shim, H.-K. *Macromolecules* **1993**, *26*, 1799. (c) Jin, J.-I.; Lee, Y.-H.; Shim, H.-K. *Macromolecules* **1993**, *26*, 1805.

79. Φ stands for quantum yield.

80. Chen, S. A.; Chuang, K. R.; Chao, C. I.; Lee, H. T. *Synth. Met.* **1996**, *82*, 207.

81. Granström, M. *Polym. Adv. Technol.* **1997**, *8*, 424.

82. (a) Shen, Z.; Burrows, P. E.; Bulovic, V.; Forrest, S. R.; Thompson, M. E. *Science* **1997**, *276*, 2009. (b) Burrows, P. E.; Gu, G.; Bulovic, V.; Shen, Z.; Forrest, S. R.; Thompson, M. E. *IEEE Trans. Electron Devices* **1997**, *44*, 1188.

83. Chapter 3 presents evidence suggesting the dialkoxy-PNVs have twisted backbones resulting from steric interactions of the alkoxy side chains with the vinyl units. This twisted backbone results in a shorter π-conjugation length and blue shifted emission (from what one would expect based on the electronic effect of the alkoxy

substituents).

84. The fluorescence data here is actually of a diblock copolymer of **18a** (20 repeat units) attached to **18b** (40 repeat units) for solubility. See polymer **16** in Chapter 3.

85. A random copolymer analog of **33** was synthesized, but it was poorly soluble and the quantum yield could not be accurately measured.

86. The following reference was used for help with NMR spectra interpretation: Silverstein, R. M.; Bassler, G. C.; Morrill, T. C. *Spectrometric Identification of Organic Compounds*, 5th ed., John Wiley & Sons: New York, 1991; pp 165-265.

87. Pangborn, A. B.; Giardello, M. A.; Grubbs, R. H.; Rosen, R. K.; Timmers, F. J. *Organometallics* **1996**, *15*, 1518.

88. Fox, H. H.; Lee, J.-K.; Park, L. Y.; Cai, S.; Schrock, R. R. *Organometallics* **1992**, *12*, 759.

89. Oskam, J. H.; Fox, H. H.; Yap, K. B.; McConville, D. H.; O'Dell, R.; Lichenstein, B. J.; Schrock, R. R. *J. Organomet. Chem.* **1993**, *459*, 185.

90. See Chapter 3 of this *Thesis*.

91. Feldman, J.; Schrock, R. R. *Prog. Inorg. Chem.* **1991**, *39*, 1.

92. Polymers are very slightly air-sensitive, and care is taken to not expose them to large amounts of air during work-up. Thus degassed solvents are used and polymer is kept under argon during purification. Also, polymer is kept under argon for long-term storage.

93. The batch of **17a** used in this polymerization was slightly impure resulting in its polymerization at nearly the same rate as **15**. When **17a** is purified more completely by crystallization (rather than chromatography), it is able to ROMP at a much faster rate than **15**.

94. (a) Nakamaru, K. *Bull. Chem. Soc. Jpn.* **1982**, *55*, 2697. (b) Juris, A.; Balzani, V. *Coord. Chem. Rev.* **1988**, *84*, 85.